GnRH neurons recruit astrocytes in infancy to facilitate network integration and sexual maturation

Giuliana Pellegrino, Marion Martin, Cécile Allet, Tori Lhomme, Sarah Geller, Delphine Franssen, Virginie Mansuy, Maria Manfredi-Lozano, Adrian Coutteau-Robles, Virginia Delli, et al.

Submission: 1/10/21 9:10
Nature Neuroscience

GnRH neurons recruit astrocytes in infancy to facilitate network integration and sexual maturation

Giuliana Pellegrino[1]*, Marion Martin[1]*, Cécile Allet[1]*, Tori Lhomme[1], Sarah Geller[2], Delphine Franssen[3], Virginie Mansuy[4], Maria Manfredi-Lozano[1], Adrian Coutteau-Robles[1], Virginia Delli[1], S. Rasika[1], Danièle Mazur[1], Anne Loyens[1], Manuel Tena-Sempere[5], Juergen Siepmann[6], François P. Pralong[4], Philippe Ciofi[7], Gabriel Corfas[8], Anne-Simone Parent[3], Sergio R. Ojeda[9], Ariane Sharif[1$] and Vincent Prevot[1$]

[1]Univ. Lille, Inserm, CHU Lille, Laboratory of Development and Plasticity of the Neuroendocrine Brain, Lille Neuroscience & Cognition, UMR-S 1172, FHU 1000 days for Health, Lille, France.
[2]Center for Integrative Genomics, University of Lausanne, Lausanne, Switzerland.
[3]Neuroendocrinology Unit, GIGA Neurosciences, University of Liège, Liège, Belgium.
[4]Service of Endocrinology, Diabetology and Metabolism, University Hospital and Faculty of Biology and Medicine, 1011 Lausanne, Switzerland.
[5]Department of Cell Biology, Physiology and Immunology, University of Cordoba, Cordoba, Spain; Instituto Maimonides de InvestigaciónBiomédica de Cordoba (IMIBIC/HURS), Cordoba, Spain; CIBER Fisiopatología de la Obesidad y Nutrición, Instituto de Salud Carlos III, Cordoba, Spain.
[6] Univ. Lille, Inserm, CHU Lille, U1008, Lille, France.
[7]Inserm U1215, Neurocentre Magendie, Bordeaux, France;University of Bordeaux, Bordeaux, France.
[8]Kresge Hearing Research Institute, Department of Otolaryngology-Head and Neck Surgery, University of Michigan, Ann Arbor, Michigan 48109.
[9]Division of Neuroscience, Oregon National Primate Research Center-Oregon Health & Science University, Beaverton, OR 97006, USA.

*These authors contributed equally; [$]These authors jointly supervised this work.

[$]Correspondingauthors:
Vincent Prevot, Ph.D., Inserm U1172, Bâtiment Biserte, Place de Verdun, 59045 Lille Cedex, France
Tel: +33 6-12-90-38-76
E-mail: vincent.prevot@inserm.fr
ORCID number: https://orcid.org/0000-0001-7185-3615

Ariane Sharif, Ph.D., Inserm U1172, Bâtiment Biserte, Place de Verdun, 59045 Lille Cedex, France
E-mail: ariane.sharif@inserm.fr
ORCID number: https://orcid.org/0000-0003-0810-400X

ABSTRACT

Neurons producing gonadotropin-releasing hormone (GnRH), which control fertility, complete their nose-to-brain migration by birth. However, their function depends on integration within a complex neuroglial network during postnatal development. Here, we show that GnRH neurons during the infantile period use a prostaglandin-D2/DP1-receptor signaling mechanism to recruit newborn astrocytes that “escort” them into adulthood, and the impairment of postnatal hypothalamic gliogenesis dramatically alters sexual maturation by preventing this recruitment, a process mimicked by the endocrine disruptor bisphenol-A. DP1 signaling inhibition in the infantile preoptic region, where GnRH cell bodies reside, disrupts the correct wiring and firing of GnRH neurons, alters minipuberty or the first activation of the hypothalamic-pituitary-gonadal axis during infancy, and delays the timely acquisition of reproductive capacity. These findings uncover a previously unknown neuron-to-neural-progenitor communication pathway and demonstrate that postnatal astrogenesis is a basic component of a complex set of mechanisms used by the neuroendocrine brain to control sexual maturation.

INTRODUCTION

Neuroendocrine GnRH neurons, which ensure species survival by controlling the ability of individuals to reproduce, are principally located in the preoptic region, a basal forebrain region harboring diverse neuronal populations[1]. Unlike other hypothalamic neurons driving bodily functions, GnRH neurons are not born in the brain but originate in the olfactory placode, and migrate from the nose to the brain during embryogenesis[2]. Although this migration is complete at birth, GnRH neurons recruit other neuronal populations, notably those expressing kisspeptin and neuronal nitric oxide synthase (nNOS), during postnatal development to establish a complex circuit that fine-tunes GnRH production and release by providing precisely coordinated excitatory and inhibitory inputs[3, 4], thus orchestrating sexual maturation, puberty and adult fertility[5]. However, the mechanisms by which GnRH neurons sculpt their own microenvironment and establish the connections necessary to control reproduction remain unexplored.

The GnRH network is not exclusively neuronal but includes at least two glial cell types: tanycytes, which control the access of GnRH neurosecretory terminals to the pericapillary space of pituitary portal vessels, into which the hormone is released, and astrocytes, whose communication with GnRH neurons is essential for reproductive function[6]. Glial cells, especially astrocytes, also help generate physiological responses by forming a hub with neurons that integrates internal and external cues within the adult brain[6]. Additionally, they act as cartographers of synaptogenesis and neural circuit formation in the developing central nervous system[7, 8]. Conversely, studies in the neocortex suggest that astrocyte formation is regulated by extrinsic signals generated by neurons, the development of which precedes gliogenesis[9]. We therefore asked whether GnRH neurons could themselves be responsible for the circuit formation subtending reproductive function in adulthood by establishing a glial entourage during postnatal development.

Here, we demonstrate that GnRH neurons in the infantile period attract newborn progenitor cells that differentiate into astrocytes and remain closely associated with them, essentially “escorting” these neurons into adulthood. Additionally, local inhibition of infantile

gliogenesis in the preoptic region, which harbors GnRH neuronal somata, delays puberty. The interaction between GnRH neurons and newborn astrocytes underlying correct sexual maturation depends on reciprocal prostaglandin-mediated signaling, and especially the expression of the prostaglandin D2 receptor DP1 by these newborn cells. Our findings thus identify a novel neuron-to-neural-progenitor communication mechanism that unfolds during the infantile period and times the pubertal activation of the reproductive axis.

RESULTS

GnRH neurons assemble a glial entourage during early infancy

GnRH neuronal somata in rats are loosely distributed between the medial septum/diagonal bands of Broca and the preoptic nuclei, being densest in the median preoptic nucleus (MePO) at the level of the organum vasculosum laminae terminalis (OVLT). To determine if the birth of new cells in the vicinity of GnRH neurons shapes their microenvironment, we used the thymidine analog, bromodeoxyuridine (BrdU) to map cell proliferation in the OVLT and its surroundings, referred to hereafter as the “preoptic region”, in female rats at different stages of postnatal development [postnatal day (P)1 and P5: neonatal period; P8 and P12: infantile period; P20 and P24: juvenile period, i.e. after weaning] (**Fig. 1a**). In agreement with a previous report[10], more cells incorporated BrdU in the infantile versus the juvenile period (**Supplementary Fig. 1a,b**). BrdU colocalization with proliferating-cell nuclear antigen (PCNA), an endogenous cell-cycle marker (**Supplementary Fig. 1c**), the occurrence of pairs of closely apposed $BrdU^+$ nuclei (**inset in Fig. 1b, Supplementary Fig. 1d**), and doubling of the $BrdU^+$ cell population between 2h and 24h after BrdU injection (**Supplementary Fig. 1e**) strongly suggested that BrdU-labeled cells were entering the cell cycle. Seven days after BrdU injection, most newborn cells expressed either glial fibrillary acidic protein (GFAP) in conjunction with an astrocyte-like morphology, denoting their differentiation into astrocytes, or adenomatosis polyposis coli (APC) – a marker of oligodendrocytes, while a very small number expressed the neuronal marker, HuC/D (**Supplementary Fig. 2a-j**). The presence of multipotent progenitors in the postnatal

preoptic region was confirmed *in vitro* by culturing clonally-derived neurospheres capable of differentiating into all three neural cell types (**Supplementary Fig. 2k-m**).

Interestingly, co-immunolabeling revealed the close proximity of some GnRH neuronal cell bodies to $BrdU^+$ newborn cells (**Fig. 1b**). Biocytin filling of patch-clamped astrocytes in living brain slices from infantile rats showed that preoptic astrocytes had a radius of 20-40 µm (**Supplementary Fig. 3a**). We therefore decided to look for newborn progenitors, which presumably have smaller arborizations, at a conservative distance of 10 µm from GnRH neurons. Two hours after BrdU injection, GnRH neurons accompanied by $BrdU^+$ progenitors were more frequent in neonatal and infantile rats than in juvenile animals (**Fig. 1c**). GnRH neurons preferentially associated with proliferating cells, since 12.8% of GnRH neurons were juxtaposed to $BrdU^+$ cells 2h after BrdU injection at P8, versus only 3.6% of non-GnRH neurons (**Fig. 1c,d**). At this time-point, these proximal $BrdU^+$ cells expressed the progenitor cell marker, Sox2, but not GFAP (**Fig. 1e-g**). Twenty-four hours later, 27.2% of GnRH neurons were associated with $BrdU^+$ cells labelled by a single injection at P8 (**Fig. 1c**). This increased association persisted even after seven days, when 22.3% of GnRH neurons had a companion $BrdU^+$ cell (**Fig. 1c,d**). Notably, this proportion reached 80.3 ± 2.7% (n = 4 rats) when the BrdU regimen was increased to three injections per day from P6 to P8 (**Fig. 1h**). Because the number of GnRH neurons in the preoptic region remained unchanged during postnatal development (367.2±43.5 neurons at P8 versus 342.9 ± 22.3 neurons at P15, two-sided unpaired t-test, $t_{(14)}$ = 0.498, P = 0.626; n = 8 rats per group), the increased proportion of GnRH neurons associated with $BrdU^+$ cells could either stem from a global increase in the number of $BrdU^+$ cells in the preoptic region after proliferation (**Supplementary Fig. 1e**) or the migration of $BrdU^+$ cells towards GnRH neurons. We analyzed the neighborhood of GnRH neurons 2h after a single BrdU injection at P8, and identified all neurons that would be considered associated with a $BrdU^+$ cell 24h later if the proliferation of existing $BrdU^+$ cells were to give rise to a daughter cell lying within 10µm of the GnRH neuronal soma (**Supplementary Fig. 3b,c**). However, even under the very

broad assumption that every proliferative event would give rise to a newborn cell within the perimeter described, the resulting theoretical percentage of GnRH neurons with associated $BrdU^+$ cells was still significantly lower than the actual percentage measured (**Supplementary Fig. 3d**), indicating that cell division in the neighborhood of GnRH neurons could not fully account for the increased proportion of GnRH neurons with a $BrdU^+$ companion cell. GnRH neurons are thus likely attract newborn cells to their immediate vicinity during the early infantile period.

The association between GnRH neurons and cells born at P8 was maintained until adulthood (**Fig. 1c**). Notably, the increase in GnRH neurons with $BrdU^+$ companions between 2h and 7 days after BrdU injection was seen only in the group injected at P8 (**Fig. 1c**), indicating that the beginning of the infantile period is a critical time-window for GnRH neurons to enrich their immediate cellular environment. Triple immunolabeling for GnRH, BrdU and GFAP, APC or HuC/D showed that P8-born cells accompanying GnRH neurons mainly differentiated into GFAP-expressing astrocytes (**Fig. 1g,i-k**). Physical proximity to GnRH neurons did not alter the fate of P8-born cells (phenotype of $BrdU^+$ cells in the vicinity of GnRH neurons (n = 6-7 rats) vs. all newborn cells in the preoptic region (n = 3 rats): GFAP, Mann-Whitney test: $U = 9$, $P = 0.833$; APC, Mann-Whitney test: $U = 6$, $P = 0.500$; HuC/D, Mann-Whitney test:$U = 3$, $P = 0.167$) (compare **Supplementary Fig. 2j** and **Fig. 1g**).

Blocking infantile preoptic cell proliferation delays puberty

To determine if the birth of new cells in the infantile preoptic region is involved in sexual maturation, we locally inhibited cell proliferation in P6 or P7 female rats by stereotaxically injecting biodegradable poly(D,L-lactic-co-glycolic acid) (PLGA)-based microparticles (**Fig. 2a,c**), designed to release the antimitotic compound, paclitaxel, in a time-controlled manner[11], just above the MePO. An initial assay revealed that this release was complete by 6 days, i.e. before the end of the infantile period when proliferation in the preoptic area peaks (**Supplementary Fig. 4a**). Control animals were injected with blank-

loaded microparticles (**Fig. 2a,b**), and a single BrdU injection carried out at P8 as before in both groups. We then monitored puberty onset and adult estrous cyclicity. At adulthood, paclitaxel-treated animals showed decreased cell density (**Fig. 2c,d, Supplementary Fig. 4b,c**), fewer $BrdU^+$ cells at the injection site (**Fig. 2e, Supplementary Fig. 4b,c**) and a lower proportion of GnRH neurons associated with $BrdU^+$ cells in the MePO (**Fig. 2f**), although the total number of GnRH neurons in the preoptic region remained unaffected (**Fig. 2g**). In the anteroventral periventricular nucleus (AVPV), a more ventral preoptic nucleus that extends well beyond the OVLT caudally and relays the estrogen positive feedback[12], chronic intracerebroventricular administration of another antimitotic, AraC, during the peripubertal period has been shown to block proliferation[13]. However, paclitaxel treatment did not affect the number of $BrdU^+$ cells, neurons or astrocytes in the AVPV (**Supplementary Fig. 5**), indicating that our administration method had extremely localized antimitotic effects. Paclitaxel-treated animals exhibited a marked delay in puberty onset compared to control animals, as indicated by delayed vaginal opening (**Fig. 2h,i**) and first estrus (**Fig. 2j,k**). In addition, while the two milestones coincided in control animals, they were uncoupled in paclitaxel-treated animals, which experienced their first estrus ~3.5 days after vaginal opening (**Fig. 2l**,**m**), a phenomenon rarely observed in rats[5]. Notably, paclitaxel-treated animals had similar body weights to control animals (**Supplementary Fig. 4d**), indicating that the delay in sexual maturation was not due to a growth deficit. Paclitaxel-treated animals also exhibited fewer complete 4-day estrous cycles (**Fig. 2l,n**). Taken together, these results suggest that the presence of newborn cells in the environment of preoptic GnRH neurons during the infantile period, rather than GnRH neurons *per se*, is necessary for the timely onset of puberty and contributes to fertility in adulthood.

Endocrine disruptors alter GnRH neuron-progenitor interaction

A common adverse condition for the development and function of the gonadotropic axis is exposure to endocrine-disrupting chemicals (EDCs) during perinatal life. While the gonads have long been considered the main targets of EDCs, a growing number of studies

highlight their neuroendocrine effects, such as GnRH neuronal network alterations[14]. Intriguingly, rat pups exposed for the first 15 days after birth to a very low but environmentally relevant dose [15] of the plasticizer bisphenol A (BPA; 25 ng/kg per day) tend towards delayed vaginal opening[16], phenocopying our paclitaxel-treated rat pups. Additionally, these BPA-exposed rats also demonstrate an altered frequency of GnRH secretion at P20[16], suggesting a perturbation of the first postnatal activation of the hypothalamic-pituitary-gonadal (HPG) axis, known as minipuberty. This phenomenon, which occurs at P12 in rats and 1 month of age in humans, helps establish an adult pattern of pulsatile GnRH secretion that, in baby girls and female rodents alike, triggers an FSH surge that is essential for subsequent gonadal maturation and hence, fertility[5, 17]. To verify whether the adverse effects of EDCs on gonadotropic axis maturation could stem from their interference with the ability of GnRH neurons to recruit neighboring cells, we treated female rat pups with 25 ng/kg per day of BPA from P1[16], then injected them with BrdU at P8 and assessed GnRH neuron association with $BrdU^+$ cells 2h and 7d later (**Fig. 3a**). Contrary to paclitaxel, BPA exposure did not affect cell birth near GnRH neurons at P8 (**Fig. 3b**). Additionally, the total number of GnRH neurons in the preoptic region at P8 also remained unchanged (255.7 ± 34.95 in control P8 rats versus 218.9 ± 30.38 in BPA-treated P8 rats, Mann-Whitney test: $U = 22$, $P = 0.3282$; $n = 8$ rats per group). However, unlike untreated rats, BPA-exposed animals showed reduced association between GnRH neurons and P8-born $BrdU^+$ cells 1 week later (**Fig. 3b**) even though there was no depletion of $BrdU^+$ cells in the preoptic region (**Fig. 3c**), further supporting the view that rather than proliferation, it is the recruitment of new glial progenitors by GnRH neurons that influences later reproductive function. From a broader viewpoint, these results also open up the possibility that the effects of EDCs on fertility and brain maturation are at least partly due to their interference with the ability of select neuronal populations to shape their glial environment during postnatal development.

GnRH neurons use PGD2 to recruit preoptic progenitor cells

Considering that the increased proportion of GnRH neurons associated with $BrdU^+$ cells between P8 + 2h and P8 + 24h is likely due to $BrdU^+$ cell recruitment rather than proliferation (**Supplementary Fig. 3**), we wondered whether GnRH neurons themselves released chemotropic factors to attract glial progenitors that would eventually differentiate into astrocytes in their vicinity and remain associated with them into adulthood (**Fig. 1i**). We first probed a set of molecules expressed in female rodent GnRH neurons: GnRH, neurotensin (NT), cholecystokinin (CCK), galanin, glutamate and GABA[18, 19]. Double immunolabeling showed that infantile GnRH neuronal perikarya contained galanin but lacked CCK and NT (**Supplementary Fig. 6a-i**). However, the vesicular transporters for glutamate and γ-aminobutyric acid (GABA), v-Glut and v-GAT, respectively, colocalized at the GnRH termination field in the median eminence (**Supplementary Fig. 6j-o**), suggesting that postnatal GnRH neurons could also influence proliferating cells through the local glutamate or GABA release.

To assess the putative chemotactic effects of GnRH, galanin, glutamate and GABA produced by GnRH neurons, we next developed adherent primary cultures of progenitor cells from the rat preoptic region at P1-P2 (**Supplementary Fig. 7a**). Cultured cells exhibited an antigenic profile typical of neural progenitors, predominantly expressing nestin, BLBP, Sox2 and vimentin (**Fig. 4a, Supplementary Fig. 7b-e**). However, in transwell assays, their migration was not significantly affected by GnRH, galanin, glutamate or GABA (**Fig. 4b**), suggesting that other factors might be responsible for their chemoattraction by GnRH neurons.

Next, since postnatal progenitor recruitment by GnRH neurons occurs in the global context of astrogenesis[8], and GnRH neurons are tightly surrounded by GFAP-expressing processes at P8 (**Fig. 1f**), we searched for candidate genes in GnRH neurons that could be regulated by astroglial factors. We conducted a transcriptomic analysis of GnV3 cells, an *in vitro* model of postnatal rat GnRH neurons [20], exposed to medium conditioned with or without hypothalamic astrocytes for 4 days (**Fig. 4c**). In all, 512 genes were differentially expressed (212 upregulated and 300 downregulated) when GnV3 cells were treated with astrocyte-

conditioned medium (See Source Data Files in **Supplementary Data 1**). The most upregulated gene was *Ptgds* encoding brain-type prostaglandin D2 (PGD2) synthase, a molecule with potent chemoattractant properties[21], which displayed a 133-fold increase in response to astrocyte-conditioned medium (**Supplementary Data 1**). RT-PCR analysis confirmed this upregulation (**Fig. 4d**). Moreover, PGD2 stimulated the passage of preoptic neural progenitors from the upper to the lower compartment in transwell migration assays (**Fig. 4b**), but did not affect their proliferation (**Fig. 4e**). As gliogenesis continues during postnatal development, these data suggest that GnRH neurons respond to incoming glial signals by synthesizing PGD2 and thus attracting newborn cells in their vicinity.

PGD2 functions *via* the G protein-coupled receptors, DP1 (*Ptgdrl*) and DP2 (*Gpr44*) [21, 22], both expressed in primary cultures of preoptic neural progenitors (**Fig. 4f**). Since DP1 signaling is already known to be involved in regulating hypothalamic function[22], we used BWA868C, a specific antagonist of DP1[22, 23], to determine whether the effect of PGD2 on hypothalamic progenitor cell migration was mediated by DP1. BWA868C treatment of preoptic neural progenitors not only drastically inhibited the stimulatory effect of PGD2 on cell migration (**Fig. 4g,h**), it also reduced the PGD2-induced phosphorylation of the mitogen-activated protein kinase (MAPK) ERK (**Fig. 4i**), confirming that PGD2 signaling was active in these progenitors.

PGD2/DP1 signaling mediates preoptic precursor recruitment

Next, to investigate whether GnRH neurons produce PGD2 during postnatal development *in vivo*, we analyzed *Ptgds* expression in cells isolated by fluorescence-activated cell sorting (FACS) from transgenic rats expressing enhanced green fluorescent protein (EGFP) under the control of the GnRH promoter[24] using real-time PCR (**Fig. 5a**, **Supplementary Fig. 8a,b**). *Gnrh* mRNA was only detected in the EGFP-positive cell fraction, demonstrating the accuracy of the sorting procedure (**Supplementary Fig. 8c-e**). Using this approach, we found that *Ptgds* transcripts were indeed enriched in rat GnRH neurons and

that their expression significantly increased between P8 and P20 in these neurons (**Fig. 5b**) but remained unchanged in preoptic cells lacking EGFP (**Fig. 5c**).

To gain further insight into the involvement of the PGD2/DP1 signaling pathway in the communication between GnRH neurons and neural progenitors *in vivo*, we evaluated *Ptgds* and *PtgdrI* expression in the postnatal preoptic region. Multiplex *in situ* hybridization in female rats at P8 confirmed the expression of *Ptgds* transcripts in GnRH neurons (**Fig. 5d**, upper row), while neighboring Sox2-expressing neural progenitors expressed *PtgdrI* mRNA (**Fig. 5d**, lower row). Moreover, the fraction of GnRH neurons expressing *Ptgds* increased between P8 and P12, an increase still seen at P20 (**Fig. 5e**), explaining the increased *Ptgds* expression observed in FACS-sorted cells above (**Fig. 5b**); however, the abundance of *Ptgds* transcripts per GnRH neuron did not significantly increase across the infantile period (**Fig. 5f**). In contrast, *PtgdrI* expression in *Sox2*$^{+}$ progenitors showed no significant variation between P8 and P20 (**Fig. 5g,h**). Altogether, these data show that the increased *Ptgds* expression in GnRH neurons during infantile development corresponds to an increase in the proportion of PGD2-synthesizing GnRH neurons during the period of enhanced astrogenesis in the preoptic area (**Supplementary Fig. 1**, **Supplementary Fig. 2)**.

To confirm that the PGD2/DP1 signaling pathway is indeed involved in progenitor cells recruitment by GnRH neurons *in vivo*, we acutely injected BWA868C stereotaxically into the preoptic region of P7 female rats, 2h after a single BrdU injection, and quantified the proportion of GnRH neurons associated with BrdU^{+} cells after 24h (**Fig. 6a**). This proportion increased in control animals but not in BWA868C-treated rats (**Fig. 6b**). Since BWA868C treatment did not affect the total number of BrdU^{+} cells in the preoptic region (**Fig. 6c**), the inhibitory effect of BWA868C on the physical proximity between GnRH neurons and BrdU^{+} cells was not due to neural progenitors depletion but to the blockade of the trophic influence of GnRH neurons on nearby glial progenitors. Together with our *in vitro* findings, these results indicate that functional PGD2/DP1 signaling is necessary for GnRH neurons to recruit or attract a glial entourage during the infantile period in rats.

Inhibiting DP1 disrupts GnRH network maturation and function

To assess the functional involvement of DP1 signaling in postnatal sexual maturation, we implanted BWA868C pellets (10 nM in cocoa butter) in the preoptic region of P8 female rats[25] and monitored the occurrence of the first postnatal FSH surge indicative of minipuberty (**Fig. 6d**). Similar to acute injection, BWA868C released chronically from a pellet also significantly hampered the association of GnRH neurons with $BrdU^+$ cells one week later (**Fig. 6e**), although the total number of $BrdU^+$ cells in the preoptic region remained unaffected (**Fig. 6f**). While the treatment had no effect on somatic growth (**Supplementary Fig. 9**), the FSH surge at minipuberty was blunted in BWA868C-treated pups in comparison to vehicle-treated littermates (**Fig. 6g**), suggesting that the activity of infantile GnRH neurons was impaired by their inability to attract newborn astrocytic precursors.

Next, since minipuberty has previously been shown to be a critical period for the switch in the transcriptional control of GnRH expression [4], we assessed whether BWA868C treatment at P7 influenced this process. RT-qPCR analyses in FACS-isolated rat GnRH neurons at P12-P13 indicated that BWA868C implantation had no apparent impact on *Gnrh* expression (**Fig. 7a**). However, it decreased the expression of *Cebpb*, a repressor of the *Gnrh* promoter, but left unchanged the expression of another repressor, *Zeb1*, as well as *Kiss1r* and *Otx2*, two stimulators of *GnRH* expression, and *Dicer*, an RNAse-III endonuclease essential for microRNA biogenesis and the microRNA-mediated infantile *Gnrh* transcriptional switch[4] (**Fig. 7a**). Surprisingly, BWA868C treatment also impacted several other genes involved in prostaglandin synthesis and signaling in infantile GnRH neurons (**Fig. 7b**). In addition to a significant decrease in *Ptgds* expression (**Fig. 7c**), in line with our transcriptomic analysis showing *Ptgds* regulation by astrocyte-derived factors (**Fig. 4d**, **Supplementary Data 1**), BWA868C treatment downregulated transcripts for *Ptger1* and *Ptger3*, encoding the PGE2 receptors EP1 and EP3, respectively, in infantile rat GnRH neurons (**Fig. 7c**). These results are in keeping with previous *in vitro* studies showing that astrocyte-conditioned medium modulates the sensitivity of GnRH neurons to astrocytic

PGE2, a stimulator of GnRH release, by upregulating EP1 and EP3 expression[26], and suggest that the BWA868C-mediated decrease in astrocyte recruitment by GnRH neurons interferes with astrocytic PGE2-stimulated GnRH release rather than GnRH production.

We next investigated whether, in addition to altering astrocyte-to-GnRH-neuron communication processes, BWA868C treatment could also influence neuronal connectivity, in particular the apposition of glutamatergic or GABAergic terminals onto GnRH neuronal cell bodies, and consequently GnRH neuronal activity during the infantile period. The BWA868C-mediated inhibition of DP1 signaling in the preoptic region significantly decreased the number of appositions of vesicular glutamate transporter 2 (vGluT2)-immunoreactive punctae but not of vesicular GABA transporter (vGaT)-immunoreactive punctae on GnRH somata at P15 (**Fig. 7d**).

Given this robust decrease in putative excitatory synaptic inputs to GnRH neurons, we next performed *ex vivo* whole-cell patch-clamp recordings of GnRH neurons in living brain slices containing the OVLT from P10-P15 infantile *Gnrh::Egfp* rats treated either with vehicle or with BWA868C *in vivo* at P7-P8 (**Fig. 7e,f**). We found no significant difference between the two conditions in the resting membrane potential (Vm) (**Fig. 7g**), membrane resistance (Rm) (**Fig. 7h**), voltage threshold for action potential (AP) generation (V_{TH}) (**Fig. 7i**) or time constant (control time constant = 0.47 ± 0.07 ms, *n* = 15 cells from 8 rats; BWA868C time constant = 0.43 ± 0.05 ms, *n* = 22 cells from 7 rats; Mann-Whitney test: *U* = 149.5, *P* = 0.641). These findings demonstrate that the integrative properties and intrinsic excitability of GnRH neurons were not modified by BWA868C treatment. However, we observed a significant attenuation of the spontaneous firing rate in GnRH neurons partly deprived of glutamatergic synapses (**Fig. 7j**and **f,** left), reminiscent of the increased interpulse interval of GnRH neurosecretion in BPA-treated rat pups[16]. This was not accompanied by modifications in spike properties such as full amplitude (control spike amplitude = 57.73 ± 2.75 mV, *n* = 10 cells from 8 rats; BWA868C spike amplitude = 61.13 ± 1.88 mV, *n* = 10 cells from 8 rats; two-sided unpaired *t*-test, *t*(18) = 1.02, *P* = 0.321), half-

368 width duration (control half-width duration = 1.85 ± 0.17 ms, *n* = 10 cells from 8 rats;
369 BWA868C half-width duration = 1.74 ± 0.07 ms, *n* = 10 cells from 8 rats; Mann-Whitney test:
370 *U* = 49, *P* = 0.970) or after-hyperpolarization potential (AHP) amplitude (control AHP
371 amplitude = 7.52 ± 0.55 mV, *n* = 10 cells from 8 rats; BWA868C AHP amplitude = 7.18 ±
372 0.30 mV, *n* = 10 cells from 8 rats; two-sided unpaired *t*-test, *t*(18) = 0.535, *P* = 0.599) or
373 duration (control AHP duration = 470.9 ± 69.52 ms, *n* = 10 cells from 8 rats; BWA868C AHP
374 duration = 465.7 ± 65.53 ms, *n* = 10 cells from 8 rats; two-sided unpaired *t*-test, *t*(18) = 0.055,
375 *P* = 0.957) as measured from isolated APs. We further analyzed spike generation in neurons
376 in which clear baseline synaptic activity was detected on the trace (n = 10 neurons from 8
377 rats per condition). In the control group, in 5 neurons, firing was triggered by a slowly
378 developing temporal summation of fast depolarizing events (**Fig. 7f**, top right), reminiscent of
379 depolarizing postsynaptic potentials. This dramatically differed from most BWA868C-treated
380 neurons, in which AP firing was apparently elicited by intrinsic mechanisms (n = 4 neurons,
381 **Fig. 7f**, bottom right, AP #1 and #2) or the cooperative effect of intrinsic and synaptic
382 mechanisms (n = 4 neurons, **Fig. 7f**, bottom right, AP #3). Only two BWA868C-treated
383 neurons analyzed displayed APs elicited by an excitatory synaptic barrage. Altogether, these
384 findings indicate that BWA868C treatment does not alter the resting membrane or integrative
385 properties of GnRH neurons but significantly reduces their functional output, likely due to
386 decreased glutamatergic synaptic connections.

387 Finally, we analyzed the effects of infantile BWA868C treatment on the acquisition of
388 mature reproductive function. Even though BWA868C implantation in the preoptic region
389 during the infantile period did not alter the age at vaginal opening (**Fig. 8a,b**), which
390 coincided with first estrus (**Fig. 8a**), it significantly delayed the onset of regular estrous
391 cyclicity (**Fig. 8a,c**). During the first two weeks after vaginal opening, BWA868C-treated
392 females spent more time in estrus at the expense of proestrus, indicating a dysregulation of
393 pulsatile GnRH release, in contrast to control (vehicle-treated) littermates, which quickly
394 acquired a regular 4-day estrous cycle.

Altogether, these results show that the integrity of GnRH neuron-glia communication in the preoptic region during the infantile period is critical for the recruitment of newborn glial precursors that accompany these neurons into adulthood as well as the establishment of functional synaptic inputs to GnRH neurons. Furthermore, this communication, mediated by PGD2/DP1 signaling, is essential for the correct initiation of sexual maturation, reciprocal signaling by astrocytes of the GnRH neural network, and adult pattern of estrous cyclicity.

DISCUSSION

The ability to reproduce is acquired through a long and complex process that relies on the fine regulation of GnRH neuronal network activity during the postnatal period. This process involves intrinsic and extrinsic modifications to functional gene networks[4, 27] and neuronal circuits converging onto GnRH neurons[28, 29], as well as the increased stimulatory influence of glial cells[6]. Our data provide the first neuroanatomical and physiological evidence that GnRH neurons build their own glial environment during a circumscribed period after birth via a specific cell-cell communication pathway with neural progenitors born during a wave of astrogenesis, and that this reciprocal communication is essential for the maturation of the hypothalamic neuroendocrine system controlling the survival of the species.

Astrocytes have long been known to play a role in the control of GnRH neuronal function, particularly during postnatal sexual maturation[25], being sophisticated sensors[8] and regulators of neuronal activity via both the timely trafficking of energy metabolites[30] and gliotransmission[31]. They communicate with GnRH neurons by releasing bioactive molecules such as PGE2[32, 33], known to be released at active synapses in response to glutamate[34, 35]. Glutamate-stimulated PGE2 release within the GnRH neural network may involve the activation of the ErbB signaling pathway [36], also important for puberty onset [25, 37], in hypothalamic astrocytes. Here, we pinpoint the production of another prostaglandin, PGD2, by GnRH neurons themselves as a potent communication signal used by these neurons to attract infantile astroglial progenitors to their vicinity. Our findings demonstrate that inhibiting

cell proliferation or impairing PGD2/DP1 signaling in the preoptic region during this period significantly alters sexual maturation, indicating that astrogenesis in the vicinity of GnRH neurons during postnatal development is an important component of the homeostatic mechanism required for GnRH neural network maturation. While recent advances in glial cell biology have provided substantial insights into how astrocytes influence neuronal function (see [38] for review), the concept that neurons could stably recruit astrocytic progenitors as companions or "escorts", i.e. allow newborn neighboring astrocytes to become structurally/functionally associated with them during development and maintain this relationship into adulthood, has rarely been evoked.

Interestingly, the birth of new cells in the infantile preoptic region could also be modulated by neuronal factors released by other components of the GnRH neuroglial network. For example, some incoming fibers from the developing arcuate nucleus of the hypothalamus release β-endorphin[39, 40], which has recently been shown to activate quiescent neural stem cells in the adult brain[41], and could thus be a candidate to regulate this infantile proliferation. While we cannot rule out an indirect influence of the proliferation or signaling of neural progenitors on reproductive function through similar mechanisms in other components of the GnRH network, e.g. by altering astrocyte-kisspeptin-neuron interactions in the adjacent AVPV, the fact that paclitaxel did not modify BrdU+ cells in this nucleus suggests that the physiological changes we observed were selectively due to perturbed astrocyte-GnRH neuron association, rather than alterations in the neuroglial interactions of afferent neurons. Nevertheless, paclitaxel affected the reproductive phenotype more severely than BWA868C, suggesting that the progenitor depletion might have been harder to compensate for than simply inadequate GnRH neuron connectivity due to impaired association with glial progenitors.

Interestingly, deficient DP1 signaling in the preoptic region also blunts the FSH surge at P12, i.e. during minipuberty, the first centrally driven and gonad-independent activation of the HPG axis[5]. This phenotype is highly reminiscent of that of mice in which astrocytic function is selectively altered by expressing a dominant-negative ErbB4 receptor (DN-ErbB4)

under the control of the GFAP promoter[37]. On the other hand, the disrupted estrous cycle triggered by blocking preoptic DP1 signaling in rats phenocopies transgenic mice expressing a dominant negative mutation of the adhesion molecule SynCAM1 under the GFAP promoter[42]. SynCAM1 expression, required to maintain the physical contact between astrocytes and GnRH neuronal cell bodies[43], is activated by astroglial ErbB4 signaling[42]. Altogether, these findings evoke a scenario in which the birth of new astrocytes during postnatal development promotes a selective increase in the expression of the PGD2-producing enzyme, PGDS, in infantile GnRH neurons via an as yet unidentified signaling pathway involving soluble factors. The choice of candidate signaling factors is large, with astrocytes releasing not only gliotransmitters but numerous neuroactive substances, including thrombospondin, TNFα and TGFβ1 (see for review [44-46]). Regardless of its identity, PGD2 released by GnRH neurons attracts DP1-expressing neural progenitors that eventually differentiate into astrocytes and remain associated with these neurons until adulthood, an "escort" function that could facilitate their integration into functional networks and sexual maturation (**Extended Data Fig. 1**), and that could require other neuron-to-glia communication processes similar to those involving infantile ErbB4 signaling[42, 43]. While such experiments in rats are beyond the technical scope of this study, preliminary experiments in *Gfap::DN-ErbB4* mice indicate that newborn cells that are morphologically associated with infantile GnRH neurons fail to accompany them into adulthood, in contrast to wild-type littermates, despite the unaltered proliferation and long-term survival of these cells (**Supplementary Note**; **Supplementary Fig. 10**).

Astrocytes also play key roles in the control of synapse formation and functional efficacy[47, 48], shaping synaptic properties to fit ongoing developmental and functional needs, thus providing contextual guidance to the synapses[49, 50]. During postnatal development, synaptic punctae in the brain appear concurrently with astrogenesis[47]. Remarkably, our results show that preventing GnRH neurons from attracting glial progenitors in their immediate neighborhood by blocking DP1 signaling markedly decreases the number of vGluT2 appositions on GnRH neurons and significantly attenuates GnRH neuron firing, primarily by

478 decreasing the rate of depolarizing postsynaptic potentials. Since the FSH surge at
479 minipuberty is also blunted in these pups, we can postulate that the birth of new astrocytes
480 near infantile GnRH neurons is required for the establishment of excitatory glutamatergic
481 inputs onto GnRH neurons, confirming the long-suspected notion that such afferents
482 contribute to the gonad-independent maturation of the HPG axis in infantile rats[51, 52]. These
483 excitatory synaptic inputs are thought to develop after GABAergic inputs[53, 54], which,
484 contrarily, do not appear to require infantile gliogenesis for their establishment or
485 maintenance (**Fig. 7d**). Intriguingly, in the interconnected GnRH neuroglial network[6],
486 glutamate spillover at the synaptic cleft by the co-activation of metabotropic and AMPA
487 glutamatergic receptors in hypothalamic astrocytes[36] or their progenitors may initiate a
488 signaling cascade that allows ErbB4 receptor recruitment[36], promotes astrogenesis[55] and
489 thus leads to the stabilization and maturation of glutamatergic synapses. This causes
490 increased PGE2 synthesis and release by astrocytes [36], which can then signal back to
491 GnRH-secreting neurons[6]. An infantile GnRH neuron-dependent modulation of astrogenesis
492 may therefore contribute to building a signaling network capable of delivering coordinated
493 trans-synaptic and astroglial inputs to GnRH neurons themselves for the initiation of puberty
494 and the timely acquisition of adult reproductive capacity (**Extended Data Fig. 1**)[4].

495 Recent human and animal studies increasingly demonstrate that the GnRH neural
496 network is particularly sensitive to environmental pollutants, in particular endocrine
497 disruptors, during early postnatal development[14]. Exposure to EDCs such as the plasticizer
498 BPA during the critical perinatal period is indeed reported to be associated with early or late
499 puberty onset and subsequent reproductive impairments in both boys and girls (see for
500 review [14]) , and to affect the central control of puberty, including glutamatergic and
501 GABAergic inputs to GnRH neurons, in preclinical animal models[16, 56, 57]. While the underlying
502 mechanisms remain elusive, glial cells, which play a central role in GnRH neuronal network
503 development and function[6], would be the obvious suspects to mediate this EDC-induced
504 pathophysiological process[14]. Our results intriguingly show that treating infantile rats with
505 very low but environmentally relevant doses of BPA[15] known to cause alterations in sexual

maturation, phenocopying paclitaxel-treated rats[16], alters the recruitment of newborn neighboring cells by GnRH neurons at minipuberty, without appearing to affect overall cell proliferation in the infantile preoptic region. This raises the possibility that early-life exposure to chemicals in contact with food[58], such as BPA, may perturb puberty onset and durably impact reproductive function at least partially by interfering with the capacity of GnRH neurons to build a proper glial environment through altered PGDS expression[59] or ErbB signaling[60], resulting in their miswiring during postnatal development.

To summarize, our findings shed light on a hitherto unsuspected neuron-to-neural-progenitor communication process that shapes the glial environment of GnRH neurons during postnatal development and is required for the proper wiring and function of these neurons, which control the survival of the species in mammals.

ACKNOWLEDGEMENTS

G.P. and M.M. were PhD students funded by the University of Lille and C.A. by the CHU Lille. We are most grateful to Stéphane Charpier (Institut du Cerveau – ICM, UPMC-P6 UM 75, Paris, France) for his precious insights in analyzing electrophysiological data and Paolo Giacobini (Inserm, Lille, France) for his comments on the manuscript. We thank Dr. Alexandre Dawid for data analysis (LiPhy, Grenoble), Aude Caillet (U1172), Nathalie Jouy (cytometry core facility, UMS2014-US41), Meryem Tardivel and Antonino Bongiovanni (microscopy core facility, UMS2014-US41), Martin Fourdrinier (animal core facility, University of Lille) and Arlette Gérard (University of Liège) for expert technical assistance. We are indebted to Gaetan Ternier for his help in image analysis using IMARIS and Sreekala Nampoothiri for English editing. This research was supported by the Fondation pour la Recherche Médicale (FRM, INE 2002), Agence Nationale de la Recherche (ANR, France) ANR-15-CE14–0025 (to V.P.), ANR-16-CE37-0006 (to V.P.), ANR-17-CE16-0015 (to V.P. and P.C.), the laboratory of excellence DISTALZ (ANR-11-LABX-0009 to VP) and I-SITE ULNE (ANR-16-IDEX-0004 ULNE to VP), the Association pour l'Etude des Anomalies Congénitales (AEAC) (to A.S.), and the National Institute of Health (USA) 1RO1 HD-084542

and 8P51OD011092 (to S.R.O).

AUTHOR CONTRIBUTIONS

A.S., A.-S. P. and V.P. designed the experiments. G.P., M.M., C.A., T.L., S.G., D.F., V.M., M. M.-L., A C.-R., V.D., D.M., A.L., M.T.S., P.C., A.S. and V.P. performed the experiments. A.S. and V.P. analyzed the data. J.S., G.C. and F.P. contributed material. All authors discussed the results and made edits to the manuscript. A.S., S.R., S.R.O. and V.P. wrote the manuscript.

COMPETING FINANCIAL INTERESTS

The authors declare no competing financial interests.

FIGURE LEGENDS

Figure 1. Postnatally-born astrocytes preferentially associate with GnRH neuronal cell bodies. (**a**) Experimental protocol. (**b**) Representative coronal section of the preoptic region immunolabeled for GnRH (green) and BrdU (magenta), nuclei counterstained with Hoechst (white), illustrating quantifications in **c**. Arrow, arrowheads: GnRH neuronal cell bodies. Inset: higher magnification of the GnRH neuron indicated, showing physical proximity to a $BrdU^+$ cell (yellow arrows). Scale bars: 100µm (main panel), 10 µm (inset). (**c**) Percentage of GnRH neurons associated with $BrdU^+$ cells 2h, 24h, 7d or 60d after a single BrdU injection at P1, P5, P8, P12, P20 or P24 (n=9,6,7,6,8,5,10,5,5,6,9,3,3,6,9,3,4,9,5 rats/group) (two-way ANOVA: age at BrdU injection, $F_{(5,73)}$=44.92, P<0.0001; survival time (2h, 7d), $F_{(1,73)}$=3.116, P=0.0817; interaction, $F_{(5,73)}$= 8.392, P< 0.0001; Tukey's multiple comparison test, P8+2h versus P8+7d: $q_{(73)}$ = 8.583, P<0.0001; P8, Kruskal-Wallis one-way ANOVA on ranks: $H_{(4)}$=20.98, P=0.0001; Dunn's multiple comparison: 2h versus 24h, P=0.0274; 2h versus 60d, P>0.9999). (**d**) Percentage of GnRH- or HuC/D-expressing neurons associated with $BrdU^+$ cells 2h or 7d after a single BrdU injection at P8 (% of GnRH neurons versus % of HuC/D^+

neurons associated with $BrdU^+$ cells: Mann-Whitney test, 2h: U=0, P=0.004; n=8,4 rats/group, respectively; 7d: U=0, P=0.002; n=10,4 rats/group).(**e**,**f**,**i-k**) Representative triple immunofluorescence labeling for GnRH (green), BrdU (magenta) and Sox2 (**e**, white), GFAP (**f,i,** white), APC (**j**, white) or HuC/D (**k**, white) in the female rat preoptic region injected with BrdU at P8 and sacrificed 2h (**e,f**) or 7d later (**i-k**), illustrating quantifications in **g**. Yellow arrows: $BrdU^+$ cells associated with GnRH neurons co-expressing the indicated markers. Scale bars: 20µm. (**g**) Percentage of $BrdU^+$ cells associated with GnRH neurons co-expressing Sox2, GFAP, APC or HuC/D in animals injected with BrdU at P8 and sacrificed 2h or 7d later (GFAP, Mann-Whitney test: U=0, P=0.0012, n=6,7 rats/group). (**h**) Co-immunolabeling for GnRH (green) and BrdU (magenta), nuclei counterstained with Hoechst (white), in female rats injected with BrdU thrice daily from P6 to P8 and sacrificed at P15, showing two GnRH neurons with companion $BrdU^+$ cells (yellow arrows). n=4 animals. Scale bar: 20µm. (**c**,**d**,**g**) Values: means ± s.e.m.; *P<0.05; **P<0.01; i.p., intraperitoneal; neo, neonatal period; OVLT, organum vasculosum laminae terminalis.

Figure 2. Inhibiting GnRH neuron association with newborn glia delays the onset of puberty and impairs mature estrous cyclicity. (**a**) Diagram of the experimental protocol, with a coronal view of the rat brain showing the anatomical localization of the microparticle implantation site (red line) in the preoptic region (dashed area). (**b, c**) Coronal sections from adult animals injected with blank- (b) or paclitaxel-loaded microparticles (c) at P6, immunolabeled for GnRH (green) and counterstained with the nuclear marker Hoechst (white). The region delimited by the dashed white line in **c** shows the hypocellular region around the injection site (asterisk). ac, anterior commissure. Scale bars: 200µm.(**d-g**) Cell nuclear density at the injection site (**d**: two-tailed unpaired t-test, $t_{(10)}$=4.366, P=0.0014, n=6 rats/group), number of $BrdU^+$ cells at the injection site (**e**: two-tailed unpaired t-test, $t_{(11)}$=4.2, P=0.0015; n=7,6 rats/group), percentage of GnRH neurons associated with $BrdU^+$ cells (**f**: two-tailed unpaired t-test with Welch's correction, $t_{(6.9)}$=4.24, P=0.0040; n=7 rats/group) and total number of GnRH neurons in the preoptic region (**g**: two-tailed unpaired t-test,

589 $t_{(15)}$=2.075, P=0.0556; n=7,10 rats/group) of control and paclitaxel-treated rats. (**h-i**)
590 Cumulative percentage (**h**) and age of vaginal opening (**i**: Mann-Whitney test: U=69.5,
591 P=0.0428, n=17,14 rats/group) in control and paclitaxel-treated rats. (**j-k**) Cumulative
592 percentage (**j**) and age of first estrus (**k**: Mann-Whitney test: U=32, P=0.0002, n=17,14
593 rats/group) in control and paclitaxel-treated rats. (**l**) Representative estrous cycle profiles of
594 control and paclitaxel-implanted animals showing the day of vaginal opening (vo) and first
595 estrus (red dot). The first paclitaxel-treated animal has a normal estrous cycle while the next
596 three are examples of altered estrous cyclicity. D, diestrus; E, estrus; P, proestrus. (**m**)
597 Difference between age at vaginal opening and at first estrus in control and paclitaxel-treated
598 animals (Mann-Whitney test: U=28.5, P<0.0001, n=17,14 rats/group). (**n**) Percentage of
599 complete estrous cycles in control and paclitaxel-treated animals (Mann-Whitney test:
600 U=80.5, P=0.0156, n=17,18 rats/group). (**d-g**,**i**,**k**,**m**-**n**) Values: means ± s.e.m.*P<0.05;
601 **P<0.01; ***P<0.001.
602
603 **Figure 3. Early exposure to bisphenol A inhibits infantile GnRH neuron-progenitor**
604 **association.** (**a**) Schematic of the protocol used to evaluate the effect of bisphenol A (BPA)
605 on the association between GnRH neurons and progenitors. (**b**) Percentage of GnRH
606 neurons associated with $BrdU^+$ cells in control and BPA-treated animals (one-way ANOVA:
607 $F_{(3,26)}$=16.6, P<0.0001, n=11,4, 8,7 rats/group; Tukey's multiple comparisons test: 2h control
608 versus 7d control, $q_{(26)}$=7.739, P<0.0001; 2h BPA versus 7d BPA, $q_{(26)}$=4.46, P=0.0198; 2h
609 control versus 2h BPA, $q_{(26)}$=1.412, P=0.7517). (**c**) Total number of $BrdU^+$ cells 2h and 7d
610 after a single injection of BrdU at P8 in animals treated with BPA from P1 to P15 (two-tailed
611 unpaired t-test, $t_{(11)}$=0.4553, P=0.6578; n=6,7 rats/group). (**b,c**) Values: means ±
612 s.e.m.*P<0.05; ***P<0.001.
613
614 **Figure 4. PGD2 is a chemoattractant for preoptic progenitor cells *in vitro*.** (**a**)
615 Immunofluorescence labeling for Sox2, nestin and BLBP in one primary progenitor culture
616 representative of three independent cultures. Cell nuclei were stained with Hoechst (blue).

Insets: higher magnification views of cells co-expressing the three markers (arrows). Scale bars: 50µm. (**b**) Quantification of transwell assays showing the effect of different factors on the migration of preoptic progenitor cells across a porous membrane. Epidermal growth factor (EGF) was used as a positive control[61] (Kruskal-Wallis one-way ANOVA on ranks: $H_{(6)}$=25.731, P<0.001; Dunn's multiple comparison method: control versus treatment: PGD2, $Q_{(6)}$=4.255, P<0.001; EGF, $Q_{(6)}$=3.925, P=0.0018; n=18,19,12,17,10,10,12 wells/condition; N=5 independent experiments). (**c**) Strategy used to identify astrocyte-regulated gene expression in GnRH neurons (See **Supplementary Data 1**). (**d**) Real-time PCR analysis of *Ptgds* mRNA levels in GnV3 cells treated with hypothalamic astrocyte-conditioned medium (ACM) or non-conditioned medium (control) (Mann-Whitney test: U=195, P<0.001; n=13,15 replicates/condition; N=3 independent experiments). ACM values are expressed relative to control values, arbitrarily set at 1. (**e**) Percentage of preoptic progenitor cells expressing the proliferation marker Ki67 after *in vitro* treatment with the same factors as in **b**. Fibroblast growth factor 2 (FGF2) was used as a positive control[62] (Kruskal-Wallis one-way ANOVA on ranks: $H_{(6)}$=38.576, P<0.001; Dunn's multiple comparison method: control versus FGF2, $Q_{(6)}$=4.798, P<0.001; n=23,22,16,17,15,16,16 wells/condition; N = 3 independent experiments). (**f**) Real-time PCR analysis of *Ptgdrl* and *Gpr44* mRNA levels in primary preoptic progenitor cell cultures (n=4 cultures). Values expressed relative to mRNA levels in the total brain, arbitrarily set at 1 (blue line). (**g**) Representative photomicrographs of the Hoechst-stained lower side of transwell assay membranes, illustrating quantifications in **h**. Scale bar: 100µm. (**h**) Quantification of transwell assays (Kruskal-Wallis one-way ANOVA on ranks: $H_{(5)}$=25.995, P<0.001; Dunn's multiple comparison method: control versus PGD2, $Q_{(5)}$=3.277, P=0.0157; PGD2 versus PGD2 + BWA 10nM, $Q_{(5)}$=3.321, P=0.0135; PGD2 versus PGD2 + BWA 1µM, $Q_{(5)}$=4.548, P<0.001; n=11,11,12,12,11,10 wells/condition; N=3 independent experiments). (**i**) ERK1/2 phosphorylation (pERK) in progenitors treated with PGD2 (1µM) and/or the DP1 receptor antagonist BWA868C (BWA). Representative immunoblot of three independent experiments. tERK, total ERK. (**b,d-f,h**) Values: means ± s.e.m.*P<0.05; **P <0.01; ***P<0.001.

Figure 5. *In vivo* expression of *Ptgds* and *PtgdrI* in the preoptic region of infantile female rats. (**a**) Procedure used to isolate GnRH neurons from the preoptic region (POA) of GnRH-EGFP transgenic rats. FACS, fluorescence-activated cell sorting; Pos, EGFP-positive fraction; Neg, EGFP-negative fraction. (**b,c**) Real-time PCR analysis of the expression of *Ptgds* mRNA in EGFP-positive- (b) or negative cells (c) at different postnatal ages (**b**: Kruskal-Wallis one-way ANOVA on ranks: $H_{(2)}$=7.476, P=0.024, n=10 rats/group; Dunn's multiple comparisons method: P8 versus P20, $Q_{(2)}$=3.844, P=0.0191; **c**: Kruskal-Wallis one-way ANOVA on ranks: $H_{(2)}$=5.280, P=0.071, n=10 rats/group). Values expressed relative to P8 values, arbitrarily set at 1. n.s., non-significant. (**d**) Representative confocal images of fluorescent *in situ* hybridization for *Gnrh*, *Sox2*, *Ptgds* and *PtgdrI* mRNAs in the preoptic region of P8 female rats, illustrating quantifications in **e-h**. (Upper row) Arrow: a GnRH neuron containing *Ptgds* mRNA (magenta dots) and surrounded by *Sox2*-expressing cells (arrowheads, white dots). (Lower row) Arrow: a GnRH neuron surrounded by *Sox2*-expressing cells (white arrowheads). Purple arrowheads: two *Sox2*-expressing cells next to the GnRH neuron, co-expressing *PtgdrI* mRNA (magenta dots). No such dots could be seen in any section of the negative controls (see methods). Sections were counterstained with the nuclear marker DAPI (blue). Scale bar: 5µm. (**e,f**) Percentage of GnRH neurons that contain *Ptgds* mRNA (**e**: one-way ANOVA: $F_{(2,16)}$=10.96, P=0.001, n=7,6,6 rats/group; Tukey's multiple comparison test: P8 versus P12, $q_{(16)}$=5.185, P=0.0056; P8 versus P20, $q_{(16)}$=6.046, P=0.0016) and of the average number of *Ptgds* dots per *Ptgds*-expressing GnRH neuron (**f**: Kruskal-Wallis one-way ANOVA on ranks: $H_{(3)}$=5.484, P=0.0585, n=7,6,6 rats/group) determined from fluorescent *in situ* hybridization experiments. (**g,h**) Percentage of *Sox2*-expressing cells that contain *PtgdrI* mRNAs (**g**: one-way ANOVA: $F_{(2,15)}$=1.528, P=0.2489, n=6 rats/group) and average number of *PtgdrI* dots per *Sox2/PtgdrI*-co-expressing cell (**h**: Kruskal-Wallis one-way ANOVA on ranks: $H_{(3)}$=3.029, P=0.2306, n=6 rats/group) determined from fluorescent *in situ* hybridization experiments. (**b-c**,**e**-**h**) Values: means ± s.e.m.*P<0.05; **P<0.01.

673

674 **Figure 6**. **Activation of DP1 signaling in the infantile preoptic region controls GnRH**
675 **neuron-progenitor association, and is involved in sexual maturation**. (**a**) Protocol used
676 to evaluate the involvement of DP1 signaling in the recruitment of progenitors by GnRH
677 neurons. Drawing: coronal view of the rat brain showing the anatomical localization of the
678 injection site, i.e. the preoptic region (dashed area). i.c., intracerebral; i.p., intraperitoneal. (**b**)
679 Percentage of GnRH neurons associated with $BrdU^+$ cells 24h after a single BrdU injection at
680 P7 in the absence (control) or presence of the DP1 antagonist BWA868C (BWA) (one-way
681 ANOVA: $F_{(2,11)}$=12.933, P=0.001, n=4,5,5 rats/group; Tukey's multiple comparison test: 2h
682 versus 24h groups: 24h-control, $q_{(11)}$=6.778, P=0.002; 24h-BWA, $q_{(11)}$=1.763, P=0.452; 24h-
683 control versus 24h-BWA, $q_{(11)}$=5.319, P=0.008).(**c**) Total number of $BrdU^+$ cells in the
684 preoptic region of control or BWA-treated animals (one-way ANOVA: $F_{(2,11)}$=20.887, P<0.001,
685 n=4,5,5 rats/group; Tukey's multiple comparison test: 2h versus 24h-control, $q_{(11)}$=8.019,
686 P<0.001; 2h versus 24h-BWA, $q_{(11)}$=8.102, P<0.001; 24h-control versus 24h-BWA,
687 $q_{(11)}$=0.0883, P=0.998). (**d**) Protocol used to evaluate the involvement of DP1 signaling in
688 sexual maturation. (**e**) Percentage of GnRH neurons associated with $BrdU^+$ cells 7d after a
689 single BrdU injection at P8 in the absence or presence of BWA868C (two-tailed unpaired t-
690 test, $t_{(6)}$=2.532, P=0.045; n=3,5 rats/group). (**f**) Total number of $BrdU^+$ cells in the preoptic
691 region of control or BWA-treated animals (two-tailed unpaired t-test, $t_{(6)}$=0.771, P=0.470;
692 n=3,5 rats/group). (**g**) Circulating FSH levels at P12 in BWA868C (BWA)-injected- and
693 control animals (two-tailed unpaired t-test, $t_{(20)}$=3.075, P=0.006; n=8,14 rats/group). Values:
694 means ± s.e.m.; *P<0.05; **P<0.01; ***P<0.001.

695

696 **Figure 7. Blocking DP1 signaling in the infantile period impairs GnRH neuron**
697 **maturation and functional activation.** (**a,c**) RT-PCR in control versus BWA868C-treated
698 FACS-sorted GnRH-EGFP neurons for (**a**) *Gnrh* and upstream regulators (Mann-Whitney
699 tests: *Gnrh*, U=27, P=0.7925; *Cebpb*, U=8, P=0.0426; *Kiss1r*, U=27, P>0.9999; two-tailed
700 unpaired t-tests: *Dicer*, $t_{(13)}$=0.6232, P=0.5439; *Otx2*, $t_{(11)}$=0.7906, P=0.4459; *Zeb1*,

$t_{(14)}$=0.2605, *P*=0.7983; *n*=6,10,6,8,6,9,6,9,5,8,6,10 rats/group) and (**c**) prostaglandin pathway genes (Mann-Whitney tests: *Ptgs-2*, *U*=18, *P*=0.3277; *Ptges*, *U*=19, *P*=0.3884; *Ptger1*, *U*=4, *P*=0.0140; *Ptger2*, *U*=16, *P*=0.2238; *Ptger3*, *U*=4, *P*=0.0048; two-tailed unpaired *t*-tests: *Pla2g4a*, $t_{(14)}$=0.1837, *P*=0.8569; *Ptgs-1*, $t_{(13)}$=0.1135, *P*=0.9113; *Ptgds*, $t_{(11)}$=2.671, *P*=0.0218; *Ptger4*, $t_{(14)}$=1.656, *P*=0.12; *n*=6,10,6,9,6,9,6,7,6,9,6,7,6,9,6,9,6,10 rats/group). Values expressed relative to control values, set at 1. (**b**) Prostaglandin biosynthesis. (**d**) Representative GnRH neuronal soma (red) with apposed vGluT2- (*left*, green) and vGaT- (*right*, green) immunoreactive (ir) punctae (arrowheads) in control (*top*) and BWA868C-treated animals (*bottom*). Scale bar: 10µm. *Bar graphs*: vGluT2- (two-tailed unpaired *t*-test, $t_{(12)}$=3.057, *P*=0.0099; *n*=7 rats/group) and vGaT-immunoreactive punctae (two-tailed unpaired *t*-test, $t_{(10)}$=1.61, *P*=0.1384; *n*=6 rats/group) per GnRH soma. (**e**) Representative fluorescent (*top*) and infrared-differential-interference-contrast (IR-DIC) (*bottom*) photomicrographs of acute brain slice from a *Gnrh::Egfp* infantile female rat, showing a patched preoptic GnRH neuron (green). Scale bar: 25µm. (**f**) *Left*: Whole-cell recording of spontaneous activity in representative GnRH neurons from control (*top*) and BWA868C-treated (*bottom*) animals. Arrowhead bottom left: resting membrane potential. *Right*: Expansion of action potentials (APs) indicated at left. Note: Control cell APs (*top*) were driven by temporal summation of small-amplitude depolarizing events (oblique lines in expansion), while APs from BWA868C-treated animals (*bottom*) were preceded by a smooth, relatively fast depolarization without synaptic events, except in recording #3. Threshold for AP generation: dashed line. (**g**-**j**) Electrophysiological cell properties: mean resting membrane potential (Vm) (**g**: Mann-Whitney test: *U*=602, *P*=0.760; *n*=37 cells, 21 control rats; *n*=34 cells, 14 BWA868C-treated rats), membrane resistance (Rm) (**h**: Mann-Whitney test: *U*=157, *P*=0.589; *n*=16 cells, 8 control rats; *n*=22 cells, 7 BWA868C-treated rats), voltage threshold for AP generation (VTH) (**i**: two-tailed unpaired *t*-test, $t_{(18)}$=0.963, *P*=0.348; *n*=10 cells, 8 control rats; *n* = 10 cells, 8 BWA868C-treated rats), spontaneous firing rate (**j**: Mann-Whitney test: *U*=285.5, *P*<0.0001; *n*=37 cells, 21 control rats; *n*=34 cells, 14 BWA868C-treated rats). Values: means ± s.e.m.; **P*<0.05; ***P*<0.01; ****P*<0.001.

Figure 8. Inhibition of DP1 signaling in the infantile period leads to perturbed estrous cyclicity. (**a**) Examples of estrous cycles in two control (*upper panels*) and two BWA-treated animals (*lower panels*). Red dots: first estrus. D, diestrus; E, estrus; P, proestrus; vo, vaginal opening. (**b**) Age at vaginal opening in BWA868C (BWA)-treated and control animals (two-tailed unpaired *t*-test, $t_{(17)}$=0.837, *P*=0.414; *n*=9,10 rats/group). (**c**) Quantification of time spent in the different phases of the estrous cycle during the first 15 days after vaginal opening in control and BWA-treated animals (Diestrus, two-tailed unpaired *t*-test, $t_{(17)}$=-1.160, *P*=0.262; Proestrus, Mann-Whitney test: *U*=12.5, *P*=0.006; Estrus, Mann-Whitney test: *U*=71.5, *P*=0.023; *n*=9,10 rats/group).(**b-c**) Values: means ± s.e.m.*$P<0.05$; **$P<0.01$.

REFERENCES

1. Moffitt, J.R.*, et al.* Molecular, spatial, and functional single-cell profiling of the hypothalamic preoptic region. *Science* **362** (2018).
2. Casoni, F.*, et al.* Development of the neurons controlling fertility in humans: new insights from 3D imaging and transparent fetal brains. *Development* **143**, 3969-3981 (2016).
3. Chachlaki, K., Garthwaite, J. & Prevot, V. The gentle art of saying NO: how nitric oxide gets things done in the hypothalamus. *Nat Rev Endocrinol* **13**, 521-535 (2017).
4. Messina, A.*, et al.* A microRNA switch regulates the rise in hypothalamic GnRH production before puberty. *Nat Neurosci* **19**, 835-844 (2016).
5. Prevot, V. Puberty in mice and rats. in *Knobil and Neill's Physiology of Reproduction* (ed. T.M. Plant & J. Zeleznik) pp 1395-1439 (Elsevier, New York, 2015).
6. Clasadonte, J. & Prevot, V. The special relationship: glia-neuron interactions in the neuroendocrine hypothalamus. *Nat Rev Endocrinol* **14**, 25-44 (2018).
7. Sloan, S.A. & Barres, B.A. Mechanisms of astrocyte development and their contributions to neurodevelopmental disorders. *Curr Opin Neurobiol* **27**, 75-81 (2014).
8. Verkhratsky, A. & Nedergaard, M. Physiology of Astroglia. *Physiol Rev* **98**, 239-389 (2018).
9. Barnabe-Heider, F.*, et al.* Evidence that embryonic neurons regulate the onset of cortical gliogenesis via cardiotrophin-1. *Neuron* **48**, 253-265 (2005).
10. Bandeira, F., Lent, R. & Herculano-Houzel, S. Changing numbers of neuronal and non-neuronal cells underlie postnatal brain growth in the rat. *Proc Natl Acad Sci U S A* **106**, 14108-14113 (2009).
11. Elkharraz, K.*, et al.* Paclitaxel-loaded microparticles and implants for the treatment of brain cancer: preparation and physicochemical characterization. *Int J Pharm* **314**, 127-136 (2006).
12. Wang, L.*, et al.* Genetic dissection of the different roles of hypothalamic kisspeptin neurons in regulating female reproduction. *Elife* **8** (2019).
13. Mohr, M.A., DonCarlos, L.L. & Sisk, C.L. Inhibiting Production of New Brain Cells during Puberty or Adulthood Blunts the Hormonally Induced Surge of Luteinizing Hormone in Female Rats. *eNeuro* **4** (2017).
14. Lopez-Rodriguez, D., Franssen, D., Bakker, J., Lomniczi, A. & Parent, A.S. Cellular and molecular features of EDC exposure: consequences for the GnRH network. *Nat Rev Endocrinol* **17**, 83-96 (2021).
15. Geens, T.*, et al.* A review of dietary and non-dietary exposure to bisphenol-A. *Food Chem Toxicol* **50**, 3725-3740 (2012).
16. Franssen, D.*, et al.* Delayed Neuroendocrine Sexual Maturation in Female Rats After a Very Low Dose of Bisphenol A Through Altered GABAergic Neurotransmission and Opposing Effects of a High Dose. *Endocrinology* **157**, 1740-1750 (2016).
17. Kuiri-Hanninen, T., Sankilampi, U. & Dunkel, L. Activation of the hypothalamic-pituitary-gonadal axis in infancy: minipuberty. *Horm Res Paediatr* **82**, 73-80 (2014).
18. Ciofi, P. Phenotypical segregation among female rat hypothalamic gonadotropin-releasing hormone neurons as revealed by the sexually dimorphic coexpression of cholecystokinin and neurotensin. *Neuroscience* **99**, 133-147 (2000).
19. Chachlaki, K.*, et al.* Phenotyping of nNOS neurons in the postnatal and adult female mouse hypothalamus. *J Comp Neurol* **525**, 3177-3189 (2017).
20. Mansuy, V.*, et al.* Phenotypic and molecular characterization of proliferating and differentiated GnRH-expressing GnV-3 cells. *Mol Cell Endocrinol* **332**, 97-105 (2011).
21. Hirai, H.*, et al.* Prostaglandin D2 selectively induces chemotaxis in T helper type 2 cells, eosinophils, and basophils via seven-transmembrane receptor CRTH2. *J Exp Med* **193**, 255-261 (2001).
22. Ohinata, K.*, et al.* Central prostaglandin D(2) stimulates food intake via the neuropeptide Y system in mice. *FEBS Lett* **582**, 679-684 (2008).
23. Tokudome, S.*, et al.* Glucocorticoid protects rodent hearts from ischemia/reperfusion injury by activating lipocalin-type prostaglandin D synthase-derived PGD2 biosynthesis. *J Clin Invest* **119**, 1477-1488 (2009).

24. Kato, M., Ui-Tei, K., Watanabe, M. & Sakuma, Y. Characterization of voltage-gated calcium currents in gonadotropin-releasing hormone neurons tagged with green fluorescent protein in rats. *Endocrinology* **144**, 5118-5125 (2003).
25. Ma, Y.J., Junier, M.P., Costa, M.E. & Ojeda, S.R. Transforming growth factor-alpha gene expression in the hypothalamus is developmentally regulated and linked to sexual maturation. *Neuron* **9**, 657-670 (1992).
26. Rage, F., Lee, B.J., Ma, Y.J. & Ojeda, S.R. Estradiol enhances prostaglandin E2 receptor gene expression in luteinizing hormone-releasing hormone (LHRH) neurons and facilitates the LHRH response to PGE2 by activating a glia-to-neuron signaling pathway. *J.Neurosci.* **17**, 9145-9156 (1997).
27. Lomniczi, A., Wright, H. & Ojeda, S.R. Epigenetic regulation of female puberty. *Front Neuroendocrinol* **36**, 90-107 (2015).
28. Boehm, U., Zou, Z. & Buck, L.B. Feedback loops link odor and pheromone signaling with reproduction. *Cell* **123**, 683-695 (2005).
29. Yoon, H., Enquist, L.W. & Dulac, C. Olfactory inputs to hypothalamic neurons controlling reproduction and fertility. *Cell* **123**, 669-682 (2005).
30. Clasadonte, J., Scemes, E., Wang, Z., Boison, D. & Haydon, P.G. Connexin 43-Mediated Astroglial Metabolic Networks Contribute to the Regulation of the Sleep-Wake Cycle. *Neuron* **95**, 1365-1380 e1365 (2017).
31. Araque, A.*, et al.* Gliotransmitters travel in time and space. *Neuron* **81**, 728-739 (2014).
32. Clasadonte, J.*, et al.* Prostaglandin E2 release from astrocytes triggers gonadotropin-releasing hormone (GnRH) neuron firing via EP2 receptor activation. *Proc Natl Acad Sci U S A* **108**, 16104-16109 (2011).
33. Glanowska, K.M. & Moenter, S.M. Endocannabinoids and prostaglandins both contribute to GnRH neuron-GABAergic afferent local feedback circuits. *J Neurophysiol* **106**, 3073-3081 (2011).
34. Bezzi, P.*, et al.* Prostaglandins stimulate calcium-dependent glutamate release in astrocytes. *Nature* **391**, 281-285 (1998).
35. Zonta, M.*, et al.* Neuron-to-astrocyte signaling is central to the dynamic control of brain microcirculation. *Nat.Neurosci.* **6**, 43-50 (2003).
36. Dziedzic, B.*, et al.* Neuron-to-glia signaling mediated by excitatory amino acid receptors regulates ErbB receptor function in astroglial cells of the neuroendocrine brain. *J.Neurosci.* **23**, 915-926 (2003).
37. Prevot, V.*, et al.* Normal female sexual development requires neuregulin-erbB receptor signaling in hypothalamic astrocytes. *J.Neurosci.* **23**, 230-239 (2003).
38. Nagai, J.*, et al.* Behaviorally consequential astrocytic regulation of neural circuits. *Neuron* **109**, 576-596 (2021).
39. Bouret, S.G., Draper, S.J. & Simerly, R.B. Trophic action of leptin on hypothalamic neurons that regulate feeding. *Science* **304**, 108-110 (2004).
40. Caron, E., Ciofi, P., Prevot, V. & Bouret, S.G. Alteration in neonatal nutrition causes perturbations in hypothalamic neural circuits controlling reproductive function. *J Neurosci* **32**, 11486-11494 (2012).
41. Paul, A., Chaker, Z. & Doetsch, F. Hypothalamic regulation of regionally distinct adult neural stem cells and neurogenesis. *Science* **356**, 1383-1386 (2017).
42. Sandau, U.S.*, et al.* SynCAM1, a synaptic adhesion molecule, is expressed in astrocytes and contributes to erbB4 receptor-mediated control of female sexual development. *Endocrinology* **152**, 2364-2376 (2011).
43. Sandau, U.S.*, et al.* The synaptic cell adhesion molecule, SynCAM1, mediates astrocyte-to-astrocyte and astrocyte-to-GnRH neuron adhesiveness in the mouse hypothalamus. *Endocrinology* **152**, 2353-2363 (2011).
44. Allen, N.J. & Eroglu, C. Cell Biology of Astrocyte-Synapse Interactions. *Neuron* **96**, 697-708 (2017).
45. Verkhratsky, A., Matteoli, M., Parpura, V., Mothet, J.P. & Zorec, R. Astrocytes as secretory cells of the central nervous system: idiosyncrasies of vesicular secretion. *EMBO J* **35**, 239-257 (2016).
46. Kofuji, P. & Araque, A. G-Protein-Coupled Receptors in Astrocyte-Neuron Communication. *Neuroscience* **456**, 71-84 (2021).

47. Ullian, E.M., Sapperstein, S.K., Christopherson, K.S. & Barres, B.A. Control of synapse number by glia. *Science* **291**, 657-661 (2001).
48. Pfrieger, F.W. & Barres, B.A. Synaptic efficacy enhanced by glial cells in vitro. *Science* **277**, 1684-1687 (1997).
49. Papouin, T., Dunphy, J.M., Tolman, M., Dineley, K.T. & Haydon, P.G. Septal Cholinergic Neuromodulation Tunes the Astrocyte-Dependent Gating of Hippocampal NMDA Receptors to Wakefulness. *Neuron* **94**, 840-854 e847 (2017).
50. Mu, Y.*, et al.* Glia Accumulate Evidence that Actions Are Futile and Suppress Unsuccessful Behavior. *Cell* **178**, 27-43 e19 (2019).
51. Bourguignon, J.P., Gerard, A., Alvarex-Gonzalez, M.L., Fawe, L. & Franchimont, P. Gonadal-independent developmental changes in activation of N-methyl-D-aspartate receptors involved in gonadotropin-releasing hormone secretion. *Neuroendocrinology* **55**, 634-641 (1992).
52. Carbone, S., Szwarcfarb, B., Otero Losada, M.E. & Moguilevsky, J.A. Effects of ovarian steroids on the gonadotropin response to N-methyl-D-aspartate and on hypothalamic excitatory amino acid levels during sexual maturation in female rats. *Endocrinology* **130**, 1365-1370 (1992).
53. DeFazio, R.A., Heger, S., Ojeda, S.R. & Moenter, S.M. Activation of A-type gamma-aminobutyric acid receptors excites gonadotropin-releasing hormone neurons. *Mol Endocrinol* **16**, 2872-2891 (2002).
54. Berg, T., Silveira, M.A. & Moenter, S.M. Prepubertal Development of GABAergic Transmission to Gonadotropin-Releasing Hormone (GnRH) Neurons and Postsynaptic Response Are Altered by Prenatal Androgenization. *J Neurosci* **38**, 2283-2293 (2018).
55. Sardi, S.P., Murtie, J., Koirala, S., Patten, B.A. & Corfas, G. Presenilin-dependent ErbB4 nuclear signaling regulates the timing of astrogenesis in the developing brain. *Cell* **127**, 185-197 (2006).
56. Veiga-Lopez, A., Beckett, E.M., Abi Salloum, B., Ye, W. & Padmanabhan, V. Developmental programming: prenatal BPA treatment disrupts timing of LH surge and ovarian follicular wave dynamics in adult sheep. *Toxicol Appl Pharmacol* **279**, 119-128 (2014).
57. Rasier, G.*, et al.* Mechanisms of interaction of endocrine-disrupting chemicals with glutamate-evoked secretion of gonadotropin-releasing hormone. *Toxicol Sci* **102**, 33-41 (2008).
58. Muncke, J.*, et al.* Impacts of food contact chemicals on human health: a consensus statement. *Environ Health* **19**, 25 (2020).
59. O'Brien, E., Dolinoy, D.C. & Mancuso, P. Perinatal bisphenol A exposures increase production of pro-inflammatory mediators in bone marrow-derived mast cells of adult mice. *J Immunotoxicol* **11**, 205-212 (2014).
60. Lamartiniere, C.A., Jenkins, S., Betancourt, A.M., Wang, J. & Russo, J. Exposure to the Endocrine Disruptor Bisphenol A Alters Susceptibility for Mammary Cancer. *Horm Mol Biol Clin Investig* **5**, 45-52 (2011).
61. Burrows, R.C., Wancio, D., Levitt, P. & Lillien, L. Response diversity and the timing of progenitor cell maturation are regulated by developmental changes in EGFR expression in the cortex. *Neuron* **19**, 251-267 (1997).
62. Gensburger, C., Labourdette, G. & Sensenbrenner, M. Brain basic fibroblast growth factor stimulates the proliferation of rat neuronal precursor cells in vitro. *FEBS Lett* **217**, 1-5 (1987).

METHODS

Animals. Sprague-Dawley rats were obtained from Janvier Laboratories (Saint Berthevin, France). GnRH-EGFP transgenic rats, which express the enhanced green fluorescent protein (EGFP) under the control of the rat GnRH promoter (NBRP Rat No: 0469, The

National BioResource Project for the Rat, Japan) [24, 63] was a kind gift from Dr. Masakatsu Kato (University of Tokyo Health Sciences, Tokyo, Japan). Wild-type and transgenic mice expressing a dominant-negative form of the ErbB4 receptor in astrocytes (*GFAP*::*DN-ErbB4*) were generated as described previously [37]. The animals were maintained at 23-25°C on a 12-h light-dark cycle, with food and water available *ad libitum*. Animal studies were approved by the Institutional Ethics Committee for the Care and Use of Experimental Animals of the University of Lille (APAFIS#2617-2015110517317420 v5). The bisphenol A treatment experiment was performed on Wistar rats purchased from the University of Liège and carried out with the approval of the Belgian Ministry of Agriculture and the Ethical Committee at the University of Liège. Animals were raised in polypropylene cages (Ref 1291H006, Tecnilab, 323 Netherlands), fed with low phytoestrogen chow (V135 R/Z low phytoestrogen pellets, SSNIFF 324 Diet, Netherlands). Water was supplied in glass bottles to reduce EDC contamination. All experiments were performed in accordance with the guidelines for animal use specified by the European Union Council Directive of September 22, 2010 (2010/63/EU). All experiments were performed in female animals, except the preparation of primary cultures of preoptic progenitors, for which both sexes were used.

BrdU injections. Unless otherwise stated, animals received a single intraperitoneal (i.p.) injection of BrdU (Sigma) at a dose of 300 mg/kg body weight at different postnatal ages and were allowed to survive for 2h, 24h, 7 days or ≥ 60 days. A group of rats received 3 i.p. injections of BrdU (150 mg/kg) per day for 3 consecutive days (P6-P8) and were sacrificed at P15.

Stereotactic brain injection of paclitaxel-loaded microparticles. The preparation, physicochemical characterization and drug release kinetics of paclitaxel-loaded, poly(D,L-lactic-*co*-glycolic acid) (PLGA)-based microparticles have been described [11]. Briefly, Paclitaxel (Zyo Pharma Trade, Hamburg, Germany) was encapsulated into PLGA-based

931 microparticles at a drug loading of 40% (w/w) (Carlina Technologies, Angers, France). Drug-
932 free microparticles were prepared accordingly without adding paclitaxel. Female rats at P6 or
933 P7 (*n* = 35) were anesthetized with an i.p. dose of a mixture of ketamine hydrochloride
934 (50 mg/ml; 60 mg/kg) and xylazine hydrochloride (2%; 10 mg/kg), secured in a stereotaxic
935 apparatus, and injected medially with 1 µl of a suspension of 50 µg paclitaxel-loaded or drug-
936 free microparticles in sterile water using a microsyringe with a 21 gauge needle (Hamilton,
937 Reno, NV) into the preoptic region of the hypothalamus, dorsal to the MePO (bregma:
938 0.0 mm, 6 mm deep from the skull) [64]. All animals received an i.p. injection of BrdU at P8 and
939 were sacrificed at adult age. Brains were processed for immunofluorescent labeling of BrdU,
940 GnRH and GFAP, and cell nuclei counter-staining using the nuclear marker Hoechst or DAPI
941 to determine the implantation site of microparticles. Animals with an implantation site located
942 outside the preoptic region were excluded from the analysis.
943
944 **Bisphenol-A treatment**. Exposure to bisphenol A (BPA) was performed as described
945 previously [16]. Briefly, female pups were subcutaneously injected (0.05 mL) with either vehicle
946 (corn oil) or BPA (Ref 23,9658; Sigma-Aldrich) at a dose of 25 ng/kg.d. Injections were given
947 every 24 hours from P1 to P15. All animals received an i.p. injection of BrdU at P8 and were
948 sacrificed 2 hours or 7 days later. Brains were extracted and processed for
949 immunofluorescent staining of BrdU and GnRH.
950
951 **Stereotaxic brain infusions of BWA868C.**
952 *Acute injections.* Female rats received an i.p. injection of BrdU at P7. A group of animals (*n* =
953 4) was sacrificed 2h after the injection. The other animals were placed in a stereotaxic frame
954 (Kopf® Instruments, California) under anesthesia (isoflurane), and 2 burr holes were drilled
955 0.5 mm apart from the bregma, according to a rat brain atlas [64]. A 10 µl Hamilton syringe was
956 slowly inserted into the preoptic region (5.2 mm deep relative to the dura), and 1 µl of a
957 solution containing 10 nM BWA868C (Cayman Chemical, Ann Arbor, Michigan, USA) (*n* = 5)
958 or vehicle (saline solution 0.9%, *n* = 5) was injected bilaterally using an infusion pump (KD

Scientific, Holliston, MA) over 5 min. Animals were killed 24h later and their brains processed for immunofluorescent labeling of BrdU and GnRH.

BWA868C implants. Female rats were placed in a stereotaxic frame under anesthesia, and one burr hole was drilled at the level of the bregma as detailed above. A stainless steel 5 mm cannula filled at its tip with BWA868C (10 nM) or vehicle mixed with melted cocoa butter was stereotaxically implanted in the preoptic region at the level of the bregma, as previously described [65]. After implantation, the cannulas were fixed to the skull with superglue, and the skin wound sutured. Blood was collected via submandibular bleeding from animals at P12 for plasma FSH measurements using a procedure described previously by others [66].

Physiological measurements.

Puberty onset and estrous cyclicity. Animals were monitored daily for imperforation of the vaginal membrane (i.e. vaginal opening). After vaginal opening, vaginal smears were performed daily and analyzed under an inverted microscope to identify the specific day of the estrous cycle. The percentage of complete estrus cycles was calculated as the number of occurrences of the sequence “Diestrus-Diestrus-Proestrus-Estrus”, defined as a complete estrus cycle, divided by the theoretical maximum possible number of complete estrus cycles over the recorded period of time for each animal (> 2 weeks).

Follicle-stimulating hormone level measurements. Serum FSH levels were measured using radioimmunoassay as previously described [4]. The accuracy of hormone measurements was confirmed by the assessment of rodent serum samples of known concentration (external controls).

Electrophysiology.

Brain slices preparation. Electrophysiological recordings were performed on living brain slices containing the preoptic region from 10- to 15-days-old GnRH-EGFP transgenic rats. Rats were anesthetized with isoflurane and decapitated. The brain was removed and rapidly placed in ice-cold artificial cerebrospinal fluid (aCSF) containing (in mM): 120 NaCl, 3.2 KCl,

1 NaH_2PO_4, 26 $NaHCO_3$, 1 $MgCl_2$, 2 $CaCl_2$, 10 glucose (300 mOsm, pH 7.4) and bubbled with 95% O_2-5% CO_2. 200-μm coronal slices were cut using a vibratome (VT1200; Leica). Slices were incubated at 34°C in oxygenated aCSF for a recovery period of 1 hour, and then at room temperature until recording.

Patch-clamp recording. For patch-clamp recording, individual brain slices were placed in a submerged recording chamber (Warner Instruments), immobilized by a nylon grid and continuously perfused at 3 ml/min with oxygenated aCSF maintained at 32.8°C by a heater controller (TC-344C; Warner Instruments). GnRH neurons were visualized and identified under 10x and 40x magnification using an upright fluorescent microscope with infrared differential interference contrast (Leica DM-LFSA) and an ORCA-Flash 4.0 digital CMOS camera (Hamamatsu). Recording pipettes were pulled from borosilicate glass capillaries (1.5 mm outer diameter; 1.12 mm inner diameter; World Precision Instruments) using P1000 Flaming Brown puller (Sutter Instruments Co) and had resistance from 7 to 9 MΩ when filled with an internal solution containing (in mM): 140 K-gluconate, 10 KCl, 1 EGTA, 2 Na_2-ATP and 10 HEPES, pH 7.3 with KOH. Pipettes were placed in contact with GnRH neurons using a PCS-5400 micromanipulator (Thorlabs). Whole-cell patch-clamp recordings were performed in current-clamp mode using a Multiclamp 700B Amplifier, digitized with the Digidata 1322A interface and acquired with pClamp 10.2 software (Molecular Devices). Data were filtered at 1 kHz and sampled at 5 kHz. Recordings were analyzed with Clampfit 10.2 from pClamp software (Molecular Devices). Resting membrane potential, spontaneous firing rate, membrane resistance, voltage threshold for action potential generation, full amplitude and half width duration of action potentials, after-hyperpolarizing potential amplitude and duration, and time constant were determined as previously described [32, 67]. Only cells which showed less than 20% change in access resistance throughout the recording were included in this study. Junction potential was corrected in the data analysis.

Biocytin labeling of preoptic astrocytes. Slices were incubated during 30 minutes in 100 nM sulforhodamine 101 (SR101, Sigma), a fluorescent dye that is selectively taken up by astrocytes, and were pretreated for 20 minutes with 50 μM carbenoxolone (Sigma) to inhibit

gap junctions. Biocytin (2 mg/ml, Sigma) was added to the internal solution and astrocytes were patched in whole-cell configuration for 20 minutes. Electrical membrane properties of astrocytes were measured in voltage-clamp mode by applying a series of voltage pulses from -100 mV to +100 mV (300 ms, 10 mV increments) from a holding potential of -80 mV as previously described[30]. Astrocytes showed typical glial cell membrane properties including a highly polarized membrane potential and a linear current-voltage (I-V) relationship[30]. Slices were fixed with 4% paraformaldehyde overnight at 4°C, incubated with Streptavidin Alexa Fluor 647 (1:250, Invitrogen) in PBS containing 0.5% Triton X-100 overnight at 4°C, counterstained with DAPI (1:1000) and mounted on glass slides with Mowiol.

Preoptic neurosphere cultures. The preoptic region of female rats aged 10 or 19 days was dissected and minced on 80 µm nylon mesh (Buisine, Clermont de l'Oise, France). The dissected region corresponded to a 1-mm-thick triangular tissue located behind the diagonal band of Broca just before the OVLT, i.e., the beginning of the third ventricle, and the optic chiasm. We checked that our dissection excluded the subventricular zone of the lateral ventricle. The cell suspension was transferred to a culture flask (BD Biosciences, San Jose, CA) and cultured in neurosphere medium composed of Dulbecco's Modified Eagle's Medium (DMEM)/F-12 with L-glutamine, 15 mM HEPES (#31330-038) supplemented with 2% (v/v) B-27 (#17504-044), 20 ng/ml EGF (human recombinant; #PHG0311), 20 ng/ml FGF2 (human recombinant; #13256-029), 2 mM L-glutamine (25030-024), and 100 units of penicillin and 100 µg of streptomycin/ml (#15140-122) (all from Gibco, Carlsbad, CA) under a humid atmosphere of 5% CO2-95% air at 37°C. Cells were grown in hypoxic conditions by covering flask caps with parafilm. Neurospheres were formed after ~1 week. Thereafter, the neurospheres were collected twice a week through centrifugation, dissociated by mechanical trituration and passaged in half-renewed neurosphere medium to form further generations of neurospheres. Neurospheres were kept for up to 31 passages, the longest time examined.

Clonogenicity. To evaluate the generation of secondary neurospheres from single cells, primary neurospheres were dissociated into single cells by either mechanical dissociation

through 20 µm nylon mesh (Buisine) or enzymatic digestion using StemProAccutase Cell Dissociation Reagent (Gibco) for 10 min at room temperature. Cells were plated in 96-well culture plates at a density of 50, 75 or 100 cells per well in 50 µl of neurosphere medium. Wells containing cell aggregates 24h after plating were excluded from the analysis. Cultures were fed with 100 % (v/v) fresh neurosphere medium every 3 days until day 10, when wells were examined for the presence of neurospheres.

Differentiation experiments. To evaluate their differentiation potential, neurospheres were transferred to 24-well plates on poly-L-lysine (0.01%; #P4832, Sigma)-coated glass coverslips and grown in DMEM/F12 with L-glutamine, 15 mM HEPES (#31330-038) supplemented with 10% (v/v) fetal bovine serum (#10270106), 2 mM L-glutamine, and 100 units of penicillin and 100 µg of streptomycin/ml (all from Gibco) for 7 days.

Adherent cultures of preoptic progenitors. The preoptic region of rats aged 1 or 2 days was dissected as described above and minced on 20 µm nylon mesh (Buisine). The cell suspension was transferred to a culture flask (BD Biosciences) coated with poly-D-lysine (10 µg/ml, P7405, Sigma) and laminin (10 µg/ml, L6274, Sigma) and cultured in neurosphere medium under a humid atmosphere of 5% CO_2-95% air at 37°C. The medium was changed every 3 to 4 days. Cells were passaged once, when 70-80% confluence was reached, and were then used for migration assays, snap frozen in dry ice for gene expression analysis or seeded on 24-well plates glass coverslips for proliferation assays or immunocytochemical characterization.

GnV3 cell culture and treatment. Cells were grown in Neurobasal-A medium (10888-022) supplemented with 2% (v/v) B-27, 100 units of penicillin and 100 µg of streptomycin/ml, 25 mM GlutaMAX (35050-038), 1% fetal bovine serum, 50 µg/ml FGF2 (all from Gibco) and 1 µg/µl doxycycline (D-9891, Sigma) as described [68]. All experiments were performed on GnV3 cells at their 13th or 14th passage.

Preparation of hypothalamic astrocyte-conditioned medium. Primary astrocyte cultures were prepared from the hypothalamus of 1-2-day-old rat pups and grown in DMEM/F12 medium (#31330-038) supplemented with 10% (v/v) fetal bovine serum, 2 mM L-glutamine, and 100 units of penicillin and 100 µg of streptomycin/ml (all from Gibco) as previously described [36]. After reaching confluence (i.e., after ~7-10 days), contaminants were removed by overnight shaking. The growth medium was replaced by astrocyte-defined medium (ADM) composed of DMEM (41965-039) supplemented with 2 mM L-glutamine, 5 µg/ml insulin (I-5500, Sigma) and 100 µM putrescine (P-5780, Sigma). After two days, the culture medium (now ACM, astrocyte-conditioned medium) was collected, centrifuged at 1,000 rpm and the supernatant was kept at -80°C until use.

Treatment of GnV3 cells with hypothalamic astrocyte-conditioned medium. One day before treatment, GnV3 cells were plated at a density of $2x10^5$ cells/cm^2 in their growth medium. Cells were treated with ADM (control condition) or ACM for a total of 4 days, with a culture medium renewal after every 2 days. At the end of the 4-day treatment, GnV3 cells were collected in Trizol (Invitrogen) for microarray analysis or lysis buffer (Qiagen) for RT-qPCR analysis, and stored at -80°C until use. Treatment of GnV3 cells was performed in three experiments using ACM from three different primary astrocyte cultures.

***In vitro* migration assay.** Boyden microchemotaxis chambers were used according to the manufacturer's instructions (Neuro Probe, Gaithersburg MD, USA). In brief, primary preoptic progenitors were harvested, re-suspended in control medium (Neurobasal-A medium supplemented with 2% (v/v) B-27, 2 mM L-glutamine, and 100 units of penicillin and 100 µg of streptomycin/ml (all from Gibco)) and plated in 24-well plate chambers at a density of 150,000 cells per well on the open-bottom wells of the upper compartment, previously coated with poly-D-lysine and laminin. The two compartments of each well were separated by a polyvinylpyrrolidone-free polycarbonate porous membrane (8 µm pore size). The lower chamber was filled with control medium containing GnRH (100 ng/ml, GeneCust, Ellange, Luxembourg), PGD2 (1 µM, Sigma), galanin (2 µM, Tocris Bioscience, Bristol, UK),

glutamate (10 µM, Sigma), GABA (2 µM, Sigma) or EGF (100 ng/ml, Gibco). BWA868C (10 nM or 1 µM) was added to the cell suspension in the upper compartment. After 18h of incubation in 5% CO_2, 95% air at 37°C, cells attached to the upper side of the filter were mechanically removed with a cotton swab. Cells that had migrated to the lower side were fixed with 4% paraformaldehyde (30 minutes at room temperature) and stained with Hoechst (1:10,000). Cells were photographed with a 20x objective and counted using ImageJ 1.52p software (NIH, Bethesda).

***In vitro* proliferation assay.** Primary preoptic progenitors were transferred to 24-well plates on poly-D-lysine/laminin-coated glass coverslips and grown in neurosphere medium. Once cells were 70-80% confluent, they were transferred to neurosphere medium devoid of FGF2 (starvation medium) for 24h prior to treatment with GnRH, PGD2, galanin, glutamate, GABA (same concentrations as in migration assays) or FGF2 (100 ng/ml) in starvation medium for 24h. Coverslips were fixed and processed for Ki67 immunolabeling.

Immunofluorescence labeling

Tissue preparation. Animals were anesthetized by i.p. injection of pentobarbital (70 mg/kg). They were perfused transcardially with a rinse of saline solution (0.9% NaCl), followed by 100 ml of 4% paraformaldehyde in 0.1 M phosphate buffer(PB) (pH 7.4). The brains were removed and immersed in the same fixative for 2-3h at 4°C. They were then transferred to PB containing 20% sucrose until they had sunk, embedded in Tissue Tek® (Sakura Finetek, Villeneuve d'Ascq, France), and frozen in liquid nitrogen. Frozen 14-µm coronal sections containing the preoptic region (0.20 mm to -0.30 mm relative to bregma) [64] were prepared using a cryostat (CM3050S, Leica, Nussloch, Germany) and mounted on chrome-alum-gelatin coated slides, air-dried and subjected to immunolabeling.

Immunohistofluorescence. The sections were subjected to microwave pretreatment in a solution of sodium citrate 0.01 M (pH 6) for 4 minutes at 800 W followed by 2 cycles 5 minutes each at 400 W for antigen retrieval. After cooling at room temperature and washing

in PB, sections were incubated with primary antibodies (**Supplementary Table 1**) diluted in PB containing 0.9% sodium chloride, 0.3% Triton X-100 and 2% normal donkey serum (PBSTS) overnight at 4°C. Sections were then incubated with appropriate secondary antibodies at room temperature for 1h (**Supplementary Table 2**). After nuclei staining with Hoechst or DAPI (1/1,000), sections were coverslipped in Mowiol mounting medium (20% Mowiol, 2.5% DABCO in Tris 0.2 M pH 8.5). Control sections were incubated in the absence of primary antibody. Omission of the primary antibody resulted in no staining.

Immunocytofluorescence. Coverslips were fixed in 4% paraformaldehyde (15 min at room temperature), incubated with PBS 0.1 M containing 0.1% Triton X-100 and 0.3% normal donkey serum for 30 minutes at room temperature, and subjected to immunofluorescent labeling following the same procedure as for tissue sections. For O4 immunodetection, the anti-O4 antibody (**Supplementary Table 1**) was applied to living cells for 2h at 37°C before fixation.

Fluorescent *in situ* hybridization. FISH was performed on frozen brain sections of the preoptic region of female rats at P8, P12 and P20 with the RNAscope® Multiplex Fluorescent Kit v2 according to the manufacturer's protocol (Advanced Cell Diagnostics, Inc., Newark, CA, USA). Specific probes were used to detect *Ptgds* (486051, NM_013015.2, target region 2 - 702), *Ptgdrl* (486041, NM_022241.1, target region 224 - 1157), *Gnrh1* (502431-C2, NM_012767.2, target region 2 - 454) and *Sox2* (502441-C3, NM_001109181.1, target region 51 - 2079) mRNAs. Hybridization with a probe against the Bacillus subtilis dihydrodipicolinate reductase (dapB) gene (320871) was used as negative control.

Microscopy

Analysis of sections and acquisition of images were done using an Axio Imager Z2 Apo-Tome microscope equipped with a motorized stage (Zeiss, Germany) and an ORCA-Flash 4.0 V2 camera (Hamamatsu, Japan) driven by the Zen 2.3 (blue edition) imaging software (Zeiss). For FISH experiments and immunofluorescence labeling for vGluT2 and vGaT,

acquisition of images was performed using an inverted confocal microscope (LSM 710, Zeiss, Jena, Germany). High magnification photomicrographs were acquired with a 63x objective (NA 1.4) using the Airyscan detector (Zeiss). Images to be used for figures were pseudocolored, adjusted for brightness and contrast and merged using Adobe Photoshop 22.1.0 (Adobe Systems, San Jose, CA).

Microscopic analyses. All analyses were done in the preoptic region, as defined in the Swanson stereotaxic rat brain atlas, between plate 17 (i.e., beginning of the OVLT) and plate 20 (i.e., crossing of the anterior commissure) [69], with a particular attention to the MePO, where most GnRH neurons that stimulate the LH surge are located [70]. Analyses were made on one out of every 5 sections. Estimation of total cell populations in the preoptic region was obtained by multiplying the number of cells per section by the total number of sections per preoptic region, and then correcting for split nuclei [71].

Morphological association between GnRH neurons and BrdU$^+$ cells. Quantification was made under the fluorescent microscope at the 40x objective. A BrdU$^+$ cell was considered morphologically associated with a GnRH neuron when it was located at a distance ≤ the size of the BrdU$^+$ nucleus (i.e., ≤ 10 µm) from the GnRH neuron cell body with no interposed cell nucleus in between (**Supplementary Fig. 3**).

Number of cell nuclei at the injection site of microparticle-injected rats. The total number of Hoechst-stained nuclei was automatically quantified using the ImageJ software on microphotographs of the injection site taken at the 20x objective. Quantification represents the mean number of Hoechst-stained nuclei in a 20x microscopic field, corresponding to a surface area of 0.5 mm^2, counted on 3 sections per animal (n = 12).

Number of BrdU$^+$ cells at the injection site of microparticle-injected rats. Analysis was performed on photomontages of the preoptic region taken at the 20x objective. Quantification represents the mean number of BrdU$^+$ cells in a 1 mm square centered on the injection site, counted on 3 to 4 sections per animal (n = 13).

Quantification of vGluT2 and vGaT appositions to GnRH neuron cell bodies. Analysis was performed on high magnification images of GnRH neuron somata located at the level of the OVLT using the IMARIS 9.3 software (Bitplane) as described before [72]. Briefly, the number of vGluT2- or vGaT-immunoreactive punctae closely apposed with the GnRH neuron soma was quantified on 3D reconstructions from raw confocal image z-stacks using a channel of colocalization. A punctum was considered apposed when no black pixels were visible between the GnRH and the vGluT2 or vGaT fluorescence. The value was normalized to the number of optical sections through the z-depth of the neuron and the surface area of the neuronal soma. The resulting value was multiplied by the average number of optical sections and the average surface area of all neurons analyzed to provide a number of punctae per GnRH soma.

Western blot analyses. Preoptic primary progenitors were starved for 24h in DMEM/F-12 with L-glutamine, 15 mM HEPES supplemented with 2 mM L-glutamine, 100 units of penicillin and 100 µg of streptomycin/ml, 5 µg/ml insulin (Sigma) and 16 µg/ml putrescine (Sigma). The cells were treated with PGD2 1 µM and/or BWA868C (10 nM or 1 µM) in fresh medium for 7 minutes and snap-frozen on dry ice. Proteins were extracted and subjected to size-fractionation as previously described [4]. The proteins were then transferred onto 0.2 µm pore-size nitrocellulose membranes (Invitrogen) using the NuPAGE system (Invitrogen). Membranes were blocked for 1 h in blocking buffer (Tris buffer saline (0.05 M Tris, pH 7.4, 0.15 M NaCl) with 0.05% Tween 20 (TBST) and 5% nonfat milk) at room temperature and incubated overnight at 4°C with the appropriate primary antibody diluted in blocking buffer (rabbit polyclonal anti-phospho-p44/42 MAPK (Thr202/Tyr204) (pErk) #9101, 1:1,000; rabbit polyclonal anti-p44/42 MAPK (Erk) #9102, 1:1,000, Cell Signaling Technology, Beverly, MA, USA). After washing with TBST, membranes were exposed to horseradish peroxidase-conjugated secondary antibodies (goat anti-rabbit IgG, PI1000, 1:2000, Vector) diluted in blocking buffer for 1 h at room temperature. Immunoreactions were visualized using the ECL

detection kit (NEL101; PerkinElmer, Boston, MA). Immunoblots were scanned using a desktop scanner (Epson Expression 1680 PRO) and Adobe Photoshop.

Isolation of hypothalamic GnRH neurons using fluorescence-activated cell sorting. The preoptic regions of *Gnrh::Egfp* transgenic rats were microdissected and enzymatically dissociated using a Papain Dissociation System (Worthington, Lakewood, NJ) to obtain single-cell suspensions. FACS was performed using an ARIA SORP cell sorter cytometer and FACSDiva 8.0 software (BD Biosciences). Data were analyzed using the Kaluza 2.0 software (Beckman Coulter). The sort decision was based on measurements of EGFP fluorescence (excitation: 488 nm, 50 mW; detection: GFP bandpass 530/30 nm, autofluorescence bandpass 695/40 nm) by comparing cell suspensions from the preoptic region and from the cerebral cortex of *Gnrh::Egfp* animals. A total of 174 ± 20 (range, 44 – 700) EGFP-positive cells were sorted per animal and directly lysed into 10 µl of extraction buffer containing 0.1% Triton® X-100 (Sigma) and 0.4 unit/µl RNaseOUT™ (Life technologies).

Quantitative RT-PCR analyses. Gene expression analyses were performed on FACS-sorted GnRH neurons, primary preoptic progenitor cultures and GnV3 cells. For primary preoptic progenitors, RNAs were extracted as follows: 100 µl of Trizol (Life Scientific, Carlsbad CA, USA) were used to lyse cells before adding 100 µl of chloroform (Merck, Darmstadt, Germany) and centrifuging at 12,000 g for 15 minutes at 4°C. The aqueous phase was carefully collected and added to isopropanol at 1:1 before centrifuging at 12,000 g for 10 minutes at 4°C. The aqueous phase was then discarded and the pellet washed in 70% ethanol. After centrifugation at 12,000 g for 5 minutes at 4°C, the pellet was left to air-dry and then diluted in 10 µl DEPC water. The purity and quantity of RNA were determined by UV spectroscopy (Nanodrop 1000, Thermo Scientific, Waltham MA, USA). Messenger RNAs obtained from FACS-sorted GnRH neurons or primary progenitors were reverse transcribed using SuperScript® III Reverse Transcriptase (Life Technologies). For sorted cells, a linear

preamplification step was performed using the TaqMan®PreAmp Master Mix Kit protocol (Applied Biosystems). Real-time PCR was carried out on Applied Biosystems 7900HT Fast Real-Time PCR System using exon-boundary-specific TaqMan® Gene Expression Assays (Applied Biosystems) (**Supplementary Table 3**). Gene expression data were analyzed using SDS 2.4.1 and Data Assist 3.0.1 software (Applied Biosystems) with R45S and actin as control housekeeping mRNAs following a standardized procedure [73]. For GnV3 cells, RNAs were purified using the RNeasy Mini Kit (Qiagen, Basel, Switzerland) according to the manufacturer's instructions. The solution was treated with DNase (RNase-Free DNase Set, Qiagen, Basel, Switzerland) and eluted with 30 µl of water. RNA concentrations were determined with a Nanodrop® (ND-1000 Spectrophotometer, Witec, Luzern, Switzerland). Two hundred ng of RNA was reverse transcribed using the RT High Capacity RNA-to-cDNA Kit (Applied Biosystems, Rotkreuz, Switzerland). Real-Time PCR analysis was performed on 2 µl of cDNA using Power SYBR Green Taq polymerase master mix (Applied Biosystems, Rotkreuz, Switzerland). The primer sequences used were: Ptgds forward: 5'-TGGGTCTCTTGGGATTTCCA-3', Ptgds reverse: 5'-CCCCAGGAACTTGTCTTGTTG-3'; polymerase 2a (Polr2a, as endogenous control) forward: 5'-GTAAGGGCCACTATCTTCATCATCA-3', Polr2a reverse: 5'-CCCTCATCATACCTGGTCACATC-3'.

Microarray hybridization and data analysis. RNA purification and microarray hybridization were performed as previously described [20]. Total RNA was extracted from the cells using Trizol (Invitrogen), according to the manufacturer's instructions. Only RNA samples with RNA integrity numbers greater than 9.0 were accepted for microarray analysis. Microarray hybridization was performed with Affymetrix GeneChip Rat Gene 1.0 ST arrays according to the manufacturer's instructions and scanned with the Gene Array scanner (Affymetrix). The fluorescence images obtained were processed using the BioConductoraffy package (DAFL, Lausanne). Expression values were measured using the Robust Multi-array Average (RMA) algorithm generating expression values on a log2 scale. RMA includes background

correction, quantile normalization and probe set summary by robust regression. GnV3 signature of 22,336 transcripts was generated and annotated with Gene Symbol. Genes without an Entrez annotation were filtered out. The fold change was calculated individually for each gene. Differential hybridized features were identified using Bioconductor package "limma"[74]. Additionally, the false discovery rate, i.e. the expected proportion of rejected null hypotheses that are wrongly rejected, was estimated by a resampling procedure[75]. Genes that showed substantial up- or down-regulation by log fold changes (FC) > 1 with a FDR < 0.05 were considered as differentially expressed. For each condition (ADM or ACM), microarray analyses were performed using RNA samples derived from three wells per condition. Only the list of genes showing significant up and down-regulation is provided in the **Supplementary Data 1**.

Statistics. No statistical methods were used to pre-determine sample sizes but our sample sizes are similar to those reported in previous publications [4, 25, 26, 37, 76]. Studies were not formally randomized and investigators were not blind to treatment group. All analyses were performed using the SigmaStat 3.5 (Systat) or GraphPad Prism 7.05 (GraphPad) software. Outliers were identified using the ROUT (Q=1%) method. Statistical differences were evaluated using unpaired two-sided Student's *t*-tests for comparison of two groups and one- or two-way analysis of variance (ANOVA) with Tukey's *post hoc* tests for comparison of more than two groups. When the criterion for normality or equal variances was not met, the Mann-Whitney Rank Sum Test or the Kruskal-Wallis One Way ANOVA on Ranks Test was used to compare two or more groups, respectively. $P < 0.05$ was considered significant.

Data availability. Uncropped Western blots and Source Data Files for transcriptomic analysis of GnV3 cells are provided as Extended data. Additional data that support the findings of this study are available from the corresponding author upon request.

References.

63. Fujioka, H.*, et al.* Generation of transgenic rats expressing enhanced green fluorescent protein in gonadotropin-releasing hormone neurons. *J Reprod Dev* **49**, 523-529 (2003).
64. Paxinos, G. & Watson, C. *The rat brain in stereotaxic coordinates* (Academic press New York, 1982).
65. Ojeda, S.R. & Ramirez, V.D. Automatic control of LH and FSH secretion by short feedback circuits in immature rats. *Endocrinology* **84**, 786-797 (1969).
66. Golde, W.T., Gollobin, P. & Rodriguez, L.L. A rapid, simple, and humane method for submandibular bleeding of mice using a lancet. *Lab Anim (NY)* **34**, 39-43 (2005).
67. Altwegg-Boussac, T., Chavez, M., Mahon, S. & Charpier, S. Excitability and responsiveness of rat barrel cortex neurons in the presence and absence of spontaneous synaptic activity in vivo. *J Physiol* **592**, 3577-3595 (2014).
68. Salvi, R.*, et al.* Gonadotropin-releasing hormone-expressing neurons immortalized conditionally are activated by insulin: implication of the mitogen-activated protein kinase pathway. *Endocrinology* **147**, 816-826 (2006).
69. Swanson, L.W. *Structure of the rat brain* (Elsevier Science Publishers, Amsterdam, 2004).
70. Lee, W.S., Smith, M.S. & Hoffman, G.E. Luteinizing hormone-releasing hormone neurons express Fos protein during the proestrous surge of luteinizing hormone. *Proc Natl Acad Sci U S A* **87**, 5163-5167 (1990).
71. Abercrombie, M. Estimation of nuclear population from microtome sections. *Anat Rec* **94**, 239-247 (1946).
72. Tata, B.*, et al.* Elevated prenatal anti-Mullerian hormone reprograms the fetus and induces polycystic ovary syndrome in adulthood. *Nat Med* **24**, 834-846 (2018).
73. Schmittgen, T.D. & Livak, K.J. Analyzing real-time PCR data by the comparative C(T) method. *Nat Protoc* **3**, 1101-1108 (2008).
74. Smyth, G.K. Limma: Linear Models for Microarray Data. in *Bioinformatics and Computational Biology Solutions using R and Bioconductor* (ed. R. Gentleman, V. Carey, S. Dudoit, R. Irizarry & W. Huber) 397-420 (Springer, New York, 2005).
75. Storey, J.D. & Tibshirani, R. Statistical significance for genomewide studies. *Proc Natl Acad Sci U S A* **100**, 9440-9445 (2003).
76. Vanacker, C.*, et al.* Neuropilin-1 expression in GnRH neurons regulates prepubertal weight gain and sexual attraction. *EMBO J* **39**, e104633 (2020).

Submission: 1/10/21 9:10
Nature Neuroscience

GnRH neurons recruit astrocytes in infancy to facilitate network integration and sexual maturation

Giuliana Pellegrino[1]*, Marion Martin[1]*, Cécile Allet[1]*, Tori Lhomme[1], Sarah Geller[2], Delphine Franssen[3], Virginie Mansuy[4], Maria Manfredi-Lozano[1], Adrian Coutteau-Robles[1], Virginia Delli[1], S. Rasika[1], Danièle Mazur[1], Anne Loyens[1], Manuel Tena-Sempere[5], Juergen Siepmann[6], François P. Pralong[4], Philippe Ciofi[7], Gabriel Corfas[8], Anne-Simone Parent[3], Sergio R. Ojeda[9], Ariane Sharif[1$] and Vincent Prevot[1$]

[1]Univ. Lille, Inserm, CHU Lille, Laboratory of Development and Plasticity of the Neuroendocrine Brain, Lille Neuroscience & Cognition, UMR-S 1172, FHU 1000 days for Health, Lille, France.
[2]Center for Integrative Genomics, University of Lausanne, Lausanne, Switzerland.
[3]Neuroendocrinology Unit, GIGA Neurosciences, University of Liège, Liège, Belgium.
[4]Service of Endocrinology, Diabetology and Metabolism, University Hospital and Faculty of Biology and Medicine, 1011 Lausanne, Switzerland.
[5]Department of Cell Biology, Physiology and Immunology, University of Cordoba, Cordoba, Spain; Instituto Maimonides de InvestigaciónBiomédica de Cordoba (IMIBIC/HURS), Cordoba, Spain; CIBER Fisiopatología de la Obesidad y Nutrición, Instituto de Salud Carlos III, Cordoba, Spain.
[6] Univ. Lille, Inserm, CHU Lille, U1008, Lille, France.
[7]Inserm U1215, Neurocentre Magendie, Bordeaux, France; University of Bordeaux, Bordeaux, France.
[8]Kresge Hearing Research Institute, Department of Otolaryngology-Head and Neck Surgery, University of Michigan, Ann Arbor, Michigan 48109.
[9]Division of Neuroscience, Oregon National Primate Research Center-Oregon Health & Science University, Beaverton, OR 97006, USA.

*These authors contributed equally; [$]These authors jointly supervised this work.

[$]Corresponding authors:

Vincent Prevot, Ph.D., Inserm U1172, Bâtiment Biserte, Place de Verdun, 59045 Lille Cedex, France
Tel: +33 6-12-90-38-76
E-mail: vincent.prevot@inserm.fr
ORCID number: https://orcid.org/0000-0001-7185-3615

Ariane Sharif, Ph.D., Inserm U1172, Bâtiment Biserte, Place de Verdun, 59045 Lille Cedex, France
E-mail: ariane.sharif@inserm.fr
ORCID number: https://orcid.org/0000-0003-0810-400X

ABSTRACT

Neurons producing gonadotropin-releasing hormone (GnRH), which control fertility, complete their nose-to-brain migration by birth. However, their function depends on integration within a complex neuroglial network during postnatal development. Here, we show that GnRH neurons during the infantile period use a prostaglandin-D2/DP1-receptor signaling mechanism to recruit newborn astrocytes that “escort” them into adulthood, and the impairment of postnatal hypothalamic gliogenesis dramatically alters sexual maturation by preventing this recruitment, a process mimicked by the endocrine disruptor bisphenol-A. DP1 signaling inhibition in the infantile preoptic region, where GnRH cell bodies reside, disrupts the correct wiring and firing of GnRH neurons, alters minipuberty or the first activation of the hypothalamic-pituitary-gonadal axis during infancy, and delays the timely acquisition of reproductive capacity. These findings uncover a previously unknown neuron-to-neural-progenitor communication pathway and demonstrate that postnatal astrogenesis is a basic component of a complex set of mechanisms used by the neuroendocrine brain to control sexual maturation.

INTRODUCTION

Neuroendocrine GnRH neurons, which ensure species survival by controlling the ability of individuals to reproduce, are principally located in the preoptic region, a basal forebrain region harboring diverse neuronal populations[1]. Unlike other hypothalamic neurons driving bodily functions, GnRH neurons are not born in the brain but originate in the olfactory placode, and migrate from the nose to the brain during embryogenesis[2]. Although this migration is complete at birth, GnRH neurons recruit other neuronal populations, notably those expressing kisspeptin and neuronal nitric oxide synthase (nNOS), during postnatal development to establish a complex circuit that fine-tunes GnRH production and release by providing precisely coordinated excitatory and inhibitory inputs[3, 4], thus orchestrating sexual maturation, puberty and adult fertility[5]. However, the mechanisms by which GnRH neurons sculpt their own microenvironment and establish the connections necessary to control reproduction remain unexplored.

The GnRH network is not exclusively neuronal but includes at least two glial cell types: tanycytes, which control the access of GnRH neurosecretory terminals to the pericapillary space of pituitary portal vessels, into which the hormone is released, and astrocytes, whose communication with GnRH neurons is essential for reproductive function[6]. Glial cells, especially astrocytes, also help generate physiological responses by forming a hub with neurons that integrates internal and external cues within the adult brain[6]. Additionally, they act as cartographers of synaptogenesis and neural circuit formation in the developing central nervous system[7, 8]. Conversely, studies in the neocortex suggest that astrocyte formation is regulated by extrinsic signals generated by neurons, the development of which precedes gliogenesis[9]. We therefore asked whether GnRH neurons could themselves be responsible for the circuit formation subtending reproductive function in adulthood by establishing a glial entourage during postnatal development.

Here, we demonstrate that GnRH neurons in the infantile period attract newborn progenitor cells that differentiate into astrocytes and remain closely associated with them, essentially “escorting” these neurons into adulthood. Additionally, local inhibition of infantile

gliogenesis in the preoptic region, which harbors GnRH neuronal somata, delays puberty. The interaction between GnRH neurons and newborn astrocytes underlying correct sexual maturation depends on reciprocal prostaglandin-mediated signaling, and especially the expression of the prostaglandin D2 receptor DP1 by these newborn cells. Our findings thus identify a novel neuron-to-neural-progenitor communication mechanism that unfolds during the infantile period and times the pubertal activation of the reproductive axis.

RESULTS

GnRH neurons assemble a glial entourage during early infancy

GnRH neuronal somata in rats are loosely distributed between the medial septum/diagonal bands of Broca and the preoptic nuclei, being densest in the median preoptic nucleus (MePO) at the level of the organum vasculosum laminae terminalis (OVLT). To determine if the birth of new cells in the vicinity of GnRH neurons shapes their microenvironment, we used the thymidine analog, bromodeoxyuridine (BrdU) to map cell proliferation in the OVLT and its surroundings, referred to hereafter as the “preoptic region”, in female rats at different stages of postnatal development [postnatal day (P)1 and P5: neonatal period; P8 and P12: infantile period; P20 and P24: juvenile period, i.e. after weaning] (**Fig. 1a**). In agreement with a previous report[10], more cells incorporated BrdU in the infantile versus the juvenile period (**Supplementary Fig. 1a,b**). BrdU colocalization with proliferating-cell nuclear antigen (PCNA), an endogenous cell-cycle marker (**Supplementary Fig. 1c**), the occurrence of pairs of closely apposed $BrdU^+$ nuclei (**inset in Fig. 1b, Supplementary Fig. 1d**), and doubling of the $BrdU^+$ cell population between 2h and 24h after BrdU injection (**Supplementary Fig. 1e**) strongly suggested that BrdU-labeled cells were entering the cell cycle. Seven days after BrdU injection, most newborn cells expressed either glial fibrillary acidic protein (GFAP) in conjunction with an astrocyte-like morphology, denoting their differentiation into astrocytes, or adenomatosis polyposis coli (APC) – a marker of oligodendrocytes, while a very small number expressed the neuronal marker, HuC/D (**Supplementary Fig. 2a-j**). The presence of multipotent progenitors in the postnatal

preoptic region was confirmed *in vitro* by culturing clonally-derived neurospheres capable of differentiating into all three neural cell types (**Supplementary Fig. 2k-m**).

Interestingly, co-immunolabeling revealed the close proximity of some GnRH neuronal cell bodies to $BrdU^+$ newborn cells (**Fig. 1b**). Biocytin filling of patch-clamped astrocytes in living brain slices from infantile rats showed that preoptic astrocytes had a radius of 20-40 µm (**Supplementary Fig. 3a**). We therefore decided to look for newborn progenitors, which presumably have smaller arborizations, at a conservative distance of 10 µm from GnRH neurons. Two hours after BrdU injection, GnRH neurons accompanied by $BrdU^+$ progenitors were more frequent in neonatal and infantile rats than in juvenile animals (**Fig. 1c**). GnRH neurons preferentially associated with proliferating cells, since 12.8% of GnRH neurons were juxtaposed to $BrdU^+$ cells 2h after BrdU injection at P8, versus only 3.6% of non-GnRH neurons (**Fig. 1c,d**). At this time-point, these proximal $BrdU^+$ cells expressed the progenitor cell marker, Sox2, but not GFAP (**Fig. 1e-g**). Twenty-four hours later, 27.2% of GnRH neurons were associated with $BrdU^+$ cells labelled by a single injection at P8 (**Fig. 1c**). This increased association persisted even after seven days, when 22.3% of GnRH neurons had a companion $BrdU^+$ cell (**Fig. 1c,d**). Notably, this proportion reached 80.3 ± 2.7% (n = 4 rats) when the BrdU regimen was increased to three injections per day from P6 to P8 (**Fig. 1h**). Because the number of GnRH neurons in the preoptic region remained unchanged during postnatal development (367.2±43.5 neurons at P8 versus 342.9 ± 22.3 neurons at P15, two-sided unpaired t-test, $t_{(14)}$ = 0.498, P = 0.626; n = 8 rats per group), the increased proportion of GnRH neurons associated with $BrdU^+$ cells could either stem from a global increase in the number of $BrdU^+$ cells in the preoptic region after proliferation (**Supplementary Fig. 1e**) or the migration of $BrdU^+$ cells towards GnRH neurons. We analyzed the neighborhood of GnRH neurons 2h after a single BrdU injection at P8, and identified all neurons that would be considered associated with a $BrdU^+$ cell 24h later if the proliferation of existing $BrdU^+$ cells were to give rise to a daughter cell lying within 10µm of the GnRH neuronal soma (**Supplementary Fig. 3b,c**). However, even under the very

broad assumption that every proliferative event would give rise to a newborn cell within the perimeter described, the resulting theoretical percentage of GnRH neurons with associated $BrdU^+$ cells was still significantly lower than the actual percentage measured (**Supplementary Fig. 3d**), indicating that cell division in the neighborhood of GnRH neurons could not fully account for the increased proportion of GnRH neurons with a $BrdU^+$ companion cell. GnRH neurons are thus likely attract newborn cells to their immediate vicinity during the early infantile period.

The association between GnRH neurons and cells born at P8 was maintained until adulthood (**Fig. 1c**). Notably, the increase in GnRH neurons with $BrdU^+$ companions between 2h and 7 days after BrdU injection was seen only in the group injected at P8 (**Fig. 1c**), indicating that the beginning of the infantile period is a critical time-window for GnRH neurons to enrich their immediate cellular environment. Triple immunolabeling for GnRH, BrdU and GFAP, APC or HuC/D showed that P8-born cells accompanying GnRH neurons mainly differentiated into GFAP-expressing astrocytes (**Fig. 1g,i-k**). Physical proximity to GnRH neurons did not alter the fate of P8-born cells (phenotype of $BrdU^+$ cells in the vicinity of GnRH neurons (n = 6-7 rats) vs. all newborn cells in the preoptic region (n = 3 rats): GFAP, Mann-Whitney test: $U = 9$, $P = 0.833$; APC, Mann-Whitney test: $U = 6$, $P = 0.500$; HuC/D, Mann-Whitney test:$U = 3$, $P = 0.167$) (compare **Supplementary Fig. 2j** and **Fig. 1g**).

Blocking infantile preoptic cell proliferation delays puberty

To determine if the birth of new cells in the infantile preoptic region is involved in sexual maturation, we locally inhibited cell proliferation in P6 or P7 female rats by stereotaxically injecting biodegradable poly(D,L-lactic-co-glycolic acid) (PLGA)-based microparticles (**Fig. 2a,c**), designed to release the antimitotic compound, paclitaxel, in a time-controlled manner[11], just above the MePO. An initial assay revealed that this release was complete by 6 days, i.e. before the end of the infantile period when proliferation in the preoptic area peaks (**Supplementary Fig. 4a**). Control animals were injected with blank-

loaded microparticles (**Fig. 2a,b**), and a single BrdU injection carried out at P8 as before in both groups. We then monitored puberty onset and adult estrous cyclicity. At adulthood, paclitaxel-treated animals showed decreased cell density (**Fig. 2c,d, Supplementary Fig. 4b,c**), fewer $BrdU^+$ cells at the injection site (**Fig. 2e, Supplementary Fig. 4b,c**) and a lower proportion of GnRH neurons associated with $BrdU^+$ cells in the MePO (**Fig. 2f**), although the total number of GnRH neurons in the preoptic region remained unaffected (**Fig. 2g**). In the anteroventral periventricular nucleus (AVPV), a more ventral preoptic nucleus that extends well beyond the OVLT caudally and relays the estrogen positive feedback[12], chronic intracerebroventricular administration of another antimitotic, AraC, during the peripubertal period has been shown to block proliferation[13]. However, paclitaxel treatment did not affect the number of $BrdU^+$ cells, neurons or astrocytes in the AVPV (**Supplementary Fig. 5**), indicating that our administration method had extremely localized antimitotic effects. Paclitaxel-treated animals exhibited a marked delay in puberty onset compared to control animals, as indicated by delayed vaginal opening (**Fig. 2h,i**) and first estrus (**Fig. 2j,k**). In addition, while the two milestones coincided in control animals, they were uncoupled in paclitaxel-treated animals, which experienced their first estrus ~3.5 days after vaginal opening (**Fig. 2l**,**m**), a phenomenon rarely observed in rats[5]. Notably, paclitaxel-treated animals had similar body weights to control animals (**Supplementary Fig. 4d**), indicating that the delay in sexual maturation was not due to a growth deficit. Paclitaxel-treated animals also exhibited fewer complete 4-day estrous cycles (**Fig. 2l,n**). Taken together, these results suggest that the presence of newborn cells in the environment of preoptic GnRH neurons during the infantile period, rather than GnRH neurons *per se*, is necessary for the timely onset of puberty and contributes to fertility in adulthood.

Endocrine disruptors alter GnRH neuron-progenitor interaction

A common adverse condition for the development and function of the gonadotropic axis is exposure to endocrine-disrupting chemicals (EDCs) during perinatal life. While the gonads have long been considered the main targets of EDCs, a growing number of studies

highlight their neuroendocrine effects, such as GnRH neuronal network alterations[14]. Intriguingly, rat pups exposed for the first 15 days after birth to a very low but environmentally relevant dose [15] of the plasticizer bisphenol A (BPA; 25 ng/kg per day) tend towards delayed vaginal opening[16], phenocopying our paclitaxel-treated rat pups. Additionally, these BPA-exposed rats also demonstrate an altered frequency of GnRH secretion at P20[16], suggesting a perturbation of the first postnatal activation of the hypothalamic-pituitary-gonadal (HPG) axis, known as minipuberty. This phenomenon, which occurs at P12 in rats and 1 month of age in humans, helps establish an adult pattern of pulsatile GnRH secretion that, in baby girls and female rodents alike, triggers an FSH surge that is essential for subsequent gonadal maturation and hence, fertility[5, 17]. To verify whether the adverse effects of EDCs on gonadotropic axis maturation could stem from their interference with the ability of GnRH neurons to recruit neighboring cells, we treated female rat pups with 25 ng/kg per day of BPA from P1[16], then injected them with BrdU at P8 and assessed GnRH neuron association with $BrdU^+$ cells 2h and 7d later (**Fig. 3a**). Contrary to paclitaxel, BPA exposure did not affect cell birth near GnRH neurons at P8 (**Fig. 3b**). Additionally, the total number of GnRH neurons in the preoptic region at P8 also remained unchanged (255.7 ± 34.95 in control P8 rats versus 218.9 ± 30.38 in BPA-treated P8 rats, Mann-Whitney test: $U = 22$, $P = 0.3282$; $n = 8$ rats per group). However, unlike untreated rats, BPA-exposed animals showed reduced association between GnRH neurons and P8-born $BrdU^+$ cells 1 week later (**Fig. 3b**) even though there was no depletion of $BrdU^+$ cells in the preoptic region (**Fig. 3c**), further supporting the view that rather than proliferation, it is the recruitment of new glial progenitors by GnRH neurons that influences later reproductive function. From a broader viewpoint, these results also open up the possibility that the effects of EDCs on fertility and brain maturation are at least partly due to their interference with the ability of select neuronal populations to shape their glial environment during postnatal development.

GnRH neurons use PGD2 to recruit preoptic progenitor cells

Considering that the increased proportion of GnRH neurons associated with $BrdU^+$ cells between P8 + 2h and P8 + 24h is likely due to $BrdU^+$ cell recruitment rather than proliferation (**Supplementary Fig. 3**), we wondered whether GnRH neurons themselves released chemotropic factors to attract glial progenitors that would eventually differentiate into astrocytes in their vicinity and remain associated with them into adulthood (**Fig. 1i**). We first probed a set of molecules expressed in female rodent GnRH neurons: GnRH, neurotensin (NT), cholecystokinin (CCK), galanin, glutamate and GABA[18, 19]. Double immunolabeling showed that infantile GnRH neuronal perikarya contained galanin but lacked CCK and NT (**Supplementary Fig. 6a-i**). However, the vesicular transporters for glutamate and γ-aminobutyric acid (GABA), v-Glut and v-GAT, respectively, colocalized at the GnRH termination field in the median eminence (**Supplementary Fig. 6j-o**), suggesting that postnatal GnRH neurons could also influence proliferating cells through the local glutamate or GABA release.

To assess the putative chemotactic effects of GnRH, galanin, glutamate and GABA produced by GnRH neurons, we next developed adherent primary cultures of progenitor cells from the rat preoptic region at P1-P2 (**Supplementary Fig. 7a**). Cultured cells exhibited an antigenic profile typical of neural progenitors, predominantly expressing nestin, BLBP, Sox2 and vimentin (**Fig. 4a, Supplementary Fig. 7b-e**). However, in transwell assays, their migration was not significantly affected by GnRH, galanin, glutamate or GABA (**Fig. 4b**), suggesting that other factors might be responsible for their chemoattraction by GnRH neurons.

Next, since postnatal progenitor recruitment by GnRH neurons occurs in the global context of astrogenesis[8], and GnRH neurons are tightly surrounded by GFAP-expressing processes at P8 (**Fig. 1f**), we searched for candidate genes in GnRH neurons that could be regulated by astroglial factors. We conducted a transcriptomic analysis of GnV3 cells, an *in vitro* model of postnatal rat GnRH neurons [20], exposed to medium conditioned with or without hypothalamic astrocytes for 4 days (**Fig. 4c**). In all, 512 genes were differentially expressed (212 upregulated and 300 downregulated) when GnV3 cells were treated with astrocyte-

conditioned medium (See Source Data Files in **Supplementary Data 1**). The most upregulated gene was *Ptgds* encoding brain-type prostaglandin D2 (PGD2) synthase, a molecule with potent chemoattractant properties[21], which displayed a 133-fold increase in response to astrocyte-conditioned medium (**Supplementary Data 1**). RT-PCR analysis confirmed this upregulation (**Fig. 4d**). Moreover, PGD2 stimulated the passage of preoptic neural progenitors from the upper to the lower compartment in transwell migration assays (**Fig. 4b**), but did not affect their proliferation (**Fig. 4e**). As gliogenesis continues during postnatal development, these data suggest that GnRH neurons respond to incoming glial signals by synthesizing PGD2 and thus attracting newborn cells in their vicinity.

PGD2 functions *via* the G protein-coupled receptors, DP1 (*Ptgdrl*) and DP2 (*Gpr44*) [21, 22], both expressed in primary cultures of preoptic neural progenitors (**Fig. 4f**). Since DP1 signaling is already known to be involved in regulating hypothalamic function[22], we used BWA868C, a specific antagonist of DP1[22, 23], to determine whether the effect of PGD2 on hypothalamic progenitor cell migration was mediated by DP1. BWA868C treatment of preoptic neural progenitors not only drastically inhibited the stimulatory effect of PGD2 on cell migration (**Fig. 4g,h**), it also reduced the PGD2-induced phosphorylation of the mitogen-activated protein kinase (MAPK) ERK (**Fig. 4i**), confirming that PGD2 signaling was active in these progenitors.

PGD2/DP1 signaling mediates preoptic precursor recruitment

Next, to investigate whether GnRH neurons produce PGD2 during postnatal development *in vivo*, we analyzed *Ptgds* expression in cells isolated by fluorescence-activated cell sorting (FACS) from transgenic rats expressing enhanced green fluorescent protein (EGFP) under the control of the GnRH promoter[24] using real-time PCR (**Fig. 5a**, **Supplementary Fig. 8a,b**). *Gnrh* mRNA was only detected in the EGFP-positive cell fraction, demonstrating the accuracy of the sorting procedure (**Supplementary Fig. 8c-e**). Using this approach, we found that *Ptgds* transcripts were indeed enriched in rat GnRH neurons and

that their expression significantly increased between P8 and P20 in these neurons (**Fig. 5b**) but remained unchanged in preoptic cells lacking EGFP (**Fig. 5c**).

To gain further insight into the involvement of the PGD2/DP1 signaling pathway in the communication between GnRH neurons and neural progenitors *in vivo*, we evaluated *Ptgds* and *PtgdrI* expression in the postnatal preoptic region. Multiplex *in situ* hybridization in female rats at P8 confirmed the expression of *Ptgds* transcripts in GnRH neurons (**Fig. 5d**, upper row), while neighboring Sox2-expressing neural progenitors expressed *PtgdrI* mRNA (**Fig. 5d**, lower row). Moreover, the fraction of GnRH neurons expressing *Ptgds* increased between P8 and P12, an increase still seen at P20 (**Fig. 5e**), explaining the increased *Ptgds* expression observed in FACS-sorted cells above (**Fig. 5b**); however, the abundance of *Ptgds* transcripts per GnRH neuron did not significantly increase across the infantile period (**Fig. 5f**). In contrast, *PtgdrI* expression in *Sox2*$^{+}$ progenitors showed no significant variation between P8 and P20 (**Fig. 5g,h**). Altogether, these data show that the increased *Ptgds* expression in GnRH neurons during infantile development corresponds to an increase in the proportion of PGD2-synthesizing GnRH neurons during the period of enhanced astrogenesis in the preoptic area (**Supplementary Fig. 1**, **Supplementary Fig. 2)**.

To confirm that the PGD2/DP1 signaling pathway is indeed involved in progenitor cells recruitment by GnRH neurons *in vivo*, we acutely injected BWA868C stereotaxically into the preoptic region of P7 female rats, 2h after a single BrdU injection, and quantified the proportion of GnRH neurons associated with BrdU^{+} cells after 24h (**Fig. 6a**). This proportion increased in control animals but not in BWA868C-treated rats (**Fig. 6b**). Since BWA868C treatment did not affect the total number of BrdU^{+} cells in the preoptic region (**Fig. 6c**), the inhibitory effect of BWA868C on the physical proximity between GnRH neurons and BrdU^{+} cells was not due to neural progenitors depletion but to the blockade of the trophic influence of GnRH neurons on nearby glial progenitors. Together with our *in vitro* findings, these results indicate that functional PGD2/DP1 signaling is necessary for GnRH neurons to recruit or attract a glial entourage during the infantile period in rats.

Inhibiting DP1 disrupts GnRH network maturation and function

To assess the functional involvement of DP1 signaling in postnatal sexual maturation, we implanted BWA868C pellets (10 nM in cocoa butter) in the preoptic region of P8 female rats[25] and monitored the occurrence of the first postnatal FSH surge indicative of minipuberty (**Fig. 6d**). Similar to acute injection, BWA868C released chronically from a pellet also significantly hampered the association of GnRH neurons with $BrdU^+$ cells one week later (**Fig. 6e**), although the total number of $BrdU^+$ cells in the preoptic region remained unaffected (**Fig. 6f**). While the treatment had no effect on somatic growth (**Supplementary Fig. 9**), the FSH surge at minipuberty was blunted in BWA868C-treated pups in comparison to vehicle-treated littermates (**Fig. 6g**), suggesting that the activity of infantile GnRH neurons was impaired by their inability to attract newborn astrocytic precursors.

Next, since minipuberty has previously been shown to be a critical period for the switch in the transcriptional control of GnRH expression [4], we assessed whether BWA868C treatment at P7 influenced this process. RT-qPCR analyses in FACS-isolated rat GnRH neurons at P12-P13 indicated that BWA868C implantation had no apparent impact on *Gnrh* expression (**Fig. 7a**). However, it decreased the expression of *Cebpb*, a repressor of the *Gnrh* promoter, but left unchanged the expression of another repressor, *Zeb1*, as well as *Kiss1r* and *Otx2*, two stimulators of *GnRH* expression, and *Dicer*, an RNAse-III endonuclease essential for microRNA biogenesis and the microRNA-mediated infantile *Gnrh* transcriptional switch[4] (**Fig. 7a**). Surprisingly, BWA868C treatment also impacted several other genes involved in prostaglandin synthesis and signaling in infantile GnRH neurons (**Fig. 7b**). In addition to a significant decrease in *Ptgds* expression (**Fig. 7c**), in line with our transcriptomic analysis showing *Ptgds* regulation by astrocyte-derived factors (**Fig. 4d**, **Supplementary Data 1**), BWA868C treatment downregulated transcripts for *Ptger1* and *Ptger3*, encoding the PGE2 receptors EP1 and EP3, respectively, in infantile rat GnRH neurons (**Fig. 7c**). These results are in keeping with previous *in vitro* studies showing that astrocyte-conditioned medium modulates the sensitivity of GnRH neurons to astrocytic

PGE2, a stimulator of GnRH release, by upregulating EP1 and EP3 expression[26], and suggest that the BWA868C-mediated decrease in astrocyte recruitment by GnRH neurons interferes with astrocytic PGE2-stimulated GnRH release rather than GnRH production.

We next investigated whether, in addition to altering astrocyte-to-GnRH-neuron communication processes, BWA868C treatment could also influence neuronal connectivity, in particular the apposition of glutamatergic or GABAergic terminals onto GnRH neuronal cell bodies, and consequently GnRH neuronal activity during the infantile period. The BWA868C-mediated inhibition of DP1 signaling in the preoptic region significantly decreased the number of appositions of vesicular glutamate transporter 2 (vGluT2)-immunoreactive punctae but not of vesicular GABA transporter (vGaT)-immunoreactive punctae on GnRH somata at P15 (**Fig. 7d**).

Given this robust decrease in putative excitatory synaptic inputs to GnRH neurons, we next performed *ex vivo* whole-cell patch-clamp recordings of GnRH neurons in living brain slices containing the OVLT from P10-P15 infantile *Gnrh::Egfp* rats treated either with vehicle or with BWA868C *in vivo* at P7-P8 (**Fig. 7e,f**). We found no significant difference between the two conditions in the resting membrane potential (Vm) (**Fig. 7g**), membrane resistance (Rm) (**Fig. 7h**), voltage threshold for action potential (AP) generation (V_{TH}) (**Fig. 7i**) or time constant (control time constant = 0.47 ± 0.07 ms, n = 15 cells from 8 rats; BWA868C time constant = 0.43 ± 0.05 ms, n = 22 cells from 7 rats; Mann-Whitney test: U = 149.5, P = 0.641). These findings demonstrate that the integrative properties and intrinsic excitability of GnRH neurons were not modified by BWA868C treatment. However, we observed a significant attenuation of the spontaneous firing rate in GnRH neurons partly deprived of glutamatergic synapses (**Fig. 7j**and **f,** left), reminiscent of the increased interpulse interval of GnRH neurosecretion in BPA-treated rat pups[16]. This was not accompanied by modifications in spike properties such as full amplitude (control spike amplitude = 57.73 ± 2.75 mV, n = 10 cells from 8 rats; BWA868C spike amplitude = 61.13 ± 1.88 mV, n = 10 cells from 8 rats; two-sided unpaired t-test, $t(18)$ = 1.02, P = 0.321), half-

width duration (control half-width duration = 1.85 ± 0.17 ms, *n* = 10 cells from 8 rats; BWA868C half-width duration = 1.74 ± 0.07 ms, *n* = 10 cells from 8 rats; Mann-Whitney test: *U* = 49, *P* = 0.970) or after-hyperpolarization potential (AHP) amplitude (control AHP amplitude = 7.52 ± 0.55 mV, *n* = 10 cells from 8 rats; BWA868C AHP amplitude = 7.18 ± 0.30 mV, *n* = 10 cells from 8 rats; two-sided unpaired *t*-test, *t*(18) = 0.535, *P* = 0.599) or duration (control AHP duration = 470.9 ± 69.52 ms, *n* = 10 cells from 8 rats; BWA868C AHP duration = 465.7 ± 65.53 ms, *n* = 10 cells from 8 rats; two-sided unpaired *t*-test, *t*(18) = 0.055, *P* = 0.957) as measured from isolated APs. We further analyzed spike generation in neurons in which clear baseline synaptic activity was detected on the trace (n = 10 neurons from 8 rats per condition). In the control group, in 5 neurons, firing was triggered by a slowly developing temporal summation of fast depolarizing events (**Fig. 7f**, top right), reminiscent of depolarizing postsynaptic potentials. This dramatically differed from most BWA868C-treated neurons, in which AP firing was apparently elicited by intrinsic mechanisms (n = 4 neurons, **Fig. 7f**, bottom right, AP #1 and #2) or the cooperative effect of intrinsic and synaptic mechanisms (n = 4 neurons, **Fig. 7f**, bottom right, AP #3). Only two BWA868C-treated neurons analyzed displayed APs elicited by an excitatory synaptic barrage. Altogether, these findings indicate that BWA868C treatment does not alter the resting membrane or integrative properties of GnRH neurons but significantly reduces their functional output, likely due to decreased glutamatergic synaptic connections.

Finally, we analyzed the effects of infantile BWA868C treatment on the acquisition of mature reproductive function. Even though BWA868C implantation in the preoptic region during the infantile period did not alter the age at vaginal opening (**Fig. 8a,b**), which coincided with first estrus (**Fig. 8a**), it significantly delayed the onset of regular estrous cyclicity (**Fig. 8a,c**). During the first two weeks after vaginal opening, BWA868C-treated females spent more time in estrus at the expense of proestrus, indicating a dysregulation of pulsatile GnRH release, in contrast to control (vehicle-treated) littermates, which quickly acquired a regular 4-day estrous cycle.

Altogether, these results show that the integrity of GnRH neuron-glia communication in the preoptic region during the infantile period is critical for the recruitment of newborn glial precursors that accompany these neurons into adulthood as well as the establishment of functional synaptic inputs to GnRH neurons. Furthermore, this communication, mediated by PGD2/DP1 signaling, is essential for the correct initiation of sexual maturation, reciprocal signaling by astrocytes of the GnRH neural network, and adult pattern of estrous cyclicity.

DISCUSSION

The ability to reproduce is acquired through a long and complex process that relies on the fine regulation of GnRH neuronal network activity during the postnatal period. This process involves intrinsic and extrinsic modifications to functional gene networks[4, 27] and neuronal circuits converging onto GnRH neurons[28, 29], as well as the increased stimulatory influence of glial cells[6]. Our data provide the first neuroanatomical and physiological evidence that GnRH neurons build their own glial environment during a circumscribed period after birth via a specific cell-cell communication pathway with neural progenitors born during a wave of astrogenesis, and that this reciprocal communication is essential for the maturation of the hypothalamic neuroendocrine system controlling the survival of the species.

Astrocytes have long been known to play a role in the control of GnRH neuronal function, particularly during postnatal sexual maturation[25], being sophisticated sensors[8] and regulators of neuronal activity via both the timely trafficking of energy metabolites[30] and gliotransmission[31]. They communicate with GnRH neurons by releasing bioactive molecules such as PGE2[32, 33], known to be released at active synapses in response to glutamate[34, 35]. Glutamate-stimulated PGE2 release within the GnRH neural network may involve the activation of the ErbB signaling pathway [36], also important for puberty onset [25, 37], in hypothalamic astrocytes. Here, we pinpoint the production of another prostaglandin, PGD2, by GnRH neurons themselves as a potent communication signal used by these neurons to attract infantile astroglial progenitors to their vicinity. Our findings demonstrate that inhibiting

cell proliferation or impairing PGD2/DP1 signaling in the preoptic region during this period significantly alters sexual maturation, indicating that astrogenesis in the vicinity of GnRH neurons during postnatal development is an important component of the homeostatic mechanism required for GnRH neural network maturation. While recent advances in glial cell biology have provided substantial insights into how astrocytes influence neuronal function (see [38] for review), the concept that neurons could stably recruit astrocytic progenitors as companions or "escorts", i.e. allow newborn neighboring astrocytes to become structurally/functionally associated with them during development and maintain this relationship into adulthood, has rarely been evoked.

Interestingly, the birth of new cells in the infantile preoptic region could also be modulated by neuronal factors released by other components of the GnRH neuroglial network. For example, some incoming fibers from the developing arcuate nucleus of the hypothalamus release β-endorphin[39, 40], which has recently been shown to activate quiescent neural stem cells in the adult brain[41], and could thus be a candidate to regulate this infantile proliferation. While we cannot rule out an indirect influence of the proliferation or signaling of neural progenitors on reproductive function through similar mechanisms in other components of the GnRH network, e.g. by altering astrocyte-kisspeptin-neuron interactions in the adjacent AVPV, the fact that paclitaxel did not modify BrdU+ cells in this nucleus suggests that the physiological changes we observed were selectively due to perturbed astrocyte-GnRH neuron association, rather than alterations in the neuroglial interactions of afferent neurons. Nevertheless, paclitaxel affected the reproductive phenotype more severely than BWA868C, suggesting that the progenitor depletion might have been harder to compensate for than simply inadequate GnRH neuron connectivity due to impaired association with glial progenitors.

Interestingly, deficient DP1 signaling in the preoptic region also blunts the FSH surge at P12, i.e. during minipuberty, the first centrally driven and gonad-independent activation of the HPG axis[5]. This phenotype is highly reminiscent of that of mice in which astrocytic function is selectively altered by expressing a dominant-negative ErbB4 receptor (DN-ErbB4)

under the control of the GFAP promoter[37]. On the other hand, the disrupted estrous cycle triggered by blocking preoptic DP1 signaling in rats phenocopies transgenic mice expressing a dominant negative mutation of the adhesion molecule SynCAM1 under the GFAP promoter[42]. SynCAM1 expression, required to maintain the physical contact between astrocytes and GnRH neuronal cell bodies[43], is activated by astroglial ErbB4 signaling[42]. Altogether, these findings evoke a scenario in which the birth of new astrocytes during postnatal development promotes a selective increase in the expression of the PGD2-producing enzyme, PGDS, in infantile GnRH neurons via an as yet unidentified signaling pathway involving soluble factors. The choice of candidate signaling factors is large, with astrocytes releasing not only gliotransmitters but numerous neuroactive substances, including thrombospondin, TNFα and TGFβ1 (see for review [44-46]). Regardless of its identity, PGD2 released by GnRH neurons attracts DP1-expressing neural progenitors that eventually differentiate into astrocytes and remain associated with these neurons until adulthood, an "escort" function that could facilitate their integration into functional networks and sexual maturation (**Extended Data Fig. 1**), and that could require other neuron-to-glia communication processes similar to those involving infantile ErbB4 signaling[42, 43]. While such experiments in rats are beyond the technical scope of this study, preliminary experiments in *Gfap::DN-ErbB4* mice indicate that newborn cells that are morphologically associated with infantile GnRH neurons fail to accompany them into adulthood, in contrast to wild-type littermates, despite the unaltered proliferation and long-term survival of these cells (**Supplementary Note**; **Supplementary Fig. 10**).

Astrocytes also play key roles in the control of synapse formation and functional efficacy[47, 48], shaping synaptic properties to fit ongoing developmental and functional needs, thus providing contextual guidance to the synapses[49, 50]. During postnatal development, synaptic punctae in the brain appear concurrently with astrogenesis[47]. Remarkably, our results show that preventing GnRH neurons from attracting glial progenitors in their immediate neighborhood by blocking DP1 signaling markedly decreases the number of vGluT2 appositions on GnRH neurons and significantly attenuates GnRH neuron firing, primarily by

479 decreasing the rate of depolarizing postsynaptic potentials. Since the FSH surge at
480 minipuberty is also blunted in these pups, we can postulate that the birth of new astrocytes
481 near infantile GnRH neurons is required for the establishment of excitatory glutamatergic
482 inputs onto GnRH neurons, confirming the long-suspected notion that such afferents
483 contribute to the gonad-independent maturation of the HPG axis in infantile rats[51, 52]. These
484 excitatory synaptic inputs are thought to develop after GABAergic inputs[53, 54], which,
485 contrarily, do not appear to require infantile gliogenesis for their establishment or
486 maintenance (**Fig. 7d**). Intriguingly, in the interconnected GnRH neuroglial network[6],
487 glutamate spillover at the synaptic cleft by the co-activation of metabotropic and AMPA
488 glutamatergic receptors in hypothalamic astrocytes[36] or their progenitors may initiate a
489 signaling cascade that allows ErbB4 receptor recruitment[36], promotes astrogenesis[55] and
490 thus leads to the stabilization and maturation of glutamatergic synapses. This causes
491 increased PGE2 synthesis and release by astrocytes [36], which can then signal back to
492 GnRH-secreting neurons[6]. An infantile GnRH neuron-dependent modulation of astrogenesis
493 may therefore contribute to building a signaling network capable of delivering coordinated
494 trans-synaptic and astroglial inputs to GnRH neurons themselves for the initiation of puberty
495 and the timely acquisition of adult reproductive capacity (**Extended Data Fig. 1**)[4].

496 Recent human and animal studies increasingly demonstrate that the GnRH neural
497 network is particularly sensitive to environmental pollutants, in particular endocrine
498 disruptors, during early postnatal development[14]. Exposure to EDCs such as the plasticizer
499 BPA during the critical perinatal period is indeed reported to be associated with early or late
500 puberty onset and subsequent reproductive impairments in both boys and girls (see for
501 review [14]) , and to affect the central control of puberty, including glutamatergic and
502 GABAergic inputs to GnRH neurons, in preclinical animal models[16, 56, 57]. While the underlying
503 mechanisms remain elusive, glial cells, which play a central role in GnRH neuronal network
504 development and function[6], would be the obvious suspects to mediate this EDC-induced
505 pathophysiological process[14]. Our results intriguingly show that treating infantile rats with
506 very low but environmentally relevant doses of BPA[15] known to cause alterations in sexual

maturation, phenocopying paclitaxel-treated rats[16], alters the recruitment of newborn neighboring cells by GnRH neurons at minipuberty, without appearing to affect overall cell proliferation in the infantile preoptic region. This raises the possibility that early-life exposure to chemicals in contact with food[58], such as BPA, may perturb puberty onset and durably impact reproductive function at least partially by interfering with the capacity of GnRH neurons to build a proper glial environment through altered PGDS expression[59] or ErbB signaling[60], resulting in their miswiring during postnatal development.

To summarize, our findings shed light on a hitherto unsuspected neuron-to-neural-progenitor communication process that shapes the glial environment of GnRH neurons during postnatal development and is required for the proper wiring and function of these neurons, which control the survival of the species in mammals.

ACKNOWLEDGEMENTS

G.P. and M.M. were PhD students funded by the University of Lille and C.A. by the CHU Lille. We are most grateful to Stéphane Charpier (Institut du Cerveau – ICM, UPMC-P6 UM 75, Paris, France) for his precious insights in analyzing electrophysiological data and Paolo Giacobini (Inserm, Lille, France) for his comments on the manuscript. We thank Dr. Alexandre Dawid for data analysis (LiPhy, Grenoble), Aude Caillet (U1172), Nathalie Jouy (cytometry core facility, UMS2014-US41), Meryem Tardivel and Antonino Bongiovanni (microscopy core facility, UMS2014-US41), Martin Fourdrinier (animal core facility, University of Lille) and Arlette Gérard (University of Liège) for expert technical assistance. We are indebted to Gaetan Ternier for his help in image analysis using IMARIS and Sreekala Nampoothiri for English editing. This research was supported by the Fondation pour la Recherche Médicale (FRM, INE 2002), Agence Nationale de la Recherche (ANR, France) ANR-15-CE14–0025 (to V.P.), ANR-16-CE37-0006 (to V.P.), ANR-17-CE16-0015 (to V.P. and P.C.), the laboratory of excellence DISTALZ (ANR-11-LABX-0009 to VP) and I-SITE ULNE (ANR-16-IDEX-0004 ULNE to VP), the Association pour l'Etude des Anomalies Congénitales (AEAC) (to A.S.), and the National Institute of Health (USA) 1RO1 HD-084542

and 8P51OD011092 (to S.R.O).

AUTHOR CONTRIBUTIONS

A.S., A.-S. P. and V.P. designed the experiments. G.P., M.M., C.A., T.L., S.G., D.F., V.M., M. M.-L., A C.-R., V.D., D.M., A.L., M.T.S., P.C., A.S. and V.P. performed the experiments. A.S. and V.P. analyzed the data. J.S., G.C. and F.P. contributed material. All authors discussed the results and made edits to the manuscript. A.S., S.R., S.R.O. and V.P. wrote the manuscript.

COMPETING FINANCIAL INTERESTS

The authors declare no competing financial interests.

FIGURE LEGENDS

Figure 1. Postnatally-born astrocytes preferentially associate with GnRH neuronal cell bodies. (**a**) Experimental protocol. (**b**) Representative coronal section of the preoptic region immunolabeled for GnRH (green) and BrdU (magenta), nuclei counterstained with Hoechst (white), illustrating quantifications in **c**. Arrow, arrowheads: GnRH neuronal cell bodies. Inset: higher magnification of the GnRH neuron indicated, showing physical proximity to a $BrdU^+$ cell (yellow arrows). Scale bars: 100µm (main panel), 10 µm (inset). (**c**) Percentage of GnRH neurons associated with $BrdU^+$ cells 2h, 24h, 7d or 60d after a single BrdU injection at P1, P5, P8, P12, P20 or P24 (n=9,6,7,6,8,5,10,5,5,6,9,3,3,6,9,3,4,9,5 rats/group) (two-way ANOVA: age at BrdU injection, $F_{(5,73)}$=44.92, P<0.0001; survival time (2h, 7d), $F_{(1,73)}$=3.116, P=0.0817; interaction, $F_{(5,73)}$= 8.392, P< 0.0001; Tukey's multiple comparison test, P8+2h versus P8+7d: $q_{(73)}$ = 8.583, P<0.0001; P8, Kruskal-Wallis one-way ANOVA on ranks: $H_{(4)}$=20.98, P=0.0001; Dunn's multiple comparison: 2h versus 24h, P=0.0274; 2h versus 60d, P>0.9999). (**d**) Percentage of GnRH- or HuC/D-expressing neurons associated with $BrdU^+$ cells 2h or 7d after a single BrdU injection at P8 (% of GnRH neurons versus % of HuC/D^+

neurons associated with $BrdU^+$ cells: Mann-Whitney test, 2h: U=0, P=0.004; n=8,4 rats/group, respectively; 7d: U=0, P=0.002; n=10,4 rats/group).(**e**,**f**,**i-k**) Representative triple immunofluorescence labeling for GnRH (green), BrdU (magenta) and Sox2 (**e**, white), GFAP (**f,i,** white), APC (**j**, white) or HuC/D (**k**, white) in the female rat preoptic region injected with BrdU at P8 and sacrificed 2h (**e,f**) or 7d later (**i-k**), illustrating quantifications in **g**. Yellow arrows: $BrdU^+$ cells associated with GnRH neurons co-expressing the indicated markers. Scale bars: 20µm. (**g**) Percentage of $BrdU^+$ cells associated with GnRH neurons co-expressing Sox2, GFAP, APC or HuC/D in animals injected with BrdU at P8 and sacrificed 2h or 7d later (GFAP, Mann-Whitney test: U=0, P=0.0012, n=6,7 rats/group). (**h**) Co-immunolabeling for GnRH (green) and BrdU (magenta), nuclei counterstained with Hoechst (white), in female rats injected with BrdU thrice daily from P6 to P8 and sacrificed at P15, showing two GnRH neurons with companion $BrdU^+$ cells (yellow arrows). n=4 animals. Scale bar: 20µm. (**c**,**d**,**g**) Values: means ± s.e.m.; *P<0.05; **P<0.01; i.p., intraperitoneal; neo, neonatal period; OVLT, organum vasculosum laminae terminalis.

Figure 2. Inhibiting GnRH neuron association with newborn glia delays the onset of puberty and impairs mature estrous cyclicity. (**a**) Diagram of the experimental protocol, with a coronal view of the rat brain showing the anatomical localization of the microparticle implantation site (red line) in the preoptic region (dashed area). (**b, c**) Coronal sections from adult animals injected with blank- (b) or paclitaxel-loaded microparticles (c) at P6, immunolabeled for GnRH (green) and counterstained with the nuclear marker Hoechst (white). The region delimited by the dashed white line in **c** shows the hypocellular region around the injection site (asterisk). ac, anterior commissure. Scale bars: 200µm.(**d-g**) Cell nuclear density at the injection site (**d**: two-tailed unpaired t-test, $t_{(10)}$=4.366, P=0.0014, n=6 rats/group), number of $BrdU^+$ cells at the injection site (**e**: two-tailed unpaired t-test, $t_{(11)}$=4.2, P=0.0015; n=7,6 rats/group), percentage of GnRH neurons associated with $BrdU^+$ cells (**f**: two-tailed unpaired t-test with Welch's correction, $t_{(6.9)}$=4.24, P=0.0040; n=7 rats/group) and total number of GnRH neurons in the preoptic region (**g**: two-tailed unpaired t-test,

590 $t_{(15)}$=2.075, P=0.0556; n=7,10 rats/group) of control and paclitaxel-treated rats. (**h-i**)
591 Cumulative percentage (**h**) and age of vaginal opening (**i**: Mann-Whitney test: U=69.5,
592 P=0.0428, n=17,14 rats/group) in control and paclitaxel-treated rats. (**j-k**) Cumulative
593 percentage (**j**) and age of first estrus (**k**: Mann-Whitney test: U=32, P=0.0002, n=17,14
594 rats/group) in control and paclitaxel-treated rats. (**l**) Representative estrous cycle profiles of
595 control and paclitaxel-implanted animals showing the day of vaginal opening (vo) and first
596 estrus (red dot). The first paclitaxel-treated animal has a normal estrous cycle while the next
597 three are examples of altered estrous cyclicity. D, diestrus; E, estrus; P, proestrus. (**m**)
598 Difference between age at vaginal opening and at first estrus in control and paclitaxel-treated
599 animals (Mann-Whitney test: U=28.5, P<0.0001, n=17,14 rats/group). (**n**) Percentage of
600 complete estrous cycles in control and paclitaxel-treated animals (Mann-Whitney test:
601 U=80.5, P=0.0156, n=17,18 rats/group). (**d-g**,**i**,**k**,**m**-**n**) Values: means ± s.e.m.*P<0.05;
602 **P<0.01; ***P<0.001.
603
604 **Figure 3. Early exposure to bisphenol A inhibits infantile GnRH neuron-progenitor**
605 **association.** (**a**) Schematic of the protocol used to evaluate the effect of bisphenol A (BPA)
606 on the association between GnRH neurons and progenitors. (**b**) Percentage of GnRH
607 neurons associated with $BrdU^+$ cells in control and BPA-treated animals (one-way ANOVA:
608 $F_{(3,26)}$=16.6, P<0.0001, n=11,4, 8,7 rats/group; Tukey's multiple comparisons test: 2h control
609 versus 7d control, $q_{(26)}$=7.739, P<0.0001; 2h BPA versus 7d BPA, $q_{(26)}$=4.46, P=0.0198; 2h
610 control versus 2h BPA, $q_{(26)}$=1.412, P=0.7517). (**c**) Total number of $BrdU^+$ cells 2h and 7d
611 after a single injection of BrdU at P8 in animals treated with BPA from P1 to P15 (two-tailed
612 unpaired t-test, $t_{(11)}$=0.4553, P=0.6578; n=6,7 rats/group). (**b,c**) Values: means ±
613 s.e.m.*P<0.05; ***P<0.001.
614
615 **Figure 4. PGD2 is a chemoattractant for preoptic progenitor cells *in vitro*.** (**a**)
616 Immunofluorescence labeling for Sox2, nestin and BLBP in one primary progenitor culture
617 representative of three independent cultures. Cell nuclei were stained with Hoechst (blue).

Insets: higher magnification views of cells co-expressing the three markers (arrows). Scale bars: 50µm. (**b**) Quantification of transwell assays showing the effect of different factors on the migration of preoptic progenitor cells across a porous membrane. Epidermal growth factor (EGF) was used as a positive control[61] (Kruskal-Wallis one-way ANOVA on ranks: $H_{(6)}$=25.731, P<0.001; Dunn's multiple comparison method: control versus treatment: PGD2, $Q_{(6)}$=4.255, P<0.001; EGF, $Q_{(6)}$=3.925, P=0.0018; n=18,19,12,17,10,10,12 wells/condition; N=5 independent experiments). (**c**) Strategy used to identify astrocyte-regulated gene expression in GnRH neurons (See **Supplementary Data 1**). (**d**) Real-time PCR analysis of *Ptgds* mRNA levels in GnV3 cells treated with hypothalamic astrocyte-conditioned medium (ACM) or non-conditioned medium (control) (Mann-Whitney test: U=195, P<0.001; n=13,15 replicates/condition; N=3 independent experiments). ACM values are expressed relative to control values, arbitrarily set at 1. (**e**) Percentage of preoptic progenitor cells expressing the proliferation marker Ki67 after *in vitro* treatment with the same factors as in **b**. Fibroblast growth factor 2 (FGF2) was used as a positive control[62] (Kruskal-Wallis one-way ANOVA on ranks: $H_{(6)}$=38.576, P<0.001; Dunn's multiple comparison method: control versus FGF2, $Q_{(6)}$=4.798, P<0.001; n=23,22,16,17,15,16,16 wells/condition; N = 3 independent experiments). (**f**) Real-time PCR analysis of *Ptgdrl* and *Gpr44* mRNA levels in primary preoptic progenitor cell cultures (n=4 cultures). Values expressed relative to mRNA levels in the total brain, arbitrarily set at 1 (blue line). (**g**) Representative photomicrographs of the Hoechst-stained lower side of transwell assay membranes, illustrating quantifications in **h**. Scale bar: 100µm. (**h**) Quantification of transwell assays (Kruskal-Wallis one-way ANOVA on ranks: $H_{(5)}$=25.995, P<0.001; Dunn's multiple comparison method: control versus PGD2, $Q_{(5)}$=3.277, P=0.0157; PGD2 versus PGD2 + BWA 10nM, $Q_{(5)}$=3.321, P=0.0135; PGD2 versus PGD2 + BWA 1µM, $Q_{(5)}$=4.548, P<0.001; n=11,11,12,12,11,10 wells/condition; N=3 independent experiments). (**i**) ERK1/2 phosphorylation (pERK) in progenitors treated with PGD2 (1µM) and/or the DP1 receptor antagonist BWA868C (BWA). Representative immunoblot of three independent experiments. tERK, total ERK. (**b,d**-**f**,**h**) Values: means ± s.e.m.*P<0.05; **P <0.01; ***P<0.001.

Figure 5. *In vivo* expression of *Ptgds* and *PtgdrI* in the preoptic region of infantile female rats. (**a**) Procedure used to isolate GnRH neurons from the preoptic region (POA) of GnRH-EGFP transgenic rats. FACS, fluorescence-activated cell sorting; Pos, EGFP-positive fraction; Neg, EGFP-negative fraction. (**b,c**) Real-time PCR analysis of the expression of *Ptgds* mRNA in EGFP-positive- (b) or negative cells (c) at different postnatal ages (**b**: Kruskal-Wallis one-way ANOVA on ranks: $H_{(2)}$=7.476, P=0.024, n=10 rats/group; Dunn's multiple comparisons method: P8 versus P20, $Q_{(2)}$=3.844, P=0.0191; **c**: Kruskal-Wallis one-way ANOVA on ranks: $H_{(2)}$=5.280, P=0.071, n=10 rats/group). Values expressed relative to P8 values, arbitrarily set at 1. n.s., non-significant. (**d**) Representative confocal images of fluorescent *in situ* hybridization for *Gnrh*, *Sox2*, *Ptgds* and *PtgdrI* mRNAs in the preoptic region of P8 female rats, illustrating quantifications in **e-h**. (Upper row) Arrow: a GnRH neuron containing *Ptgds* mRNA (magenta dots) and surrounded by *Sox2*-expressing cells (arrowheads, white dots). (Lower row) Arrow: a GnRH neuron surrounded by *Sox2*-expressing cells (white arrowheads). Purple arrowheads: two *Sox2*-expressing cells next to the GnRH neuron, co-expressing *PtgdrI* mRNA (magenta dots). No such dots could be seen in any section of the negative controls (see methods). Sections were counterstained with the nuclear marker DAPI (blue). Scale bar: 5µm. (**e,f**) Percentage of GnRH neurons that contain *Ptgds* mRNA (**e**: one-way ANOVA: $F_{(2,16)}$=10.96, P=0.001, n=7,6,6 rats/group; Tukey's multiple comparison test: P8 versus P12, $q_{(16)}$=5.185, P=0.0056; P8 versus P20, $q_{(16)}$=6.046, P=0.0016) and of the average number of *Ptgds* dots per *Ptgds*-expressing GnRH neuron (**f**: Kruskal-Wallis one-way ANOVA on ranks: $H_{(3)}$=5.484, P=0.0585, n=7,6,6 rats/group) determined from fluorescent *in situ* hybridization experiments. (**g,h**) Percentage of *Sox2*-expressing cells that contain *PtgdrI* mRNAs (**g**: one-way ANOVA: $F_{(2,15)}$=1.528, P=0.2489, n=6 rats/group) and average number of *PtgdrI* dots per *Sox2/PtgdrI*-co-expressing cell (**h**: Kruskal-Wallis one-way ANOVA on ranks: $H_{(3)}$=3.029, P=0.2306, n=6 rats/group) determined from fluorescent *in situ* hybridization experiments. (**b-c**,**e**-**h**) Values: means ± s.e.m.*P<0.05; **P<0.01.

Figure 6. **Activation of DP1 signaling in the infantile preoptic region controls GnRH neuron-progenitor association, and is involved in sexual maturation**. (**a**) Protocol used to evaluate the involvement of DP1 signaling in the recruitment of progenitors by GnRH neurons. Drawing: coronal view of the rat brain showing the anatomical localization of the injection site, i.e. the preoptic region (dashed area). i.c., intracerebral; i.p., intraperitoneal. (**b**) Percentage of GnRH neurons associated with $BrdU^+$ cells 24h after a single BrdU injection at P7 in the absence (control) or presence of the DP1 antagonist BWA868C (BWA) (one-way ANOVA: $F_{(2,11)}$=12.933, P=0.001, n=4,5,5 rats/group; Tukey's multiple comparison test: 2h versus 24h groups: 24h-control, $q_{(11)}$=6.778, P=0.002; 24h-BWA, $q_{(11)}$=1.763, P=0.452; 24h-control versus 24h-BWA, $q_{(11)}$=5.319, P=0.008).(**c**) Total number of $BrdU^+$ cells in the preoptic region of control or BWA-treated animals (one-way ANOVA: $F_{(2,11)}$=20.887, P<0.001, n=4,5,5 rats/group; Tukey's multiple comparison test: 2h versus 24h-control, $q_{(11)}$=8.019, P<0.001; 2h versus 24h-BWA, $q_{(11)}$=8.102, P<0.001; 24h-control versus 24h-BWA, $q_{(11)}$=0.0883, P=0.998). (**d**) Protocol used to evaluate the involvement of DP1 signaling in sexual maturation. (**e**) Percentage of GnRH neurons associated with $BrdU^+$ cells 7d after a single BrdU injection at P8 in the absence or presence of BWA868C (two-tailed unpaired t-test, $t_{(6)}$=2.532, P=0.045; n=3,5 rats/group). (**f**) Total number of $BrdU^+$ cells in the preoptic region of control or BWA-treated animals (two-tailed unpaired t-test, $t_{(6)}$=0.771, P=0.470; n=3,5 rats/group). (**g**) Circulating FSH levels at P12 in BWA868C (BWA)-injected- and control animals (two-tailed unpaired t-test, $t_{(20)}$=3.075, P=0.006; n=8,14 rats/group). Values: means ± s.e.m.; *P<0.05; **P<0.01; ***P<0.001.

Figure 7. Blocking DP1 signaling in the infantile period impairs GnRH neuron maturation and functional activation. (**a,c**) RT-PCR in control versus BWA868C-treated FACS-sorted GnRH-EGFP neurons for (**a**) *Gnrh* and upstream regulators (Mann-Whitney tests: *Gnrh*, U=27, P=0.7925; *Cebpb*, U=8, P=0.0426; *Kiss1r*, U=27, P>0.9999; two-tailed unpaired t-tests: *Dicer*, $t_{(13)}$=0.6232, P=0.5439; *Otx2*, $t_{(11)}$=0.7906, P=0.4459; *Zeb1*,

$t_{(14)}$=0.2605, *P*=0.7983; *n*=6,10,6,8,6,9,6,9,5,8,6,10 rats/group) and (**c**) prostaglandin pathway genes (Mann-Whitney tests: *Ptgs-2*, *U*=18, *P*=0.3277; *Ptges*, *U*=19, *P*=0.3884; *Ptger1*, *U*=4, *P*=0.0140; *Ptger2*, *U*=16, *P*=0.2238; *Ptger3*, *U*=4, *P*=0.0048; two-tailed unpaired *t*-tests: *Pla2g4a*, $t_{(14)}$=0.1837, *P*=0.8569; *Ptgs-1*, $t_{(13)}$=0.1135, *P*=0.9113; *Ptgds*, $t_{(11)}$=2.671, *P*=0.0218; *Ptger4*, $t_{(14)}$=1.656, *P*=0.12; *n*=6,10,6,9,6,9,6,7,6,9,6,7,6,9,6,9,6,10 rats/group). Values expressed relative to control values, set at 1. (**b**) Prostaglandin biosynthesis. (**d**) Representative GnRH neuronal soma (red) with apposed vGluT2- (*left*, green) and vGaT- (*right*, green) immunoreactive (ir) punctae (arrowheads) in control (*top*) and BWA868C-treated animals (*bottom*). Scale bar: 10µm. *Bar graphs*: vGluT2- (two-tailed unpaired *t*-test, $t_{(12)}$=3.057, *P*=0.0099; *n*=7 rats/group) and vGaT-immunoreactive punctae (two-tailed unpaired *t*-test, $t_{(10)}$=1.61, *P*=0.1384; *n*=6 rats/group) per GnRH soma. (**e**) Representative fluorescent (*top*) and infrared-differential-interference-contrast (IR-DIC) (*bottom*) photomicrographs of acute brain slice from a *Gnrh::Egfp* infantile female rat, showing a patched preoptic GnRH neuron (green). Scale bar: 25µm. (**f**) *Left*: Whole-cell recording of spontaneous activity in representative GnRH neurons from control (*top*) and BWA868C-treated (*bottom*) animals. Arrowhead bottom left: resting membrane potential. *Right*: Expansion of action potentials (APs) indicated at left. Note: Control cell APs (*top*) were driven by temporal summation of small-amplitude depolarizing events (oblique lines in expansion), while APs from BWA868C-treated animals (*bottom*) were preceded by a smooth, relatively fast depolarization without synaptic events, except in recording #3. Threshold for AP generation: dashed line. (**g**-**j**) Electrophysiological cell properties: mean resting membrane potential (Vm) (**g**: Mann-Whitney test: *U*=602, *P*=0.760; *n*=37 cells, 21 control rats; *n*=34 cells, 14 BWA868C-treated rats), membrane resistance (Rm) (**h**: Mann-Whitney test: *U*=157, *P*=0.589; *n*=16 cells, 8 control rats; *n*=22 cells, 7 BWA868C-treated rats), voltage threshold for AP generation (VTH) (**i**: two-tailed unpaired *t*-test, $t_{(18)}$=0.963, *P*=0.348; *n*=10 cells, 8 control rats; *n* = 10 cells, 8 BWA868C-treated rats), spontaneous firing rate (**j**: Mann-Whitney test: *U*=285.5, *P*<0.0001; *n*=37 cells, 21 control rats; *n*=34 cells, 14 BWA868C-treated rats). Values: means ± s.e.m.; **P*<0.05; ***P*<0.01; ****P*<0.001.

730

731 **Figure 8. Inhibition of DP1 signaling in the infantile period leads to perturbed estrous**
732 **cyclicity.** (**a**) Examples of estrous cycles in two control (*upper panels*) and two BWA-treated
733 animals (*lower panels*). Red dots: first estrus. D, diestrus; E, estrus; P, proestrus; vo, vaginal
734 opening. (**b**) Age at vaginal opening in BWA868C (BWA)-treated and control animals (two-
735 tailed unpaired *t*-test, $t_{(17)}$=0.837, *P*=0.414; *n*=9,10 rats/group). (**c**) Quantification of time
736 spent in the different phases of the estrous cycle during the first 15 days after vaginal
737 opening in control and BWA-treated animals (Diestrus, two-tailed unpaired *t*-test, $t_{(17)}$=-1.160,
738 *P*=0.262; Proestrus, Mann-Whitney test: *U*=12.5, *P*=0.006; Estrus, Mann-Whitney test:
739 *U*=71.5, *P*=0.023; *n*=9,10 rats/group).(**b-c**) Values: means ± s.e.m.*$P<0.05$; **$P<0.01$.

740

741

REFERENCES

1. Moffitt, J.R.*, et al.* Molecular, spatial, and functional single-cell profiling of the hypothalamic preoptic region. *Science* **362** (2018).
2. Casoni, F.*, et al.* Development of the neurons controlling fertility in humans: new insights from 3D imaging and transparent fetal brains. *Development* **143**, 3969-3981 (2016).
3. Chachlaki, K., Garthwaite, J. & Prevot, V. The gentle art of saying NO: how nitric oxide gets things done in the hypothalamus. *Nat Rev Endocrinol* **13**, 521-535 (2017).
4. Messina, A.*, et al.* A microRNA switch regulates the rise in hypothalamic GnRH production before puberty. *Nat Neurosci* **19**, 835-844 (2016).
5. Prevot, V. Puberty in mice and rats. in *Knobil and Neill's Physiology of Reproduction* (ed. T.M. Plant & J. Zeleznik) pp 1395-1439 (Elsevier, New York, 2015).
6. Clasadonte, J. & Prevot, V. The special relationship: glia-neuron interactions in the neuroendocrine hypothalamus. *Nat Rev Endocrinol* **14**, 25-44 (2018).
7. Sloan, S.A. & Barres, B.A. Mechanisms of astrocyte development and their contributions to neurodevelopmental disorders. *Curr Opin Neurobiol* **27**, 75-81 (2014).
8. Verkhratsky, A. & Nedergaard, M. Physiology of Astroglia. *Physiol Rev* **98**, 239-389 (2018).
9. Barnabe-Heider, F.*, et al.* Evidence that embryonic neurons regulate the onset of cortical gliogenesis via cardiotrophin-1. *Neuron* **48**, 253-265 (2005).
10. Bandeira, F., Lent, R. & Herculano-Houzel, S. Changing numbers of neuronal and non-neuronal cells underlie postnatal brain growth in the rat. *Proc Natl Acad Sci U S A* **106**, 14108-14113 (2009).
11. Elkharraz, K.*, et al.* Paclitaxel-loaded microparticles and implants for the treatment of brain cancer: preparation and physicochemical characterization. *Int J Pharm* **314**, 127-136 (2006).
12. Wang, L.*, et al.* Genetic dissection of the different roles of hypothalamic kisspeptin neurons in regulating female reproduction. *Elife* **8** (2019).
13. Mohr, M.A., DonCarlos, L.L. & Sisk, C.L. Inhibiting Production of New Brain Cells during Puberty or Adulthood Blunts the Hormonally Induced Surge of Luteinizing Hormone in Female Rats. *eNeuro* **4** (2017).
14. Lopez-Rodriguez, D., Franssen, D., Bakker, J., Lomniczi, A. & Parent, A.S. Cellular and molecular features of EDC exposure: consequences for the GnRH network. *Nat Rev Endocrinol* **17**, 83-96 (2021).
15. Geens, T.*, et al.* A review of dietary and non-dietary exposure to bisphenol-A. *Food Chem Toxicol* **50**, 3725-3740 (2012).
16. Franssen, D.*, et al.* Delayed Neuroendocrine Sexual Maturation in Female Rats After a Very Low Dose of Bisphenol A Through Altered GABAergic Neurotransmission and Opposing Effects of a High Dose. *Endocrinology* **157**, 1740-1750 (2016).
17. Kuiri-Hanninen, T., Sankilampi, U. & Dunkel, L. Activation of the hypothalamic-pituitary-gonadal axis in infancy: minipuberty. *Horm Res Paediatr* **82**, 73-80 (2014).
18. Ciofi, P. Phenotypical segregation among female rat hypothalamic gonadotropin-releasing hormone neurons as revealed by the sexually dimorphic coexpression of cholecystokinin and neurotensin. *Neuroscience* **99**, 133-147 (2000).
19. Chachlaki, K.*, et al.* Phenotyping of nNOS neurons in the postnatal and adult female mouse hypothalamus. *J Comp Neurol* **525**, 3177-3189 (2017).
20. Mansuy, V.*, et al.* Phenotypic and molecular characterization of proliferating and differentiated GnRH-expressing GnV-3 cells. *Mol Cell Endocrinol* **332**, 97-105 (2011).
21. Hirai, H.*, et al.* Prostaglandin D2 selectively induces chemotaxis in T helper type 2 cells, eosinophils, and basophils via seven-transmembrane receptor CRTH2. *J Exp Med* **193**, 255-261 (2001).
22. Ohinata, K.*, et al.* Central prostaglandin D(2) stimulates food intake via the neuropeptide Y system in mice. *FEBS Lett* **582**, 679-684 (2008).
23. Tokudome, S.*, et al.* Glucocorticoid protects rodent hearts from ischemia/reperfusion injury by activating lipocalin-type prostaglandin D synthase-derived PGD2 biosynthesis. *J Clin Invest* **119**, 1477-1488 (2009).

24. Kato, M., Ui-Tei, K., Watanabe, M. & Sakuma, Y. Characterization of voltage-gated calcium currents in gonadotropin-releasing hormone neurons tagged with green fluorescent protein in rats. *Endocrinology* **144**, 5118-5125 (2003).
25. Ma, Y.J., Junier, M.P., Costa, M.E. & Ojeda, S.R. Transforming growth factor-alpha gene expression in the hypothalamus is developmentally regulated and linked to sexual maturation. *Neuron* **9**, 657-670 (1992).
26. Rage, F., Lee, B.J., Ma, Y.J. & Ojeda, S.R. Estradiol enhances prostaglandin E2 receptor gene expression in luteinizing hormone-releasing hormone (LHRH) neurons and facilitates the LHRH response to PGE2 by activating a glia-to-neuron signaling pathway. *J.Neurosci.* **17**, 9145-9156 (1997).
27. Lomniczi, A., Wright, H. & Ojeda, S.R. Epigenetic regulation of female puberty. *Front Neuroendocrinol* **36**, 90-107 (2015).
28. Boehm, U., Zou, Z. & Buck, L.B. Feedback loops link odor and pheromone signaling with reproduction. *Cell* **123**, 683-695 (2005).
29. Yoon, H., Enquist, L.W. & Dulac, C. Olfactory inputs to hypothalamic neurons controlling reproduction and fertility. *Cell* **123**, 669-682 (2005).
30. Clasadonte, J., Scemes, E., Wang, Z., Boison, D. & Haydon, P.G. Connexin 43-Mediated Astroglial Metabolic Networks Contribute to the Regulation of the Sleep-Wake Cycle. *Neuron* **95**, 1365-1380 e1365 (2017).
31. Araque, A.*, et al.* Gliotransmitters travel in time and space. *Neuron* **81**, 728-739 (2014).
32. Clasadonte, J.*, et al.* Prostaglandin E2 release from astrocytes triggers gonadotropin-releasing hormone (GnRH) neuron firing via EP2 receptor activation. *Proc Natl Acad Sci U S A* **108**, 16104-16109 (2011).
33. Glanowska, K.M. & Moenter, S.M. Endocannabinoids and prostaglandins both contribute to GnRH neuron-GABAergic afferent local feedback circuits. *J Neurophysiol* **106**, 3073-3081 (2011).
34. Bezzi, P.*, et al.* Prostaglandins stimulate calcium-dependent glutamate release in astrocytes. *Nature* **391**, 281-285 (1998).
35. Zonta, M.*, et al.* Neuron-to-astrocyte signaling is central to the dynamic control of brain microcirculation. *Nat.Neurosci.* **6**, 43-50 (2003).
36. Dziedzic, B.*, et al.* Neuron-to-glia signaling mediated by excitatory amino acid receptors regulates ErbB receptor function in astroglial cells of the neuroendocrine brain. *J.Neurosci.* **23**, 915-926 (2003).
37. Prevot, V.*, et al.* Normal female sexual development requires neuregulin-erbB receptor signaling in hypothalamic astrocytes. *J.Neurosci.* **23**, 230-239 (2003).
38. Nagai, J.*, et al.* Behaviorally consequential astrocytic regulation of neural circuits. *Neuron* **109**, 576-596 (2021).
39. Bouret, S.G., Draper, S.J. & Simerly, R.B. Trophic action of leptin on hypothalamic neurons that regulate feeding. *Science* **304**, 108-110 (2004).
40. Caron, E., Ciofi, P., Prevot, V. & Bouret, S.G. Alteration in neonatal nutrition causes perturbations in hypothalamic neural circuits controlling reproductive function. *J Neurosci* **32**, 11486-11494 (2012).
41. Paul, A., Chaker, Z. & Doetsch, F. Hypothalamic regulation of regionally distinct adult neural stem cells and neurogenesis. *Science* **356**, 1383-1386 (2017).
42. Sandau, U.S.*, et al.* SynCAM1, a synaptic adhesion molecule, is expressed in astrocytes and contributes to erbB4 receptor-mediated control of female sexual development. *Endocrinology* **152**, 2364-2376 (2011).
43. Sandau, U.S.*, et al.* The synaptic cell adhesion molecule, SynCAM1, mediates astrocyte-to-astrocyte and astrocyte-to-GnRH neuron adhesiveness in the mouse hypothalamus. *Endocrinology* **152**, 2353-2363 (2011).
44. Allen, N.J. & Eroglu, C. Cell Biology of Astrocyte-Synapse Interactions. *Neuron* **96**, 697-708 (2017).
45. Verkhratsky, A., Matteoli, M., Parpura, V., Mothet, J.P. & Zorec, R. Astrocytes as secretory cells of the central nervous system: idiosyncrasies of vesicular secretion. *EMBO J* **35**, 239-257 (2016).
46. Kofuji, P. & Araque, A. G-Protein-Coupled Receptors in Astrocyte-Neuron Communication. *Neuroscience* **456**, 71-84 (2021).

47. Ullian, E.M., Sapperstein, S.K., Christopherson, K.S. & Barres, B.A. Control of synapse number by glia. *Science* **291**, 657-661 (2001).
48. Pfrieger, F.W. & Barres, B.A. Synaptic efficacy enhanced by glial cells in vitro. *Science* **277**, 1684-1687 (1997).
49. Papouin, T., Dunphy, J.M., Tolman, M., Dineley, K.T. & Haydon, P.G. Septal Cholinergic Neuromodulation Tunes the Astrocyte-Dependent Gating of Hippocampal NMDA Receptors to Wakefulness. *Neuron* **94**, 840-854 e847 (2017).
50. Mu, Y.*, et al.* Glia Accumulate Evidence that Actions Are Futile and Suppress Unsuccessful Behavior. *Cell* **178**, 27-43 e19 (2019).
51. Bourguignon, J.P., Gerard, A., Alvarex-Gonzalez, M.L., Fawe, L. & Franchimont, P. Gonadal-independent developmental changes in activation of N-methyl-D-aspartate receptors involved in gonadotropin-releasing hormone secretion. *Neuroendocrinology* **55**, 634-641 (1992).
52. Carbone, S., Szwarcfarb, B., Otero Losada, M.E. & Moguilevsky, J.A. Effects of ovarian steroids on the gonadotropin response to N-methyl-D-aspartate and on hypothalamic excitatory amino acid levels during sexual maturation in female rats. *Endocrinology* **130**, 1365-1370 (1992).
53. DeFazio, R.A., Heger, S., Ojeda, S.R. & Moenter, S.M. Activation of A-type gamma-aminobutyric acid receptors excites gonadotropin-releasing hormone neurons. *Mol Endocrinol* **16**, 2872-2891 (2002).
54. Berg, T., Silveira, M.A. & Moenter, S.M. Prepubertal Development of GABAergic Transmission to Gonadotropin-Releasing Hormone (GnRH) Neurons and Postsynaptic Response Are Altered by Prenatal Androgenization. *J Neurosci* **38**, 2283-2293 (2018).
55. Sardi, S.P., Murtie, J., Koirala, S., Patten, B.A. & Corfas, G. Presenilin-dependent ErbB4 nuclear signaling regulates the timing of astrogenesis in the developing brain. *Cell* **127**, 185-197 (2006).
56. Veiga-Lopez, A., Beckett, E.M., Abi Salloum, B., Ye, W. & Padmanabhan, V. Developmental programming: prenatal BPA treatment disrupts timing of LH surge and ovarian follicular wave dynamics in adult sheep. *Toxicol Appl Pharmacol* **279**, 119-128 (2014).
57. Rasier, G.*, et al.* Mechanisms of interaction of endocrine-disrupting chemicals with glutamate-evoked secretion of gonadotropin-releasing hormone. *Toxicol Sci* **102**, 33-41 (2008).
58. Muncke, J.*, et al.* Impacts of food contact chemicals on human health: a consensus statement. *Environ Health* **19**, 25 (2020).
59. O'Brien, E., Dolinoy, D.C. & Mancuso, P. Perinatal bisphenol A exposures increase production of pro-inflammatory mediators in bone marrow-derived mast cells of adult mice. *J Immunotoxicol* **11**, 205-212 (2014).
60. Lamartiniere, C.A., Jenkins, S., Betancourt, A.M., Wang, J. & Russo, J. Exposure to the Endocrine Disruptor Bisphenol A Alters Susceptibility for Mammary Cancer. *Horm Mol Biol Clin Investig* **5**, 45-52 (2011).
61. Burrows, R.C., Wancio, D., Levitt, P. & Lillien, L. Response diversity and the timing of progenitor cell maturation are regulated by developmental changes in EGFR expression in the cortex. *Neuron* **19**, 251-267 (1997).
62. Gensburger, C., Labourdette, G. & Sensenbrenner, M. Brain basic fibroblast growth factor stimulates the proliferation of rat neuronal precursor cells in vitro. *FEBS Lett* **217**, 1-5 (1987).

METHODS

Animals. Sprague-Dawley rats were obtained from Janvier Laboratories (Saint Berthevin, France). GnRH-EGFP transgenic rats, which express the enhanced green fluorescent protein (EGFP) under the control of the rat GnRH promoter (NBRP Rat No: 0469, The

National BioResource Project for the Rat, Japan) [24, 63] was a kind gift from Dr. Masakatsu Kato (University of Tokyo Health Sciences, Tokyo, Japan). Wild-type and transgenic mice expressing a dominant-negative form of the ErbB4 receptor in astrocytes (*GFAP*::*DN-ErbB4*) were generated as described previously [37]. The animals were maintained at 23-25°C on a 12-h light-dark cycle, with food and water available *ad libitum*. Animal studies were approved by the Institutional Ethics Committee for the Care and Use of Experimental Animals of the University of Lille (APAFIS#2617-2015110517317420 v5). The bisphenol A treatment experiment was performed on Wistar rats purchased from the University of Liège and carried out with the approval of the Belgian Ministry of Agriculture and the Ethical Committee at the University of Liège. Animals were raised in polypropylene cages (Ref 1291H006, Tecnilab, 323 Netherlands), fed with low phytoestrogen chow (V135 R/Z low phytoestrogen pellets, SSNIFF 324 Diet, Netherlands). Water was supplied in glass bottles to reduce EDC contamination. All experiments were performed in accordance with the guidelines for animal use specified by the European Union Council Directive of September 22, 2010 (2010/63/EU). All experiments were performed in female animals, except the preparation of primary cultures of preoptic progenitors, for which both sexes were used.

BrdU injections. Unless otherwise stated, animals received a single intraperitoneal (i.p.) injection of BrdU (Sigma) at a dose of 300 mg/kg body weight at different postnatal ages and were allowed to survive for 2h, 24h, 7 days or ≥ 60 days. A group of rats received 3 i.p. injections of BrdU (150 mg/kg) per day for 3 consecutive days (P6-P8) and were sacrificed at P15.

Stereotactic brain injection of paclitaxel-loaded microparticles. The preparation, physicochemical characterization and drug release kinetics of paclitaxel-loaded, poly(D,L-lactic-*co*-glycolic acid) (PLGA)-based microparticles have been described [11]. Briefly, Paclitaxel (Zyo Pharma Trade, Hamburg, Germany) was encapsulated into PLGA-based

microparticles at a drug loading of 40% (w/w) (Carlina Technologies, Angers, France). Drug-free microparticles were prepared accordingly without adding paclitaxel. Female rats at P6 or P7 (*n* = 35) were anesthetized with an i.p. dose of a mixture of ketamine hydrochloride (50 mg/ml; 60 mg/kg) and xylazine hydrochloride (2%; 10 mg/kg), secured in a stereotaxic apparatus, and injected medially with 1 µl of a suspension of 50 µg paclitaxel-loaded or drug-free microparticles in sterile water using a microsyringe with a 21 gauge needle (Hamilton, Reno, NV) into the preoptic region of the hypothalamus, dorsal to the MePO (bregma: 0.0 mm, 6 mm deep from the skull) [64]. All animals received an i.p. injection of BrdU at P8 and were sacrificed at adult age. Brains were processed for immunofluorescent labeling of BrdU, GnRH and GFAP, and cell nuclei counter-staining using the nuclear marker Hoechst or DAPI to determine the implantation site of microparticles. Animals with an implantation site located outside the preoptic region were excluded from the analysis.

Bisphenol-A treatment. Exposure to bisphenol A (BPA) was performed as described previously [16]. Briefly, female pups were subcutaneously injected (0.05 mL) with either vehicle (corn oil) or BPA (Ref 23,9658; Sigma-Aldrich) at a dose of 25 ng/kg.d. Injections were given every 24 hours from P1 to P15. All animals received an i.p. injection of BrdU at P8 and were sacrificed 2 hours or 7 days later. Brains were extracted and processed for immunofluorescent staining of BrdU and GnRH.

Stereotaxic brain infusions of BWA868C.

Acute injections. Female rats received an i.p. injection of BrdU at P7. A group of animals (*n* = 4) was sacrificed 2h after the injection. The other animals were placed in a stereotaxic frame (Kopf® Instruments, California) under anesthesia (isoflurane), and 2 burr holes were drilled 0.5 mm apart from the bregma, according to a rat brain atlas [64]. A 10 µl Hamilton syringe was slowly inserted into the preoptic region (5.2 mm deep relative to the dura), and 1 µl of a solution containing 10 nM BWA868C (Cayman Chemical, Ann Arbor, Michigan, USA) (*n* = 5) or vehicle (saline solution 0.9%, *n* = 5) was injected bilaterally using an infusion pump (KD

Scientific, Holliston, MA) over 5 min. Animals were killed 24h later and their brains processed for immunofluorescent labeling of BrdU and GnRH.

BWA868C implants. Female rats were placed in a stereotaxic frame under anesthesia, and one burr hole was drilled at the level of the bregma as detailed above. A stainless steel 5 mm cannula filled at its tip with BWA868C (10 nM) or vehicle mixed with melted cocoa butter was stereotaxically implanted in the preoptic region at the level of the bregma, as previously described [65]. After implantation, the cannulas were fixed to the skull with superglue, and the skin wound sutured. Blood was collected via submandibular bleeding from animals at P12 for plasma FSH measurements using a procedure described previously by others [66].

Physiological measurements.

Puberty onset and estrous cyclicity. Animals were monitored daily for imperforation of the vaginal membrane (i.e. vaginal opening). After vaginal opening, vaginal smears were performed daily and analyzed under an inverted microscope to identify the specific day of the estrous cycle. The percentage of complete estrus cycles was calculated as the number of occurrences of the sequence “Diestrus-Diestrus-Proestrus-Estrus”, defined as a complete estrus cycle, divided by the theoretical maximum possible number of complete estrus cycles over the recorded period of time for each animal (> 2 weeks).

Follicle-stimulating hormone level measurements. Serum FSH levels were measured using radioimmunoassay as previously described [4]. The accuracy of hormone measurements was confirmed by the assessment of rodent serum samples of known concentration (external controls).

Electrophysiology.

Brain slices preparation. Electrophysiological recordings were performed on living brain slices containing the preoptic region from 10- to 15-days-old GnRH-EGFP transgenic rats. Rats were anesthetized with isoflurane and decapitated. The brain was removed and rapidly placed in ice-cold artificial cerebrospinal fluid (aCSF) containing (in mM): 120 NaCl, 3.2 KCl,

1 NaH_2PO_4, 26 $NaHCO_3$, 1 $MgCl_2$, 2 $CaCl_2$, 10 glucose (300 mOsm, pH 7.4) and bubbled with 95% O_2-5% CO_2. 200-μm coronal slices were cut using a vibratome (VT1200; Leica). Slices were incubated at 34°C in oxygenated aCSF for a recovery period of 1 hour, and then at room temperature until recording.

Patch-clamp recording. For patch-clamp recording, individual brain slices were placed in a submerged recording chamber (Warner Instruments), immobilized by a nylon grid and continuously perfused at 3 ml/min with oxygenated aCSF maintained at 32.8°C by a heater controller (TC-344C; Warner Instruments). GnRH neurons were visualized and identified under 10x and 40x magnification using an upright fluorescent microscope with infrared differential interference contrast (Leica DM-LFSA) and an ORCA-Flash 4.0 digital CMOS camera (Hamamatsu). Recording pipettes were pulled from borosilicate glass capillaries (1.5 mm outer diameter; 1.12 mm inner diameter; World Precision Instruments) using P1000 Flaming Brown puller (Sutter Instruments Co) and had resistance from 7 to 9 MΩ when filled with an internal solution containing (in mM): 140 K-gluconate, 10 KCl, 1 EGTA, 2 Na_2-ATP and 10 HEPES, pH 7.3 with KOH. Pipettes were placed in contact with GnRH neurons using a PCS-5400 micromanipulator (Thorlabs). Whole-cell patch-clamp recordings were performed in current-clamp mode using a Multiclamp 700B Amplifier, digitized with the Digidata 1322A interface and acquired with pClamp 10.2 software (Molecular Devices). Data were filtered at 1 kHz and sampled at 5 kHz. Recordings were analyzed with Clampfit 10.2 from pClamp software (Molecular Devices). Resting membrane potential, spontaneous firing rate, membrane resistance, voltage threshold for action potential generation, full amplitude and half width duration of action potentials, after-hyperpolarizing potential amplitude and duration, and time constant were determined as previously described [32, 67]. Only cells which showed less than 20% change in access resistance throughout the recording were included in this study. Junction potential was corrected in the data analysis.

Biocytin labeling of preoptic astrocytes. Slices were incubated during 30 minutes in 100 nM sulforhodamine 101 (SR101, Sigma), a fluorescent dye that is selectively taken up by astrocytes, and were pretreated for 20 minutes with 50 μM carbenoxolone (Sigma) to inhibit

gap junctions. Biocytin (2 mg/ml, Sigma) was added to the internal solution and astrocytes were patched in whole-cell configuration for 20 minutes. Electrical membrane properties of astrocytes were measured in voltage-clamp mode by applying a series of voltage pulses from -100 mV to +100 mV (300 ms, 10 mV increments) from a holding potential of -80 mV as previously described[30]. Astrocytes showed typical glial cell membrane properties including a highly polarized membrane potential and a linear current-voltage (I-V) relationship[30]. Slices were fixed with 4% paraformaldehyde overnight at 4°C, incubated with Streptavidin Alexa Fluor 647 (1:250, Invitrogen) in PBS containing 0.5% Triton X-100 overnight at 4°C, counterstained with DAPI (1:1000) and mounted on glass slides with Mowiol.

Preoptic neurosphere cultures. The preoptic region of female rats aged 10 or 19 days was dissected and minced on 80 µm nylon mesh (Buisine, Clermont de l'Oise, France). The dissected region corresponded to a 1-mm-thick triangular tissue located behind the diagonal band of Broca just before the OVLT, i.e., the beginning of the third ventricle, and the optic chiasm. We checked that our dissection excluded the subventricular zone of the lateral ventricle. The cell suspension was transferred to a culture flask (BD Biosciences, San Jose, CA) and cultured in neurosphere medium composed of Dulbecco's Modified Eagle's Medium (DMEM)/F-12 with L-glutamine, 15 mM HEPES (#31330-038) supplemented with 2% (v/v) B-27 (#17504-044), 20 ng/ml EGF (human recombinant; #PHG0311), 20 ng/ml FGF2 (human recombinant; #13256-029), 2 mM L-glutamine (25030-024), and 100 units of penicillin and 100 µg of streptomycin/ml (#15140-122) (all from Gibco, Carlsbad, CA) under a humid atmosphere of 5% CO2-95% air at 37°C. Cells were grown in hypoxic conditions by covering flask caps with parafilm. Neurospheres were formed after ~1 week. Thereafter, the neurospheres were collected twice a week through centrifugation, dissociated by mechanical trituration and passaged in half-renewed neurosphere medium to form further generations of neurospheres. Neurospheres were kept for up to 31 passages, the longest time examined.

Clonogenicity. To evaluate the generation of secondary neurospheres from single cells, primary neurospheres were dissociated into single cells by either mechanical dissociation

through 20 µm nylon mesh (Buisine) or enzymatic digestion using StemProAccutase Cell Dissociation Reagent (Gibco) for 10 min at room temperature. Cells were plated in 96-well culture plates at a density of 50, 75 or 100 cells per well in 50 µl of neurosphere medium. Wells containing cell aggregates 24h after plating were excluded from the analysis. Cultures were fed with 100 % (v/v) fresh neurosphere medium every 3 days until day 10, when wells were examined for the presence of neurospheres.

Differentiation experiments. To evaluate their differentiation potential, neurospheres were transferred to 24-well plates on poly-L-lysine (0.01%; #P4832, Sigma)-coated glass coverslips and grown in DMEM/F12 with L-glutamine, 15 mM HEPES (#31330-038) supplemented with 10% (v/v) fetal bovine serum (#10270106), 2 mM L-glutamine, and 100 units of penicillin and 100 µg of streptomycin/ml (all from Gibco) for 7 days.

Adherent cultures of preoptic progenitors. The preoptic region of rats aged 1 or 2 days was dissected as described above and minced on 20 µm nylon mesh (Buisine). The cell suspension was transferred to a culture flask (BD Biosciences) coated with poly-D-lysine (10 µg/ml, P7405, Sigma) and laminin (10 µg/ml, L6274, Sigma) and cultured in neurosphere medium under a humid atmosphere of 5% CO_2-95% air at 37°C. The medium was changed every 3 to 4 days. Cells were passaged once, when 70-80% confluence was reached, and were then used for migration assays, snap frozen in dry ice for gene expression analysis or seeded on 24-well plates glass coverslips for proliferation assays or immunocytochemical characterization.

GnV3 cell culture and treatment. Cells were grown in Neurobasal-A medium (10888-022) supplemented with 2% (v/v) B-27, 100 units of penicillin and 100 µg of streptomycin/ml, 25 mM GlutaMAX (35050-038), 1% fetal bovine serum, 50 µg/ml FGF2 (all from Gibco) and 1 µg/µl doxycycline (D-9891, Sigma) as described [68]. All experiments were performed on GnV3 cells at their 13th or 14th passage.

Preparation of hypothalamic astrocyte-conditioned medium. Primary astrocyte cultures were prepared from the hypothalamus of 1-2-day-old rat pups and grown in DMEM/F12 medium (#31330-038) supplemented with 10% (v/v) fetal bovine serum, 2 mM L-glutamine, and 100 units of penicillin and 100 µg of streptomycin/ml (all from Gibco) as previously described [36]. After reaching confluence (i.e., after ~7-10 days), contaminants were removed by overnight shaking. The growth medium was replaced by astrocyte-defined medium (ADM) composed of DMEM (41965-039) supplemented with 2 mM L-glutamine, 5 µg/ml insulin (I-5500, Sigma) and 100 µM putrescine (P-5780, Sigma). After two days, the culture medium (now ACM, astrocyte-conditioned medium) was collected, centrifuged at 1,000 rpm and the supernatant was kept at -80°C until use.

Treatment of GnV3 cells with hypothalamic astrocyte-conditioned medium. One day before treatment, GnV3 cells were plated at a density of $2x10^5$ cells/cm^2 in their growth medium. Cells were treated with ADM (control condition) or ACM for a total of 4 days, with a culture medium renewal after every 2 days. At the end of the 4-day treatment, GnV3 cells were collected in Trizol (Invitrogen) for microarray analysis or lysis buffer (Qiagen) for RT-qPCR analysis, and stored at -80°C until use. Treatment of GnV3 cells was performed in three experiments using ACM from three different primary astrocyte cultures.

***In vitro* migration assay.** Boyden microchemotaxis chambers were used according to the manufacturer's instructions (Neuro Probe, Gaithersburg MD, USA). In brief, primary preoptic progenitors were harvested, re-suspended in control medium (Neurobasal-A medium supplemented with 2% (v/v) B-27, 2 mM L-glutamine, and 100 units of penicillin and 100 µg of streptomycin/ml (all from Gibco)) and plated in 24-well plate chambers at a density of 150,000 cells per well on the open-bottom wells of the upper compartment, previously coated with poly-D-lysine and laminin. The two compartments of each well were separated by a polyvinylpyrrolidone-free polycarbonate porous membrane (8 µm pore size). The lower chamber was filled with control medium containing GnRH (100 ng/ml, GeneCust, Ellange, Luxembourg), PGD2 (1 µM, Sigma), galanin (2 µM, Tocris Bioscience, Bristol, UK),

glutamate (10 µM, Sigma), GABA (2 µM, Sigma) or EGF (100 ng/ml, Gibco). BWA868C (10 nM or 1 µM) was added to the cell suspension in the upper compartment. After 18h of incubation in 5% CO_2, 95% air at 37°C, cells attached to the upper side of the filter were mechanically removed with a cotton swab. Cells that had migrated to the lower side were fixed with 4% paraformaldehyde (30 minutes at room temperature) and stained with Hoechst (1:10,000). Cells were photographed with a 20x objective and counted using ImageJ 1.52p software (NIH, Bethesda).

***In vitro* proliferation assay.** Primary preoptic progenitors were transferred to 24-well plates on poly-D-lysine/laminin-coated glass coverslips and grown in neurosphere medium. Once cells were 70-80% confluent, they were transferred to neurosphere medium devoid of FGF2 (starvation medium) for 24h prior to treatment with GnRH, PGD2, galanin, glutamate, GABA (same concentrations as in migration assays) or FGF2 (100 ng/ml) in starvation medium for 24h. Coverslips were fixed and processed for Ki67 immunolabeling.

Immunofluorescence labeling

Tissue preparation. Animals were anesthetized by i.p. injection of pentobarbital (70 mg/kg). They were perfused transcardially with a rinse of saline solution (0.9% NaCl), followed by 100 ml of 4% paraformaldehyde in 0.1 M phosphate buffer(PB) (pH 7.4). The brains were removed and immersed in the same fixative for 2-3h at 4°C. They were then transferred to PB containing 20% sucrose until they had sunk, embedded in Tissue Tek® (Sakura Finetek, Villeneuve d'Ascq, France), and frozen in liquid nitrogen. Frozen 14-µm coronal sections containing the preoptic region (0.20 mm to -0.30 mm relative to bregma) [64] were prepared using a cryostat (CM3050S, Leica, Nussloch, Germany) and mounted on chrome-alum-gelatin coated slides, air-dried and subjected to immunolabeling.

Immunohistofluorescence. The sections were subjected to microwave pretreatment in a solution of sodium citrate 0.01 M (pH 6) for 4 minutes at 800 W followed by 2 cycles 5 minutes each at 400 W for antigen retrieval. After cooling at room temperature and washing

in PB, sections were incubated with primary antibodies (**Supplementary Table 1**) diluted in PB containing 0.9% sodium chloride, 0.3% Triton X-100 and 2% normal donkey serum (PBSTS) overnight at 4°C. Sections were then incubated with appropriate secondary antibodies at room temperature for 1h (**Supplementary Table 2**). After nuclei staining with Hoechst or DAPI (1/1,000), sections were coverslipped in Mowiol mounting medium (20% Mowiol, 2.5% DABCO in Tris 0.2 M pH 8.5). Control sections were incubated in the absence of primary antibody. Omission of the primary antibody resulted in no staining.

Immunocytofluorescence. Coverslips were fixed in 4% paraformaldehyde (15 min at room temperature), incubated with PBS 0.1 M containing 0.1% Triton X-100 and 0.3% normal donkey serum for 30 minutes at room temperature, and subjected to immunofluorescent labeling following the same procedure as for tissue sections. For O4 immunodetection, the anti-O4 antibody (**Supplementary Table 1**) was applied to living cells for 2h at 37°C before fixation.

Fluorescent *in situ* hybridization. FISH was performed on frozen brain sections of the preoptic region of female rats at P8, P12 and P20 with the RNAscope® Multiplex Fluorescent Kit v2 according to the manufacturer's protocol (Advanced Cell Diagnostics, Inc., Newark, CA, USA). Specific probes were used to detect *Ptgds* (486051, NM_013015.2, target region 2 - 702), *Ptgdrl* (486041, NM_022241.1, target region 224 - 1157), *Gnrh1* (502431-C2, NM_012767.2, target region 2 - 454) and *Sox2* (502441-C3, NM_001109181.1, target region 51 - 2079) mRNAs. Hybridization with a probe against the Bacillus subtilis dihydrodipicolinate reductase (dapB) gene (320871) was used as negative control.

Microscopy

Analysis of sections and acquisition of images were done using an Axio Imager Z2 Apo-Tome microscope equipped with a motorized stage (Zeiss, Germany) and an ORCA-Flash 4.0 V2 camera (Hamamatsu, Japan) driven by the Zen 2.3 (blue edition) imaging software (Zeiss). For FISH experiments and immunofluorescence labeling for vGluT2 and vGaT,

acquisition of images was performed using an inverted confocal microscope (LSM 710, Zeiss, Jena, Germany). High magnification photomicrographs were acquired with a 63x objective (NA 1.4) using the Airyscan detector (Zeiss). Images to be used for figures were pseudocolored, adjusted for brightness and contrast and merged using Adobe Photoshop 22.1.0 (Adobe Systems, San Jose, CA).

Microscopic analyses. All analyses were done in the preoptic region, as defined in the Swanson stereotaxic rat brain atlas, between plate 17 (i.e., beginning of the OVLT) and plate 20 (i.e., crossing of the anterior commissure) [69], with a particular attention to the MePO, where most GnRH neurons that stimulate the LH surge are located [70]. Analyses were made on one out of every 5 sections. Estimation of total cell populations in the preoptic region was obtained by multiplying the number of cells per section by the total number of sections per preoptic region, and then correcting for split nuclei [71].

Morphological association between GnRH neurons and BrdU$^+$ cells. Quantification was made under the fluorescent microscope at the 40x objective. A BrdU$^+$ cell was considered morphologically associated with a GnRH neuron when it was located at a distance ≤ the size of the BrdU$^+$ nucleus (i.e., ≤ 10 µm) from the GnRH neuron cell body with no interposed cell nucleus in between (**Supplementary Fig. 3**).

Number of cell nuclei at the injection site of microparticle-injected rats. The total number of Hoechst-stained nuclei was automatically quantified using the ImageJ software on microphotographs of the injection site taken at the 20x objective. Quantification represents the mean number of Hoechst-stained nuclei in a 20x microscopic field, corresponding to a surface area of 0.5 mm^2, counted on 3 sections per animal (n = 12).

Number of BrdU$^+$ cells at the injection site of microparticle-injected rats. Analysis was performed on photomontages of the preoptic region taken at the 20x objective. Quantification represents the mean number of BrdU$^+$ cells in a 1 mm square centered on the injection site, counted on 3 to 4 sections per animal (n = 13).

Quantification of vGluT2 and vGaT appositions to GnRH neuron cell bodies. Analysis was performed on high magnification images of GnRH neuron somata located at the level of the OVLT using the IMARIS 9.3 software (Bitplane) as described before [72]. Briefly, the number of vGluT2- or vGaT-immunoreactive punctae closely apposed with the GnRH neuron soma was quantified on 3D reconstructions from raw confocal image z-stacks using a channel of colocalization. A punctum was considered apposed when no black pixels were visible between the GnRH and the vGluT2 or vGaT fluorescence. The value was normalized to the number of optical sections through the z-depth of the neuron and the surface area of the neuronal soma. The resulting value was multiplied by the average number of optical sections and the average surface area of all neurons analyzed to provide a number of punctae per GnRH soma.

Western blot analyses. Preoptic primary progenitors were starved for 24h in DMEM/F-12 with L-glutamine, 15 mM HEPES supplemented with 2 mM L-glutamine, 100 units of penicillin and 100 µg of streptomycin/ml, 5 µg/ml insulin (Sigma) and 16 µg/ml putrescine (Sigma). The cells were treated with PGD2 1 µM and/or BWA868C (10 nM or 1 µM) in fresh medium for 7 minutes and snap-frozen on dry ice. Proteins were extracted and subjected to size-fractionation as previously described [4]. The proteins were then transferred onto 0.2 µm pore-size nitrocellulose membranes (Invitrogen) using the NuPAGE system (Invitrogen). Membranes were blocked for 1 h in blocking buffer (Tris buffer saline (0.05 M Tris, pH 7.4, 0.15 M NaCl) with 0.05% Tween 20 (TBST) and 5% nonfat milk) at room temperature and incubated overnight at 4°C with the appropriate primary antibody diluted in blocking buffer (rabbit polyclonal anti-phospho-p44/42 MAPK (Thr202/Tyr204) (pErk) #9101, 1:1,000; rabbit polyclonal anti-p44/42 MAPK (Erk) #9102, 1:1,000, Cell Signaling Technology, Beverly, MA, USA). After washing with TBST, membranes were exposed to horseradish peroxidase-conjugated secondary antibodies (goat anti-rabbit IgG, PI1000, 1:2000, Vector) diluted in blocking buffer for 1 h at room temperature. Immunoreactions were visualized using the ECL

detection kit (NEL101; PerkinElmer, Boston, MA). Immunoblots were scanned using a desktop scanner (Epson Expression 1680 PRO) and Adobe Photoshop.

Isolation of hypothalamic GnRH neurons using fluorescence-activated cell sorting. The preoptic regions of *Gnrh::Egfp* transgenic rats were microdissected and enzymatically dissociated using a Papain Dissociation System (Worthington, Lakewood, NJ) to obtain single-cell suspensions. FACS was performed using an ARIA SORP cell sorter cytometer and FACSDiva 8.0 software (BD Biosciences). Data were analyzed using the Kaluza 2.0 software (Beckman Coulter). The sort decision was based on measurements of EGFP fluorescence (excitation: 488 nm, 50 mW; detection: GFP bandpass 530/30 nm, autofluorescence bandpass 695/40 nm) by comparing cell suspensions from the preoptic region and from the cerebral cortex of *Gnrh::Egfp* animals. A total of 174 ± 20 (range, 44 – 700) EGFP-positive cells were sorted per animal and directly lysed into 10 µl of extraction buffer containing 0.1% Triton® X-100 (Sigma) and 0.4 unit/µl RNaseOUT™ (Life technologies).

Quantitative RT-PCR analyses. Gene expression analyses were performed on FACS-sorted GnRH neurons, primary preoptic progenitor cultures and GnV3 cells. For primary preoptic progenitors, RNAs were extracted as follows: 100 µl of Trizol (Life Scientific, Carlsbad CA, USA) were used to lyse cells before adding 100 µl of chloroform (Merck, Darmstadt, Germany) and centrifuging at 12,000 g for 15 minutes at 4°C. The aqueous phase was carefully collected and added to isopropanol at 1:1 before centrifuging at 12,000 g for 10 minutes at 4°C. The aqueous phase was then discarded and the pellet washed in 70% ethanol. After centrifugation at 12,000 g for 5 minutes at 4°C, the pellet was left to air-dry and then diluted in 10 µl DEPC water. The purity and quantity of RNA were determined by UV spectroscopy (Nanodrop 1000, Thermo Scientific, Waltham MA, USA). Messenger RNAs obtained from FACS-sorted GnRH neurons or primary progenitors were reverse transcribed using SuperScript® III Reverse Transcriptase (Life Technologies). For sorted cells, a linear

preamplification step was performed using the TaqMan®PreAmp Master Mix Kit protocol (Applied Biosystems). Real-time PCR was carried out on Applied Biosystems 7900HT Fast Real-Time PCR System using exon-boundary-specific TaqMan® Gene Expression Assays (Applied Biosystems) (**Supplementary Table 3**). Gene expression data were analyzed using SDS 2.4.1 and Data Assist 3.0.1 software (Applied Biosystems) with R45S and actin as control housekeeping mRNAs following a standardized procedure [73]. For GnV3 cells, RNAs were purified using the RNeasy Mini Kit (Qiagen, Basel, Switzerland) according to the manufacturer's instructions. The solution was treated with DNase (RNase-Free DNase Set, Qiagen, Basel, Switzerland) and eluted with 30 µl of water. RNA concentrations were determined with a Nanodrop® (ND-1000 Spectrophotometer, Witec, Luzern, Switzerland). Two hundred ng of RNA was reverse transcribed using the RT High Capacity RNA-to-cDNA Kit (Applied Biosystems, Rotkreuz, Switzerland). Real-Time PCR analysis was performed on 2 µl of cDNA using Power SYBR Green Taq polymerase master mix (Applied Biosystems, Rotkreuz, Switzerland). The primer sequences used were: Ptgds forward: 5'-TGGGTCTCTTGGGATTTCCA-3', Ptgds reverse: 5'-CCCCAGGAACTTGTCTTGTTG-3'; polymerase 2a (Polr2a, as endogenous control) forward: 5'-GTAAGGGCCACTATCTTCATCATCA-3', Polr2a reverse: 5'-CCCTCATCATACCTGGTCACATC-3'.

Microarray hybridization and data analysis. RNA purification and microarray hybridization were performed as previously described [20]. Total RNA was extracted from the cells using Trizol (Invitrogen), according to the manufacturer's instructions. Only RNA samples with RNA integrity numbers greater than 9.0 were accepted for microarray analysis. Microarray hybridization was performed with Affymetrix GeneChip Rat Gene 1.0 ST arrays according to the manufacturer's instructions and scanned with the Gene Array scanner (Affymetrix). The fluorescence images obtained were processed using the BioConductoraffy package (DAFL, Lausanne). Expression values were measured using the Robust Multi-array Average (RMA) algorithm generating expression values on a log2 scale. RMA includes background

correction, quantile normalization and probe set summary by robust regression. GnV3 signature of 22,336 transcripts was generated and annotated with Gene Symbol. Genes without an Entrez annotation were filtered out. The fold change was calculated individually for each gene. Differential hybridized features were identified using Bioconductor package "limma"[74]. Additionally, the false discovery rate, i.e. the expected proportion of rejected null hypotheses that are wrongly rejected, was estimated by a resampling procedure[75]. Genes that showed substantial up- or down-regulation by log fold changes (FC) > 1 with a FDR < 0.05 were considered as differentially expressed. For each condition (ADM or ACM), microarray analyses were performed using RNA samples derived from three wells per condition. Only the list of genes showing significant up and down-regulation is provided in the **Supplementary Data 1**.

Statistics. No statistical methods were used to pre-determine sample sizes but our sample sizes are similar to those reported in previous publications [4, 25, 26, 37, 76]. Studies were not formally randomized and investigators were not blind to treatment group. All analyses were performed using the SigmaStat 3.5 (Systat) or GraphPad Prism 7.05 (GraphPad) software. Outliers were identified using the ROUT (Q=1%) method. Statistical differences were evaluated using unpaired two-sided Student's *t*-tests for comparison of two groups and one- or two-way analysis of variance (ANOVA) with Tukey's *post hoc* tests for comparison of more than two groups. When the criterion for normality or equal variances was not met, the Mann-Whitney Rank Sum Test or the Kruskal-Wallis One Way ANOVA on Ranks Test was used to compare two or more groups, respectively. $P < 0.05$ was considered significant.

Data availability. Uncropped Western blots and Source Data Files for transcriptomic analysis of GnV3 cells are provided as Extended data. Additional data that support the findings of this study are available from the corresponding author upon request.

References.

63. Fujioka, H.*, et al.* Generation of transgenic rats expressing enhanced green fluorescent protein in gonadotropin-releasing hormone neurons. *J Reprod Dev* **49**, 523-529 (2003).
64. Paxinos, G. & Watson, C. *The rat brain in stereotaxic coordinates* (Academic press New York, 1982).
65. Ojeda, S.R. & Ramirez, V.D. Automatic control of LH and FSH secretion by short feedback circuits in immature rats. *Endocrinology* **84**, 786-797 (1969).
66. Golde, W.T., Gollobin, P. & Rodriguez, L.L. A rapid, simple, and humane method for submandibular bleeding of mice using a lancet. *Lab Anim (NY)* **34**, 39-43 (2005).
67. Altwegg-Boussac, T., Chavez, M., Mahon, S. & Charpier, S. Excitability and responsiveness of rat barrel cortex neurons in the presence and absence of spontaneous synaptic activity in vivo. *J Physiol* **592**, 3577-3595 (2014).
68. Salvi, R.*, et al.* Gonadotropin-releasing hormone-expressing neurons immortalized conditionally are activated by insulin: implication of the mitogen-activated protein kinase pathway. *Endocrinology* **147**, 816-826 (2006).
69. Swanson, L.W. *Structure of the rat brain* (Elsevier Science Publishers, Amsterdam, 2004).
70. Lee, W.S., Smith, M.S. & Hoffman, G.E. Luteinizing hormone-releasing hormone neurons express Fos protein during the proestrous surge of luteinizing hormone. *Proc Natl Acad Sci U S A* **87**, 5163-5167 (1990).
71. Abercrombie, M. Estimation of nuclear population from microtome sections. *Anat Rec* **94**, 239-247 (1946).
72. Tata, B.*, et al.* Elevated prenatal anti-Mullerian hormone reprograms the fetus and induces polycystic ovary syndrome in adulthood. *Nat Med* **24**, 834-846 (2018).
73. Schmittgen, T.D. & Livak, K.J. Analyzing real-time PCR data by the comparative C(T) method. *Nat Protoc* **3**, 1101-1108 (2008).
74. Smyth, G.K. Limma: Linear Models for Microarray Data. in *Bioinformatics and Computational Biology Solutions using R and Bioconductor* (ed. R. Gentleman, V. Carey, S. Dudoit, R. Irizarry & W. Huber) 397-420 (Springer, New York, 2005).
75. Storey, J.D. & Tibshirani, R. Statistical significance for genomewide studies. *Proc Natl Acad Sci U S A* **100**, 9440-9445 (2003).
76. Vanacker, C.*, et al.* Neuropilin-1 expression in GnRH neurons regulates prepubertal weight gain and sexual attraction. *EMBO J* **39**, e104633 (2020).

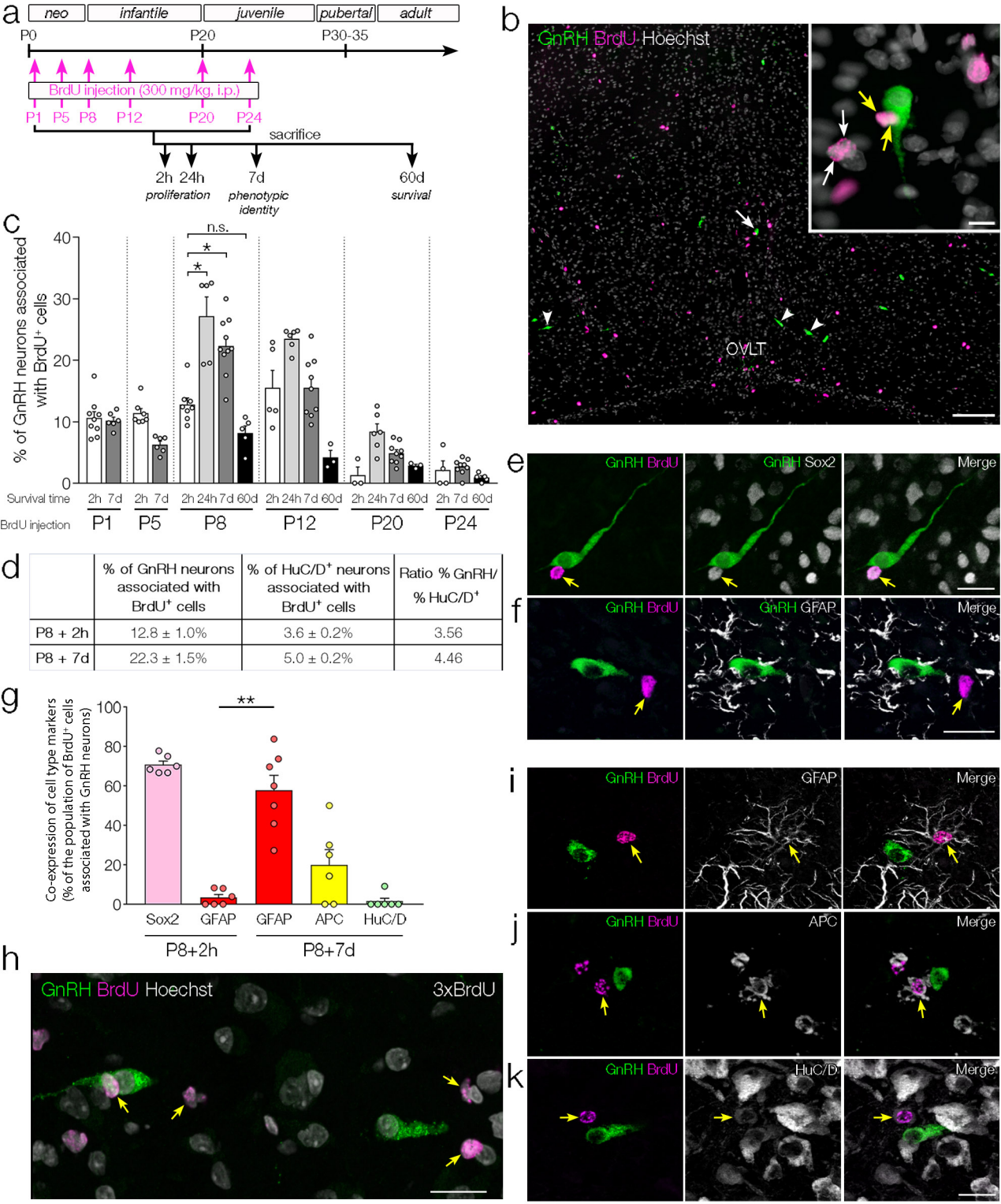

	% of GnRH neurons associated with BrdU+ cells	% of HuC/D+ neurons associated with BrdU+ cells	Ratio % GnRH/ % HuC/D+
P8 + 2h	12.8 ± 1.0%	3.6 ± 0.2%	3.56
P8 + 7d	22.3 ± 1.5%	5.0 ± 0.2%	4.46

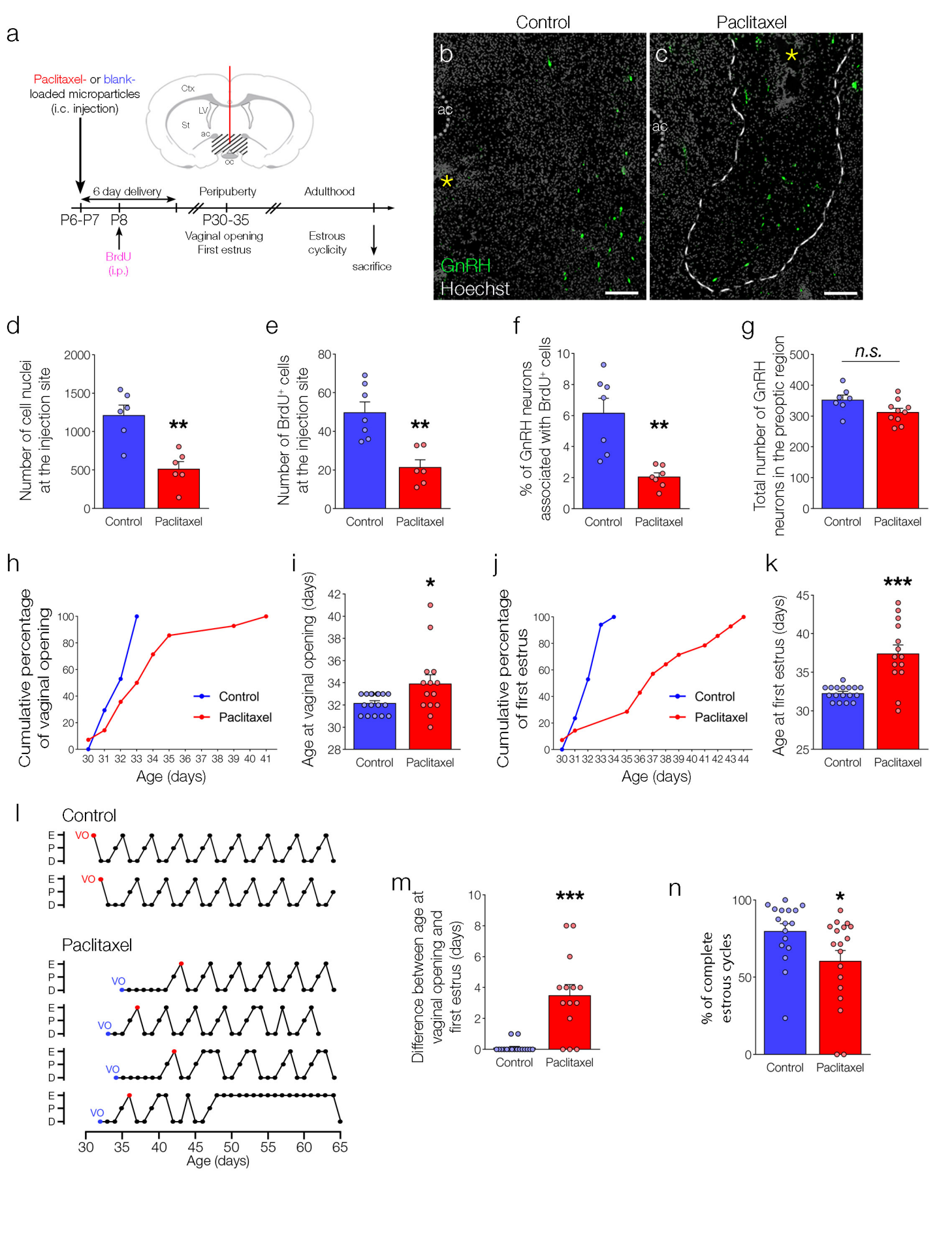
a
Paclitaxel- or blank-
loaded microparticles
(i.c. injection)
Ctx
LV
St
ac
cc
6 day delivery
Peripuberty
Adulthood
P6-P7
P8
P30-35
Vaginal opening
First estrus
Estrous
cyclicity
BrdU
(i.p.)
sacrifice
Control
Paclitaxel
b
c
ac
GnRH
Hoechst
d
Number of cell nuclei at the injection site
e
Number of BrdU+ cells at the injection site
f
% of GnRH neurons associated with BrdU+ cells
g
Total number of GnRH neurons in the preoptic region
n.s.
h
Cumulative percentage of vaginal opening
Age (days)
i
Age at vaginal opening (days)
j
Cumulative percentage of first estrus
Age (days)
k
Age at first estrus (days)
l
Control
Paclitaxel
E
P
D
VO
Age (days)
m
Difference between age at vaginal opening and first estrus (days)
n
% of complete estrous cycles

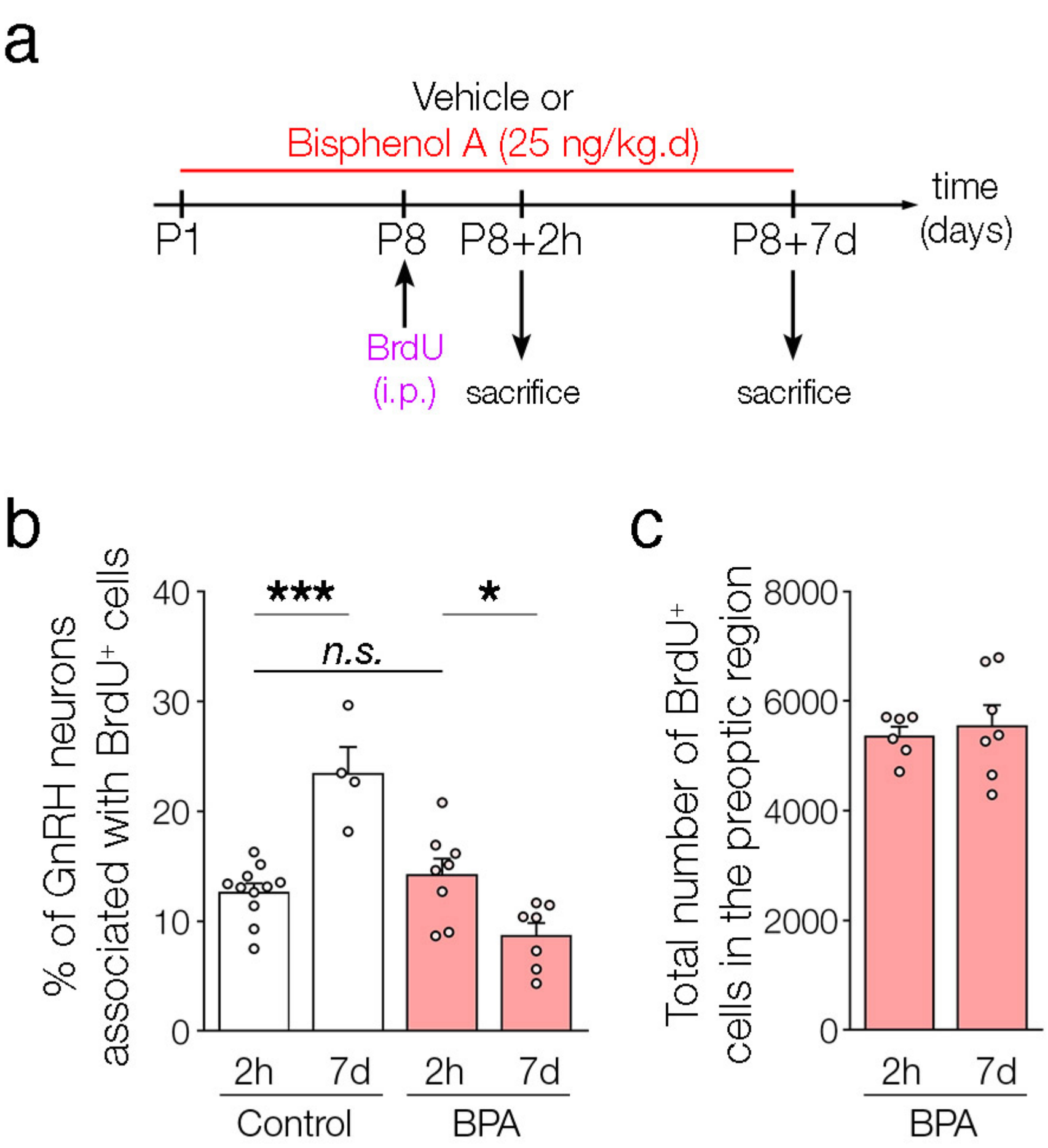
a
Vehicle or
Bisphenol A (25 ng/kg.d)
time
(days)
P1
P8
P8+2h
P8+7d
BrdU
(i.p.)
sacrifice
sacrifice
b
% of GnRH neurons
associated with BrdU+ cells
***
*
n.s.
40
30
20
10
0
2h
7d
2h
7d
Control
BPA
c
Total number of BrdU+
cells in the preoptic region
8000
6000
4000
2000
0
2h
7d
BPA

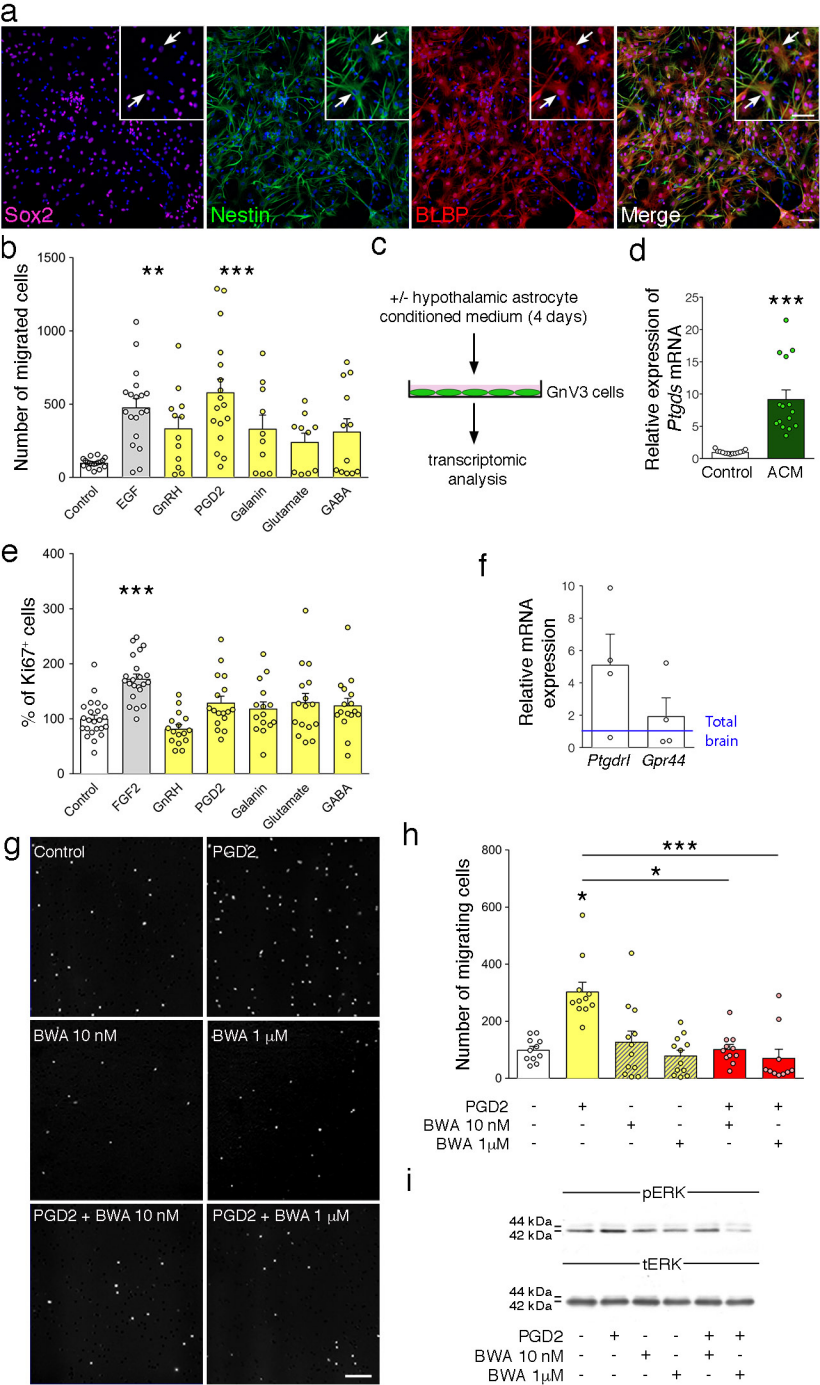
a
Sox2
Nestin
BLBP
Merge
b
Number of migrated cells
1500
1000
500
0
**
***
Control
EGF
GnRH
PGD2
Galanin
Glutamate
GABA
c
+/- hypothalamic astrocyte conditioned medium (4 days)
GnV3 cells
transcriptomic analysis
d
Relative expression of Ptgds mRNA
25
20
15
10
5
0
***
Control
ACM
e
% of Ki67+ cells
400
300
200
100
0
***
Control
FGF2
GnRH
PGD2
Galanin
Glutamate
GABA
f
Relative mRNA expression
10
8
6
4
2
0
Total brain
Ptgdrl
Gpr44
g
Control
PGD2
BWA 10 nM
BWA 1 μM
PGD2 + BWA 10 nM
PGD2 + BWA 1 μM
h
Number of migrating cells
800
600
400
200
0
***
*
*
PGD2 - + - - + +
BWA 10 nM - - + - + -
BWA 1μM - - - + - +
i
pERK
44 kDa
42 kDa
tERK
44 kDa
42 kDa
PGD2 - + - - + +
BWA 10 nM - - + - + -
BWA 1μM - - - + - +

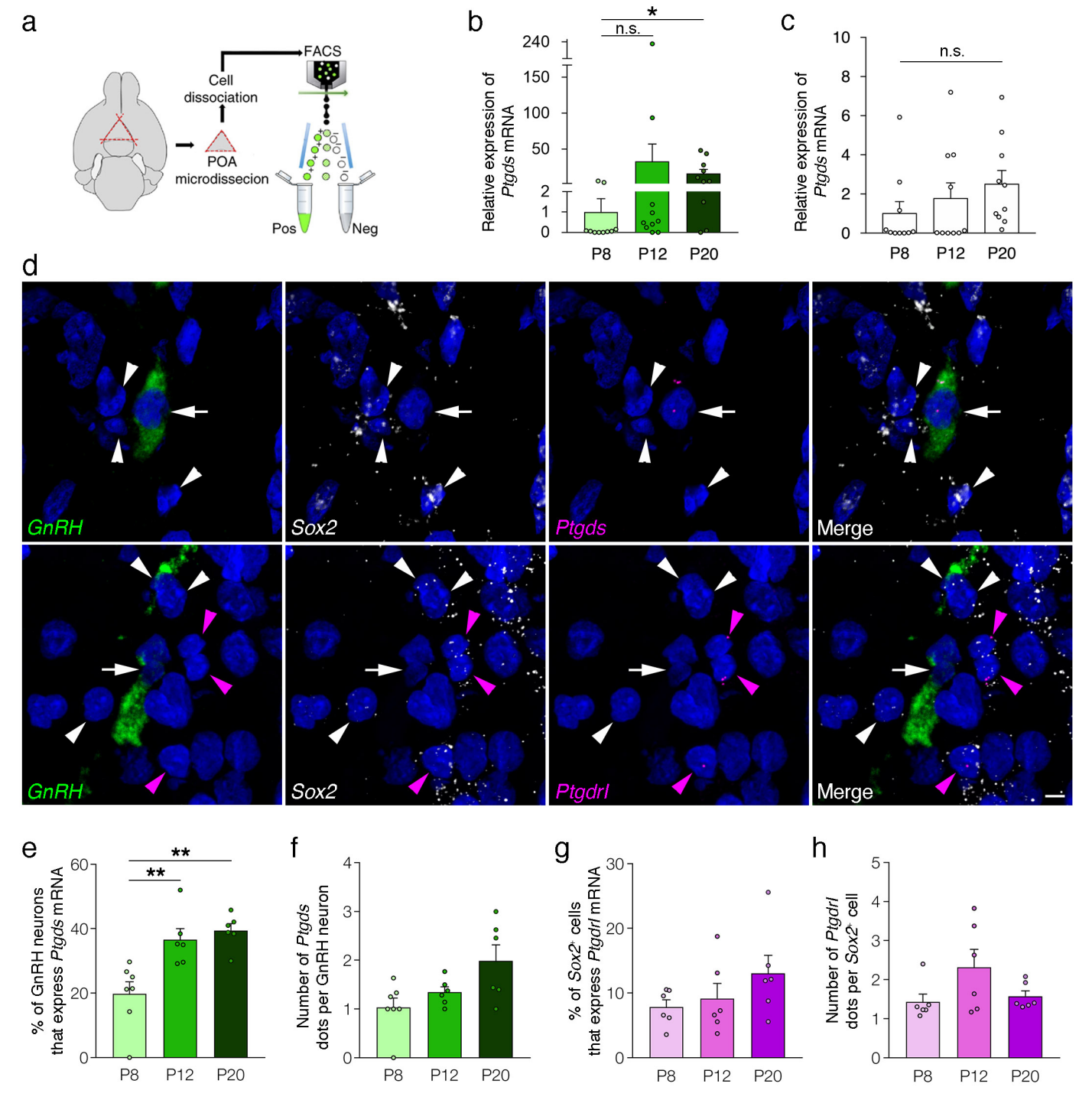
a
FACS
Cell dissociation
POA microdissecion
Pos
Neg
b
*
n.s.
Relative expression of Ptgds mRNA
240
150
100
50
2
1
0
P8
P12
P20
c
n.s.
Relative expression of Ptgds mRNA
10
8
6
4
2
0
P8
P12
P20
d
GnRH
Sox2
Ptgds
Merge
GnRH
Sox2
Ptgdrl
Merge
e
**
**
% of GnRH neurons that express Ptgds mRNA
60
40
20
0
P8
P12
P20
f
Number of Ptgds dots per GnRH neuron
4
3
2
1
0
P8
P12
P20
g
% of Sox2- cells that express Ptgdrl mRNA
30
20
10
0
P8
P12
P20
h
Number of Ptgdrl dots per Sox2- cell
5
4
3
2
1
0
P8
P12
P20

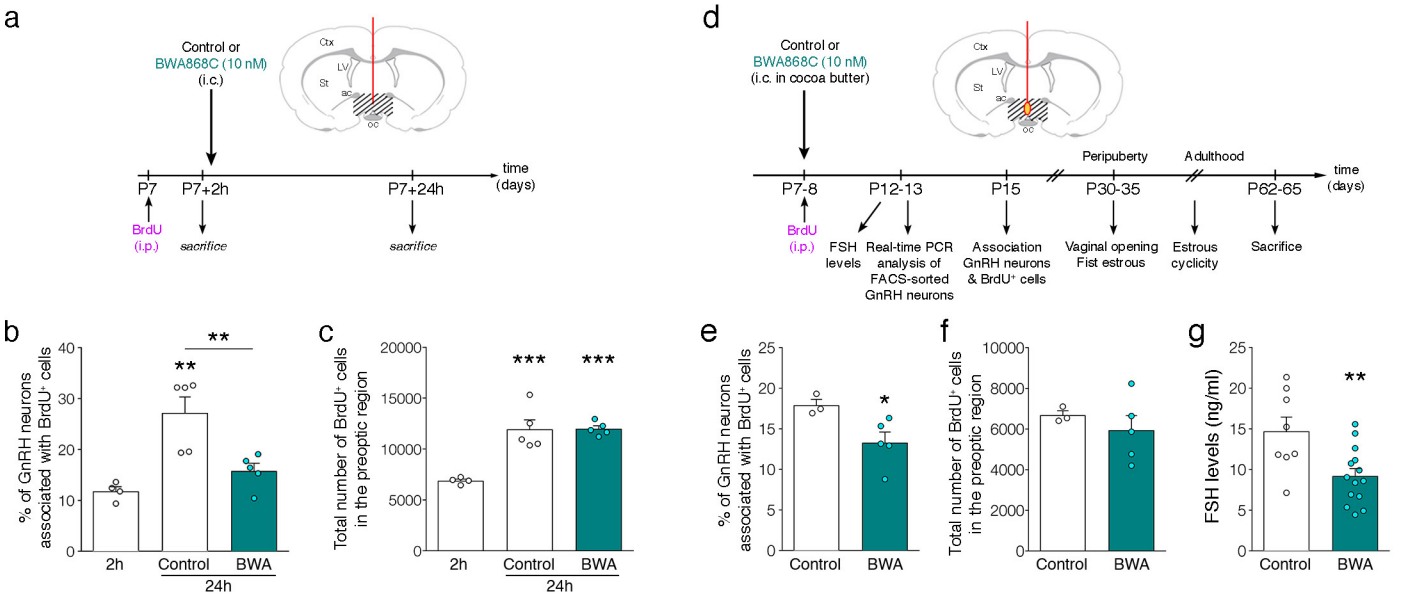
a
Control or
BWA868C (10 nM)
(i.c.)
Ctx
LV
St
ac
oc
time
(days)
P7
P7+2h
P7+24h
BrdU
(i.p.)
sacrifice
sacrifice
d
Control or
BWA868C (10 nM)
(i.c. in cocoa butter)
Ctx
LV
St
ac
oc
Peripuberty
Adulthood
time
(days)
P7-8
P12-13
P15
P30-35
P62-65
BrdU
(i.p.)
FSH
levels
Real-time PCR
analysis of
FACS-sorted
GnRH neurons
Association
GnRH neurons
& BrdU+ cells
Vaginal opening
Fist estrous
Estrous
cyclicity
Sacrifice
b
% of GnRH neurons
associated with BrdU+ cells
40
30
20
10
0
**
**
2h
Control
BWA
24h
c
Total number of BrdU+ cells
in the preoptic region
20000
15000
10000
5000
0
***
***
2h
Control
BWA
24h
e
% of GnRH neurons
associated with BrdU+ cells
25
20
15
10
5
0
*
Control
BWA
f
Total number of BrdU+ cells
in the preoptic region
10000
8000
6000
4000
2000
0
Control
BWA
g
FSH levels (ng/ml)
25
20
15
10
5
0
**
Control
BWA

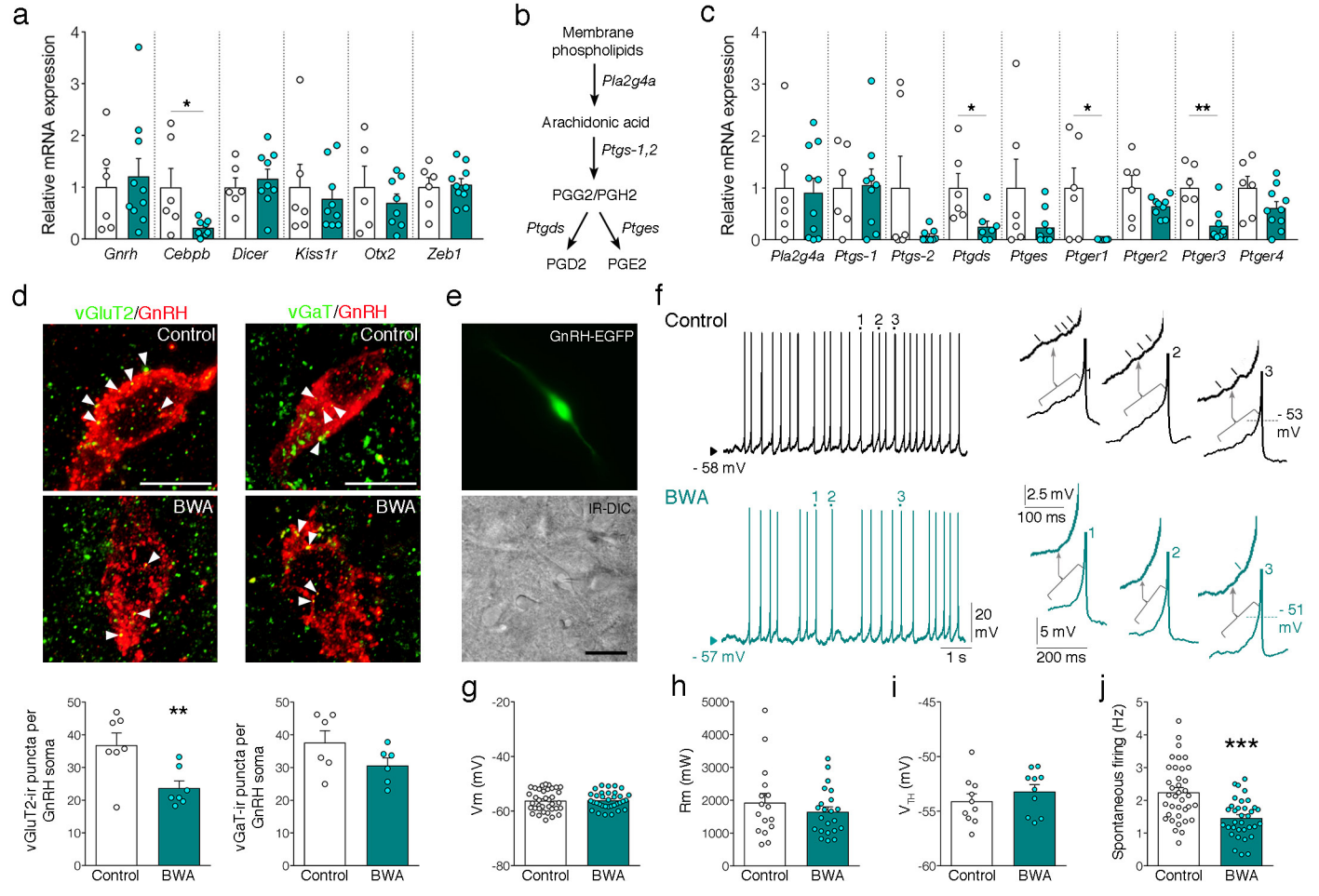
a
Relative mRNA expression
Gnrh
Cebpb
Dicer
Kiss1r
Otx2
Zeb1
b
Membrane phospholipids
Pla2g4a
Arachidonic acid
Ptgs-1,2
PGG2/PGH2
Ptgds
Ptges
PGD2
PGE2
c
Relative mRNA expression
Pla2g4a
Ptgs-1
Ptgs-2
Ptgds
Ptges
Ptger1
Ptger2
Ptger3
Ptger4
d
vGluT2/GnRH
vGaT/GnRH
Control
BWA
vGluT2-ir puncta per GnRH soma
vGaT-ir puncta per GnRH soma
e
GnRH-EGFP
IR-DIC
f
Control
- 58 mV
- 53 mV
BWA
- 57 mV
20 mV
1 s
2.5 mV
100 ms
5 mV
200 ms
- 51 mV
g
Vm (mV)
h
Rm (mW)
i
V_TH (mV)
j
Spontaneous firing (Hz)

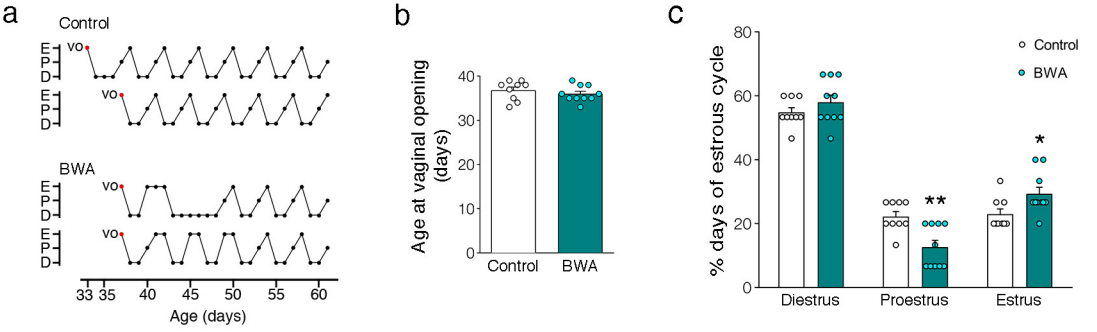
a
Control
vo
E
P
D
BWA
33 35 40 45 50 55 60
Age (days)
b
Age at vaginal opening (days)
0 10 20 30 40
Control
BWA
c
% days of estrous cycle
0 20 40 60 80
Control
BWA
**
*
Diestrus
Proestrus
Estrus